UNIVERSIDADE FEDERAL DO PARANÁ

JULIANE FAGOTTI

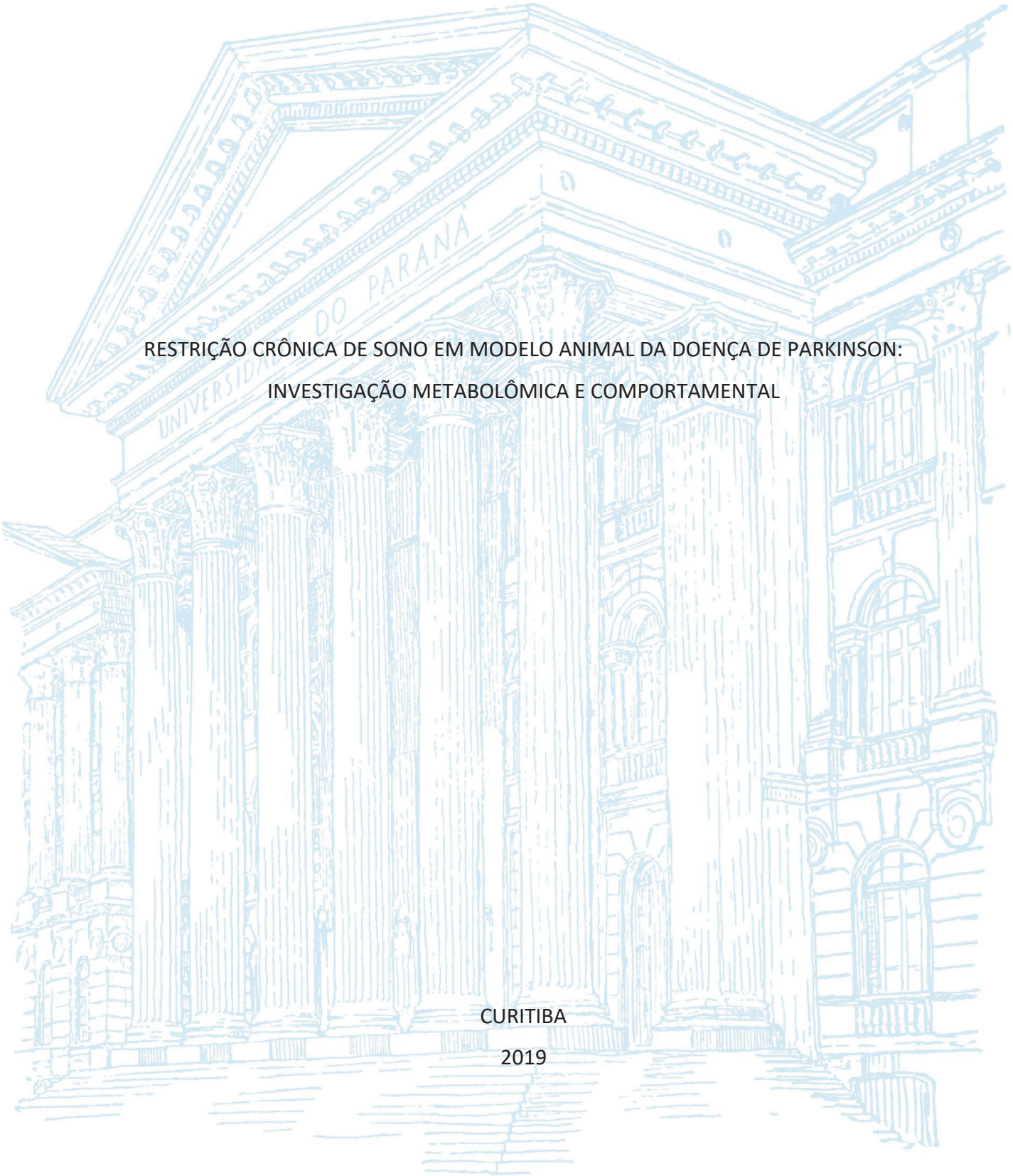

RESTRIÇÃO CRÔNICA DE SONO EM MODELO ANIMAL DA DOENÇA DE PARKINSON: INVESTIGAÇÃO METABOLÔMICA E COMPORTAMENTAL

CURITIBA

2019

JULIANE FAGOTTI

RESTRIÇÃO CRÔNICA DE SONO EM MODELO ANIMAL DA DOENÇA DE PARKINSON: INVESTIGAÇÃO METABOLÔMICA E COMPORTAMENTAL

Tese apresentada ao Programa de Pós-Graduação em Fisiologia, Setor de Ciências Biológicas, Universidade Federal do Paraná, como requisito parcial para obtenção do título de Doutor em Fisiologia.

Orientador: Marcelo de Meira Santos Lima.
Coorientador: Fernando Mazzili Louzada

CURITIBA

2019

Universidade Federal do Paraná. Sistema de Bibliotecas.
Biblioteca de Ciências Biológicas.
(Giana Mara Seniski Silva – CRB/9 1406)

Fagotti, Juliane
Restrição de sono em modelo animal da Doença de Parkinson: investigação metabolômica e comportamental. / Juliane Fagotti. – Curitiba, 2019.
113 p.: il.

Orientador: Marcelo de Meira Santos Lima
Coorientador: Fernando Mazzili Louzada

Tese (doutorado) - Universidade Federal do Paraná, Setor de Ciências Biológicas. Programa de Pós-Graduação em Fisiologia.

1. Parkinson, Doença de 2. Sono - Privação 3. Rotenona 4. Biomarcadores 5. Memória I. Título II. Lima, Marcelo de Meira Santos, 1978- III. Louzada, Fernando Mazzilli, 1964- IV. Universidade Federal do Paraná. Setor de Ciências Biológicas. Programa de Pós-Graduação em Fisiologia.

CDD (22. ed.) 616.833

MINISTÉRIO DA EDUCAÇÃO
SETOR DE CIENCIAS BIOLOGICAS
UNIVERSIDADE FEDERAL DO PARANÁ
PRÓ-REITORIA DE PESQUISA E PÓS-GRADUAÇÃO
PROGRAMA DE PÓS-GRADUAÇÃO FISIOLOGIA - 40001016072P4

TERMO DE APROVAÇÃO

Os membros da Banca Examinadora designada pelo Colegiado do Programa de Pós-Graduação em FISIOLOGIA da Universidade Federal do Paraná foram convocados para realizar a arguição da Tese de Doutorado de **JULIANE FAGOTTI**, intitulada: **RESTRIÇÃO CRÔNICA DE SONO EM MODELO ANIMAL DA DOENÇA DE PARKINSON: INVESTIGAÇÃO METABOLÔMICA E COMPORTAMENTAL**, sob orientação do Prof. Dr. MARCELO DE MEIRA SANTOS LIMA, após terem inquirido a aluna e realizado a avaliação do trabalho, são de parecer pela sua APROVAÇÃO no rito de defesa.

A outorga do título de Doutor está sujeita à homologação pelo colegiado, ao atendimento de todas as indicações e correções solicitadas pela banca e ao pleno atendimento das demandas regimentais do Programa de Pós-Graduação.

Curitiba, 12 de Dezembro de 2019.

MARCELO DE MEIRA SANTOS LIMA
Presidente da Banca Examinadora

PABLO TORTEROLO
Avaliador Externo (UNIVERSIDAD DE LA REPUBLICA - URUGUAI)

ANDERSON JOEL MARTINO ANDRADE
Avaliador Interno (UNIVERSIDADE FEDERAL DO PARANÁ)

GUSTAVO ZAMPIER DOS SANTOS LIMA
Avaliador Externo (UNIVERSIDADE FEDERAL DO RIO GRANDE DO NORTE)

GUILHERME LANZI SASSAKI
Avaliador Externo (UNIVERSIDADE FEDERAL DO PARANÁ)

AGRADECIMENTOS

Primeiramente, eu gostaria de agradecer meu orientador Professor Marcelo. Seu compromisso com a excelência é inspirador e sei que sou privilegiada por ter tido a oportunidade de compartilhar dessa sabedoria e conselhos. Sou extremamente grata por todos os seus esforços para oferecer o melhor para seus alunos. Entendo que sem a sua presença e atitudes, meu caminho até e de aqui em diante seriam completamente diferentes.

Acima de tudo, agradeço àqueles que amo incondicionalmente. Minha jornada aqui teria sido impossível sem o apoio emocional e educacional deles. Mas, principalmente, por acreditarem em mim, especialmente quando eu não acreditei e por me mostrarem o tempo todo como se orgulham e que esse amor é recíproco. Especialmente, minha mãe, a mais batalhadora, incrível e inspiradora de todos os tempos. Obrigado por tudo, eu não tenho palavras para expressar tudo o que sinto e me desculpe por não dizer o suficiente (eu sei que não digo). Ao meu pai por seu carinho, sua fé em mim e por ter sido uma fonte de sensibilidade. Meu irmão Cícero, o ser humano mais brilhante desse mundo todinho, fado sensato. Sua existência faz deste mundo um lugar melhor, sem sombra de dúvidas. Minha irmã Vanessa, te amo, obrigado pelo apoio. Eu sei que você nega, mas no fundo me ama também hihi. Mi, pisquilinha da tia, o ser mais responsável e ajuizado dessa família, te amo! Michel (*in memoriam*) eu sei que você também estaria orgulhoso da sua irmãzinha e que teria me apoiado nessa caminhada como sempre apoiou em tudo. Até mesmo sua ausência me trouxe lições valiosas e, acredito, uma serenidade que apenas a superação da dor é capaz de proporcionar.

E Leo. Aqui a Ju inabalável se desmancha. Obrigada por ter sido a minha família, meu amigo, meu parceiro. Por suportar esta jornada ao meu lado, por entender e me encorajar. Ouso dizer que provavelmente eu não estaria aqui se não fosse por você. Por todos os filmes não-vistos, as festas que eu não pude ir, os shows que eu perdi, os fins de semana e as noites em que a minha presença representava ausência. Não sei o que a vida trará para nós, mas quero que saiba (eu sei que sabe) que você foi um grande amor. Peço desculpas por não nos colocar em primeiro lugar, e sei que jamais vou conseguir exprimir em palavras o quanto tive a sorte de ter você em minha vida, de ter seu apoio, seu carinho e compreensão.

Obrigada, LABCELEBROO! Adriano, Lais, Jé, Patsi, Flávia, Luana e Anas. Vocês são maravilhosos! Obrigado pelo apoio científico, mas, sinceramente, obrigado por me deixar entrar em suas vidas e pela amizade. Os congressos não serão os mesmos sem vocês, prometam que vamos continuar indo juntos! A capybara ainda não tá cravada na cútis, mas eu agilizo isso logo, prometo. Obrigado por tornarem essa jornada muito mais divertida e os dias mais agradáveis. Aproveito também pra mandar um abraço pra todos do laboratório de Neuro. E, a todos de alguma forma envolvidos na realização dos experimentos (Fraaan, cadê você?) e a todos do departamento que contribuem para a experiência fantástica que tive nesses 5 anos (acredito ter tido a sorte de me bem-relacionar com todos – citar nomes seria injusto). Aos professores do departamento de fisiologia, obrigado pelo exemplo. Sua devoção e entusiasmo pelo ensino e pela ciência cativam e inspiram. Fábio, Hely, Rogério e Roberto, obrigado por sua dedicação.

Às amigas Josi e Gi. São tantos anos de amizade não saberia nem por onde começar. Gi, a nossa amizade já tá mais madura que a gente hahaha. É incrível como pessoas tão diferentes podem ter essa ligação tão forte e por tanto tempo. Obrigada por esse poço de fé e orgulho que você tem por mim. Josi, meu chuchu, eu continuo achano um absurdo o (pouco) tempo que passamos juntas. Mas saiba que meu coração fica mais calmo ao saber que tenho em você um porto seguro também. Amo vocês.

A todos em Curitiba, amigos, família. Indiretamente vocês fazem parte dessa minha conquista. Ter uma rede de apoio de pessoas tão maravilhosas e inspiradoras – e que ao mesmo tempo reconhecem em nós os mesmos sentimentos – é fundamental pra uma vida leve e em equilíbrio, permitindo que o trabalho seja visto da mesma maneira. Brigaduuu 😊

E, claro, tão importante quanto são os meus em Londres. Digo, faz mais de uma década! Estamos ficando velhos ... Obrigado por trazer mais pessoas incríveis para minha vida. Tim, Alex e Maria, me diverti tanto com vocês! Tim, especialmente, obrigada por me acolher em sua vida e sua família. Minha gratidão será sempre eterna.

Para todos do PDSE - Londres. Vocês foram extremamente importantes. Compartilhar os anseios e os dias de folga foram vitais e revigorantes. Aline, Victor e Sula, Five Guys não foi mais o mesmo sem vocês ☹.

A todos que conheci na Imperial e que de alguma forma ajudaram no meu crescimento não somente científico, mas também com a experiência de fazer novas amizades com

culturas tão diferentes. Fahmina, Natasa, Gordana, Simone, Antonis, Marine, Maraki, Panos, Alex, Pedro, Adesola, Virag, Olof, Katie, Matt e Jon. Obrigado pela orientação e amizade!

A todos que fizeram parte direta ou indiretamente da minha formação e da realização deste trabalho, muito obrigado, incluindo aqueles cujo trabalho inspirou o meu.

IT WAS A HELL OF A JOURNEY!

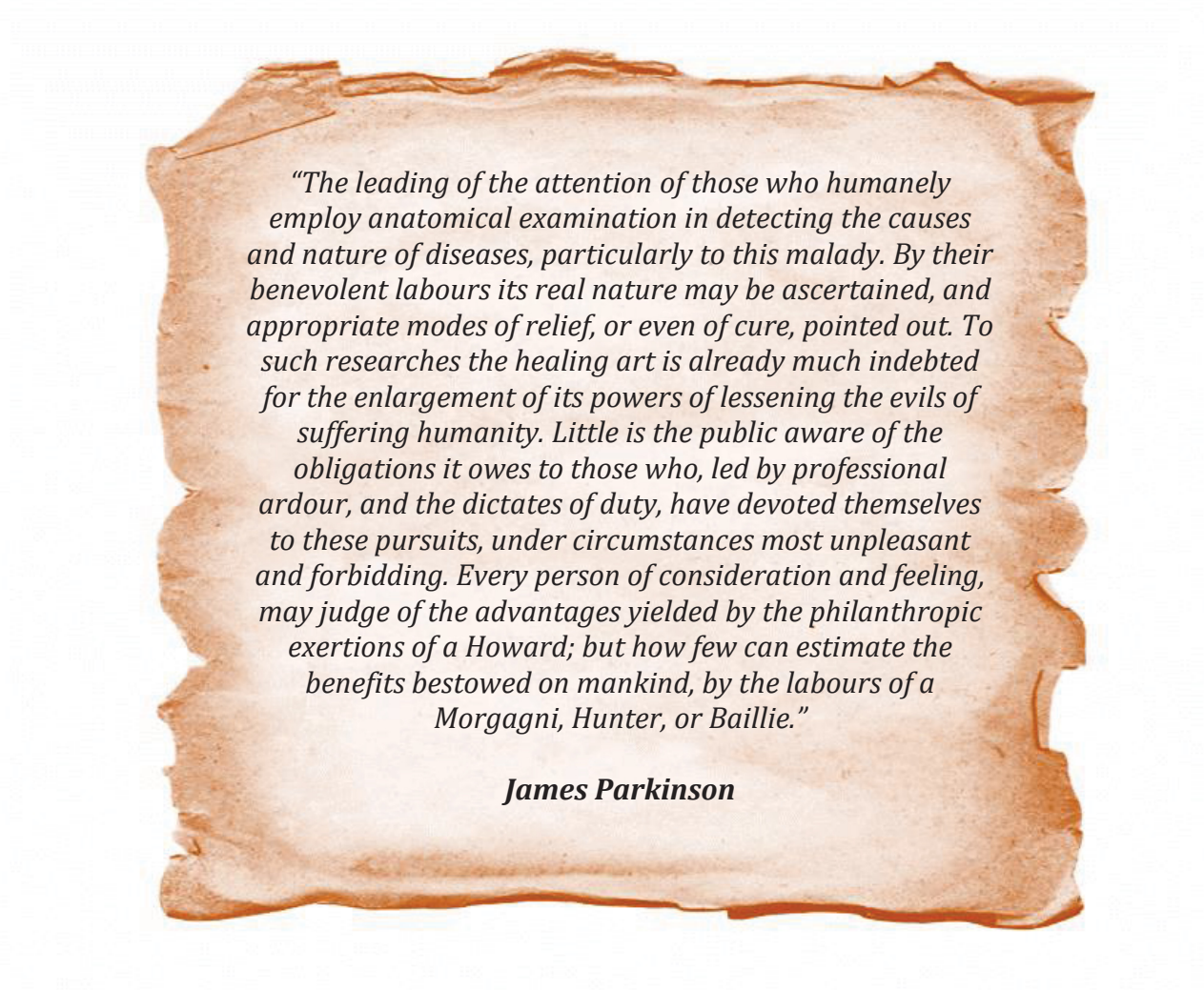

| If you try and take a cat apart |

| to see how it works, |

| the first thing you have on your hand |

| is a non-working cat. |

DOUGLAS ADAMS

incenso fosse música

isso de querer
ser exatamente aquilo
que a gente é
ainda vai
nos levar além

Paulo Leminski

RESUMO

A doença de Parkinson (DP) é o processo neurodegenerativo que mais cresce no mundo atualmente, com prevalência dobrando a cada geração, tornando um prioridade a busca por um biomarcador confiável e precoce da doença que reflita a patologia subjacente para um diagnóstico eficiente. A DP é uma condição crônica que apresenta uma série de sinais pré-motores, como distúrbios do sono e declínio cognitivo, as mais conhecidas características não motoras da doença. Cada vez mais surgem evidências de uma possível associação entre distúrbios do sono e o processo neurodegenerativo, sugerindo que o comprometimento do sono pode produzir uma assinatura metabólica detectável na doença. A fim de integrar parâmetros neurocognitivos e metabólicos, realizamos o perfilamento metabólico – não- e direcionados do modelo de PD induzido por rotenona em um contexto de restrição crônica do sono (SR) (6h/dia por 21 dias). Esse delineamento tem como objetivo a identificação de biomarcadores de DP juntamente com sintomas prodrômicos, inestimável para desenvolver um diagnóstico sensível e obter insights sobre a patogênese da DP. Demonstramos que a SR, combinada com a DP, alterou vários parâmetros comportamentais (reversão do comprometimento da atividade locomotora; comprometimento cognitivo; atraso no ritmo de atividade-repouso) e metabólicos no plasma (aminoácidos de cadeia ramificada, via do triptofano, fenilalanina e lipoproteínas, sugerindo comprometimento mitocondrial), mas nenhum modelo fenotípico metabólico capaz de diferenciar do grupo controle foi obtido a partir de amostras de cérebro, urina e fezes. Se combinados, nossos resultados trazem uma infinidade de parâmetros que podem refletir biomarcadores iniciais da PD no plasma, os quais podem ser facilmente medidos e translacionados para estudos em humanos. Ao mesmo tempo, como os perfis metabólitos das outras matrizes não foram afetados notavelmente, indicaria a resiliência das vias metabólica independentemente das variações plasmáticas observadas, dando suporte à heterogeneidade característica do pesticida rotenona como modelo de DP (que por sua vez reflete também a variabilidade da própria DP), à susceptibilidade ao efeitos da perda de sono ou, ainda, sugerir que qualquer distúrbio metabólico associado a este modelo não é rastreável com a plataforma analítica (^{1}H NMR) escolhida.

Palavras-chave: Doença de Parkinson; Rotenona; Restrição Crônica do Sono; Metabolômica; Biomarcadores; Memória de Reconhecimento; Padrão de Atividade-Repouso; TH-imuno-histoquímica

ABSTRACT

Parkinson's disease (PD) is the fastest-growing neurodegenerative disorder in the world, with prevalence rates doubling with each generation, making the search for a reliable, early-disease biomarker that reflects underlying pathology a high priority research. PD is a chronic disorder that presents a range of premotor signs, such as sleep disturbances and cognitive decline, which are key non-motor features of the disease. Increasing evidence of a possible association between sleep disruption and the neurodegenerative process suggests that sleep impairment could produce a detectable metabolic signature on the disease. In order to integrate neurocognitive and metabolic parameters, we performed untargeted and targeted metabolic profiling of the rotenone PD model in a chronic sleep restriction (SR) (6 h/day for 21 days) condition. This framework would permit the identification of PD biomarkers along with prodromal symptoms, which is inestimable to develop a sensible diagnostic and gain mechanistic insights into PD pathogenesis. We found that SR combined with PD altered several behavioural (reversal of locomotor activity impairment; cognitive impairment; delay of rest-activity rhythm) and plasma metabolic parameters (branched-chain amino acids, tryptophan pathway, phenylalanine, and lipoproteins, pointing to mitochondrial impairment), but no phenotypical model was obtained from brain samples, urine and stool metabolome. If combined, our results bring a plethora of parameters that represents reliable early-phase PD biomarkers on plasma, which can easily be measured and could be translated to human studies. At the same time, since metabolite profiles from other matrices were remarkably unaffected, it indicates resilience of the metabolic network regardless observed plasma variations, supporting the characteristic heterogeneity of the pesticide rotenone as a PD model (which is correlated with PD variability as well) and sleep loss likelihood, or suggesting that any metabolic disturbance associated with this model is untraceable with the chosen analytical platform (^{1}H NMR).

Keywords: Parkinson's disease; rotenone; chronic sleep restriction; metabolomics; biomarkers; recognition memory; rest-activity pattern; TH-immunohistochemistry

LISTA DE ABREVIATURAS E SIGLAS

5-HT: 5-Hidroxitriptamina (serotonina)
6-OHDA: 6-Hidroxidopamina
AUC: Área Sob a Curva
BCAA: Aminoácidos de Cadeia Ramificada
CT: Controle
DA: Dopamina / Dopaminérgico
DMSO: Dimetilsulfóxido
FDR: Taxa de Falsas Descobertas
GABA: Ácido γ-aminobutírico
GC: Cromatografia Gasosa
GPC: Glicerofosfocololina
ILE: Isoleucina
IMS: Espectrometria de Mobilidade Iônica
KYN: Quinurenina
KYNA: Ácido Quinurênico
L/D: Claro-Escuro
LB: Corpúsculos de Lewy
LC/MS: Cromatografia Líquida/Espectrometria de Massas
LDL: Lipoproteínas de Baixa Densidade
LEU: Leucina
MET: Metionina
MPTP: 1-metil-4-fenil-1,2,3,6-tetra-hidropiridina
MS: Espectrometria de Massas
NMR: Ressonância Magnética Nuclear
NMS: Sintomas Não-Motores
OF: Campo Aberto
OPLS-DA: Análise Ortogonal Discriminante dos Mínimos Quadrados Parciais
ORT: Teste de Reconhecimento de Objetos
PCA: Análise dos Componentes Principais
PD: Doença de Parkinson
PHE: Fenilalanina
QC: Controle de Qualidade
RBR: Distúrbio de Comportamento do Sono REM
REB: Recuperação do Sono Rebote
REM: Movimento Rápido dos Olhos
ROC: Característica de Operação do Receptor
ROT: Rotenona
ROT-CT: Grupo Rotenona, Controle para SR
ROT-REB: Grupo Rotenona Rebote
ROT-SR: Grupo Rotenona, submetido à SR
SHAM-CT: Grupo Veículo, Controle para SR
SHAM-REB: Grupo Veículo Rebote
SHAM-SR: Grupo Veículo, submetido à SR
SNPC: Substantia Nigra pars compacta
SR: Restrição de Sono
TH: Tirosina-hidroxilase
TH-ir: imunorreativo para TH
TRP: Triptofano
TSP: Ácido 3- (trimetilsilil) - [2,2,3,3, -2h4] -propiônico
TYR: Tirosina
VAL: Valine
VLDL: Lipoproteínas de Densidade Muito Baixa
A-aaa: ácido alfa-aminoadípico
A-syn: α-sinucleína

LIST OF ABBREVIATIONS AND ACRONYMS

5-HT: 5-hydroxytryptamine (serotonin)

6-OHDA: 6-hydroxydopamine

AUC: area under the curve

BCAA: branched-chain amino acids

CT: control

DA: dopamine/dopaminergic

DMSO: dimethyl sulfoxide

FDR: false discovery rate

GABA: γ-aminobutyric acid

GC: gas chromatography

GPC: glycerophosphocholine

ILE: isoleucine

IMS: ion mobility spectrometry

KYN: kynurenine

KYNA: kynurenic acid

L/D: light-dark

LB: Lewy bodies

LC/MS: liquid chromatography/mass spectrometry

LDL: low density lipoproteins

LEU: leucine

MET: methionine

MPTP: 1-methyl-4-phenyl-1,2,3,6-tetrahydropyridine

MS: mass spectrometry

NMR: nuclear magnetic resonance

NMS: non-motor symptoms

OF: open field

OPLS-DA: orthogonal partial least squares discriminant analysis

ORT: object recognition task

PCA: principal component analysis

PD: Parkinson's disease

PHE: phenylalanine

QC: quality control

RBD: REM behaviour disorder

REB: rebound sleep recovery

REM: rapid eye movement

ROC: receiver operating characteristic

ROT: rotenone

ROT-CT: rotenone control for SR group

ROT-REB: rotenone rebound group

ROT-SR: rotenone sleep restriction group

SHAM-CT: vehicle control for SR group

SHAM-REB: vehicle rebound group

SHAM-SR: vehicle sleep restriction group

SNpc: substantia nigra pars compacta

SR: sleep restriction

TH: tyrosine hydroxylase

TH-ir: TH-immunoreactive

TRP: tryptophan

TSP: 3-(trimethyl-silyl)-[2,2,3,3,-2H4]-propionic acid

TYR: tyrosine

VAL: valine

VLDL: very-low density lipoproteins

α-AAA: alpha-aminoadipic acid

α-syn: α-synuclein

SUMÁRIO

1 INTRODUCTION

1.1 PARKINSON'S DISEASE

Parkinson's disease (PD) is a progressive neurodegenerative disorder, and the fastest growing neurological disease in the world. In 2016, the number of people with PD worldwide was 6.1 million, more than doubled over the course of a generation, as in 1990 this number was 2.5 million. (DORSEY; ELBAZ; NICHOLS; ABD-ALLAH *et al.*, 2018). Epidemiological studies increasingly support a diverse etiology, with the influence of genetic, behavioural and environmental factors on disease pathogenesis and progression (ASCHERIO; SCHWARZSCHILD, 2016). However, age is still the clearest risk factor for PD, with a clear increase in prevalence with advancing age, reaching 1.7% for men and 1.2% for women aged 85 to 89 years (Figure 1), index worsened further with increase in patients' life expectancy and survival (DORSEY; ELBAZ; NICHOLS; ABD-ALLAH *et al.*, 2018). Not only that, according to United Nations projections, the number of people aged 60 and over will grow to approximately 2.1 billion by 2050, dramatically increasing the likelihood of overall incidence and prevalence for Parkinson's disease (UNITED NATIONS, DEPARTMENT OF ECONOMIC AND SOCIAL AFFAIRS, 2017).

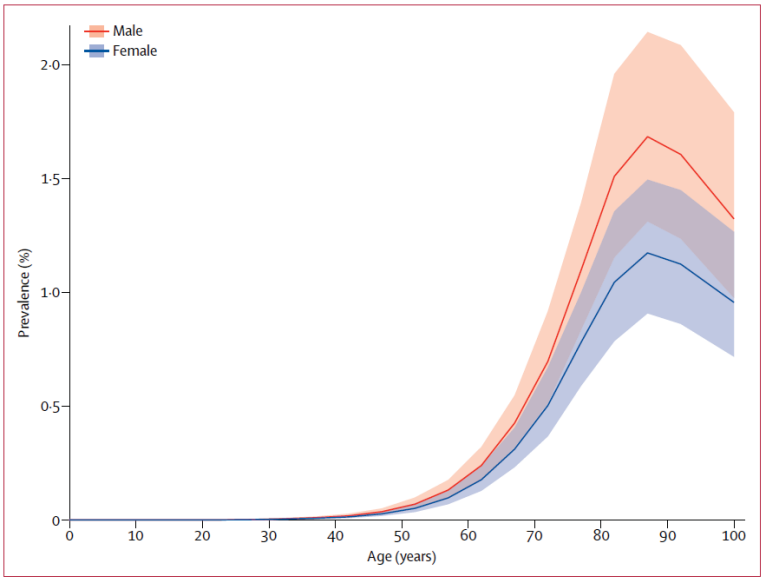

Figure 1. Overall prevalence of Parkinson's disease by age and gender, 2016. Prevalence is expressed as the percentage of the population affected by the disease. Source: DORSEY Reproduction from ELBAZ; NICHOLS; ABD-ALLAH et al. (2018).

In Brazil, the prevalence of the disease in the population over 50 years reaches approximately 128,836 (DORSEY; ELBAZ; NICHOLS; ABD-ALLAH *et al.*, 2018), but this number is fairly underestimated, since disclosure of PD is not compulsory. Unofficial data suggest that there are between 200 and 250 thousands carriers of the disease in the country (Doença de Parkinson, 2014; RIEDER, 2016), but considering the prevalence of 3.3%

(BARBOSA; CARAMELLI; MAIA; CUNNINGHAM *et al.*, 2006), we can infer that the number of PD cases nationwide may reach more than 600.000 taking into account the population aged 65 or more in the country (IBGE, 2018). In any case, available numbers are far below the projection, indicating that PD in Brazil is underrated, both due to the lack of epidemiological data but also limited diagnosis, due to the complexity of the disease, absence of specific markers and even misdiagnosis with other conditions.

PD is a complex and heterogeneous disease, with patients presenting many different characteristics (JOHNSON; STECHER; LABRIE; BRUNDIN *et al.*, 2019), involving an interplay of aging, genetics and environmental factors leading to a multifactorial pathology (KAUR; MEHAN; SINGH, 2019). Despite that PD is primarily a movement disorder, it presents a range of parallel signs that appear before being clinically defined (POSTUMA; BERG, 2019). These signs are typified as prodromal PD and comprise a range of nonmotor symptoms (NMS), including cognitive impairment and sleep disturbance (GREENLAND; WILLIAMS-GRAY; BARKER, 2019; LIMA, 2013). As a matter of fact, these symptoms appear years before the clinical onset of the disease, but they still fall poor in being taking into account in the diagnosis, even if some NMS, especially sleep disturbance, are currently more informative in following the progression of the disease than other markers (MOLLENHAUER; ZIMMERMANN; SIXEL-DORING; FOCKE *et al.*, 2016). Sleep disturbances, all leading to sleep loss, consistently emerge in PD, but they are still underestimated, even if it is known that they can worse other symptoms as memory and motor impairment (GARCIA-BORREGUERO; LARROSA; BRAVO, 2003; TANDBERG; LARSEN; KARLSEN, 1998). In this sense, it's is suggested that sleep deficiency has a bidirectional relationship with PD, but it's still unclear if sleep loss constitutes a risk-factor for the disease.

Despite much effort, there is as yet no reliable way to identify those individuals that will develop PD. Failure to establish the pathological process is the main obstacle to find a cure or treatment that alter the course of the disease, but our inability to diagnose it early enough hinder a better approach or improvement of the existing treatments. Therefore, the identification of risk factors and detection of early symptoms are a priority, since no approach to date has identified specific or sensitive signs that have a practical application in diagnosis (MILLER; O'CALLAGHAN, 2015; SILVEIRA-MORIYAMA; LEES, 2015). Strategies to identify biomarkers are being investigated, mainly to allow early diagnosis before the onset of motor symptoms. Biomarkers are the holy grail of neurodegenerative diseases, but even

in two decades of progress in the field, it has not been possible to produce a reliable and reproducible early diagnosis, mainly due to the heterogeneity of the studies and the disease itself, and the lack of specificity, making difficult to generalize the results (YILMAZ; HOPFNER; VAN EIMEREN; BERG, 2019). Metabolite phenotyping using high resolution analytical chemistry platforms coupled with multivariate statistics provides great potential for identifying reliable biomarkers of PD. The elucidation of such biochemical signatures could represent a major step towards early diagnosis, disease progression, and effective treatments (LEI; POWERS, 2013; SHARMA; MOON; KHOGALI; HAIDOUS *et al.*, 2013).

Part of the dilemma regards to the fact that it's hard to measure metabolism in humans. Standardization is not easy to achieve and many personal characteristics, like diet, have a huge effect on metabolic profiling (DAVIES; ANG; REVELL; HOLMES *et al.*, 2014). Thus, a better understanding of the mechanisms underlying the disease process may be reached with animal models (LE; SAYANA; JANKOVIC, 2014). Those represent an essential resource to investigate the pathogenesis of PD *in vivo* and access new potential outcomes. Having this in mind, the right choice of the model is critical to a successful metabolite discovery study and depends on how trustworthy the PD features are replicated (JOHNSON; BOBROVSKAYA, 2015; LEI; POWERS, 2013). In particular, neurotoxin-based models are far-reaching in enlightening many aspects of the dopaminergic neuron cell death related to PD (DAUER; PRZEDBORSKI, 2003).

From this perspective, the rotenone (ROT)-induced model, well stablished in our laboratory, is tightly connected with sleep impairment (DOS SANTOS; CASTRO; JOSE; DELATTRE *et al.*, 2013; GARCIA-GARCIA; PONCE; BROWN; CUSSEN *et al.*, 2005; MORAIS; LIMA; MARTYNHAK; SANTIAGO *et al.*, 2012; MOREIRA; BARBIERO; ARIZA; DOMBROWSKI; SABIONI; BORTOLANZA; DA CUNHA *et al.*, 2012; TARGA; RODRIGUES; NOSEDA; AURICH *et al.*, 2016), and represents a great alternative for studying the pathological and physiological processes of PD and its interplay with sleep restriction (SR).

1.2 AIMS

1.2.1 General Objective

To investigate, in the ROT animal model of PD, imposed chronic SR as a possible triggering factor for metabolic and behavioural shifts, analysing the outcomes of SR on the development of the model and the interaction between them, prospecting early-phase biomarkers of PD from a translational perspective.

1.2.2 Specific Research Objectives

- Evaluate the histological effects of SR and rotenone infusion in the long run using tyrosine hydroxylase (TH) immunohistochemistry;
- Determine the metabolic profile of plasma – using LC/MS for targeted and NMR for untargeted analysis – to explore putative alterations triggered by rotenone infusion and/or SR;
- Metabolite profiling of the SNpc, striatum, hippocampus, urine and stool, using untargeted NMR spectroscopy;
- Integrate the previously observed motor and cognitive effects of chronic sleep restriction on PD with the metabolic signatures;

1.3 JUSTIFICATIVE

Literature shows a strong correlation between sleep regulation and structures affected by PD, although we still fall short on addressing the mechanisms involved and how these conditions relate to each other. Considering that the vast majority of PD patients suffer from sleep disorders that ultimately leads to sleep loss, the chronic SR protocol in a PD setting is an interesting approach to study the relationship between both. Not only that, sleep issues are a prominent NMS of PD that could be contributing to the progression of the disease itself, possibly producing detectable changes in peripheral biofluid and tissues such

as plasma, urine and stool. Strategies to identify biomarkers are growing, mainly to allow early diagnosis before the onset of motor symptoms. Therefore, prospecting translational biomarkers based on metabolic phenotyping of an early-phase model of PD, from a neurophysiological and pathophysiological perspective, would allow a diagnosis before the onset of motor symptoms and contribute for understanding disease pathology and progression. By using two complimentary approaches for this metabolomic discovery, combining NMR and mass spectrometry (MS), we hold on the possibility of acquiring a comprehensive overview of metabolic profiles, comprising a qualitative and quantitative insight.

2 LITERATURE REVIEW

2.1 PD PATHOPHYSIOLOGY

In essence, PD is a progressive neurodegenerative condition whose ultimate characteristic is the death of dopaminergic neurons (DA) of the substantia nigra pars compacta (SNpc), and its striatal levels of its major metabolites, such as homovanilic acid and 3,4-dihydroxyphenylacetic, reflecting in SNpc depigmentation (ICKENSTEIN; KLOTZ; LANGOHR, 1999; LANE; DUNNETT, 2008; LANG; LOZANO, 1998), and consequent loss of nigral afferences. This leads to a reduction of DA inputs in the dorsal motor nucleus of the vagus (DMV) and to the striatum, affecting the modulatory function of SNpc in motor regulation within basal nuclei pathways, affecting γ-aminobutyric acid (GABA) and glutamatergic neurotransmission (Figure 2) (BOVE; TRAVAGLI, 2019). No surprise, it is the direct cause of the motor symptoms of the disease.

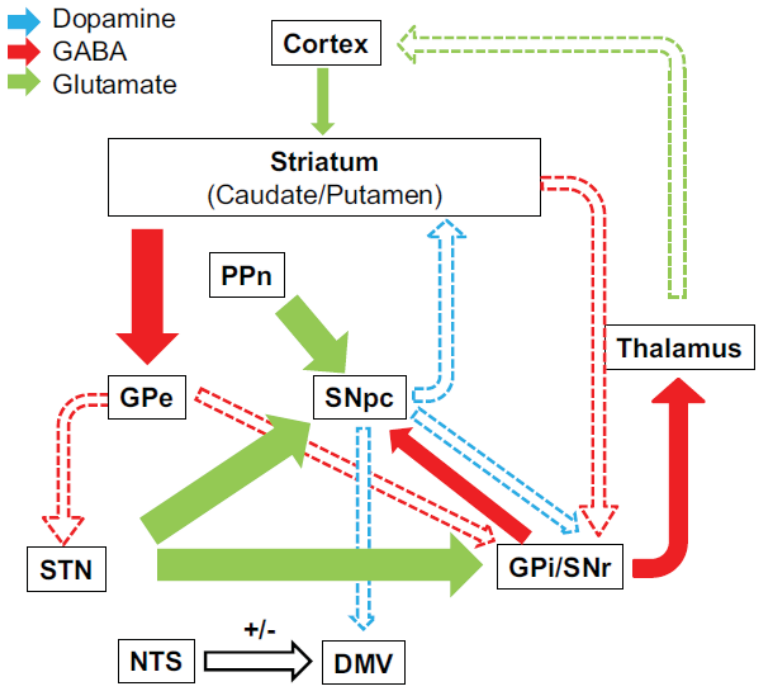

Figure 2. SNpc degeneration in PD decreases dopaminergic nigral outputs to the dorsal motor nucleus of the vagus (DMV) and the striatum. In the indirect pathway, it will cause increased GABAergic inhibitory inputs to the external segment of the globus pallidus (GPe), reducing the inhibition of the subthalamic nucleus (STN), which is going to boost glutamate release from STN. The shrunk of DA modulation in the direct pathway, on the other hand, drops GABAergic outputs to the internal segment of the globus pallidus (GPi) and the substantia nigra pars reticulata (SNr). The eventual outcome in an escalation in Thalamus inhibition, diminishing its outputs to the motor cortex. Thicker arrows: increased neurotransmission; dotted arrows: decreased neurotransmission. Reproduction from (BOVE; TRAVAGLI, 2019)

Another canonical feature of PD is the presence of Lewy bodies (LB) in the central, peripheral and autonomic nervous system (GASSER; HARDY; MIZUNO, 2011; JELLINGER, 2012). LB are eosinophilic inclusions of neurofilaments and misfolded protein aggregates of α-synuclein (α-syn), principally, but also ubiquitin and parkin (Figure 3), and it is intrinsically connected to the progression of PD (LANG; LOZANO, 1998; SCHULZ-SCHAEFFER, 2010). Although α-syn and LB are present in other synucleinopathies and Lewy pathologies, and their cause-effect relationship with PD is still under debate, it is clearly an intrinsic feature of the disease, especially in its idiopathic version (RIEDERER; BERG; CASADEI; CHENG *et al.*, 2019), which are 90% of the cases (ASCHERIO; SCHWARZSCHILD, 2016). Recently, the presence and spreading of α-syn and LB are linked to the onset of PD (KIM; KWON; KAM; PANICKER *et al.*, 2019; PAN-MONTOJO; SCHWARZ; WINKLER; ARNHOLD *et al.*, 2012) and, even more, their presence in non-dopaminergic neurons years before SNpc neurodegeneration support the most consolidated theory in PD research: the Braak Stages (Figure 4) (DEL TREDICI; BRAAK, 2012).

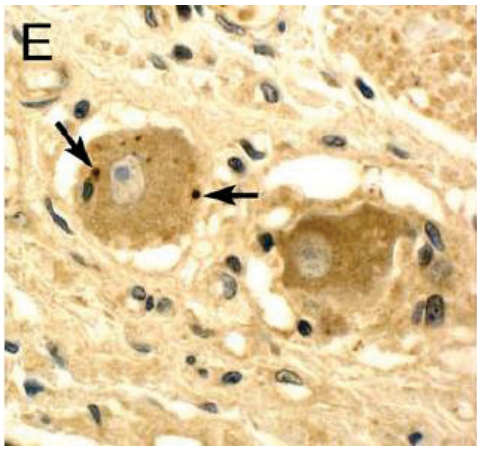

Figure 3. Onset of LB (arrows) in plexus of the enteric nervous system. Reproduction from BRAAK; GHEBREMEDHIN; RUB; BRATZKE *et al.* (2004).

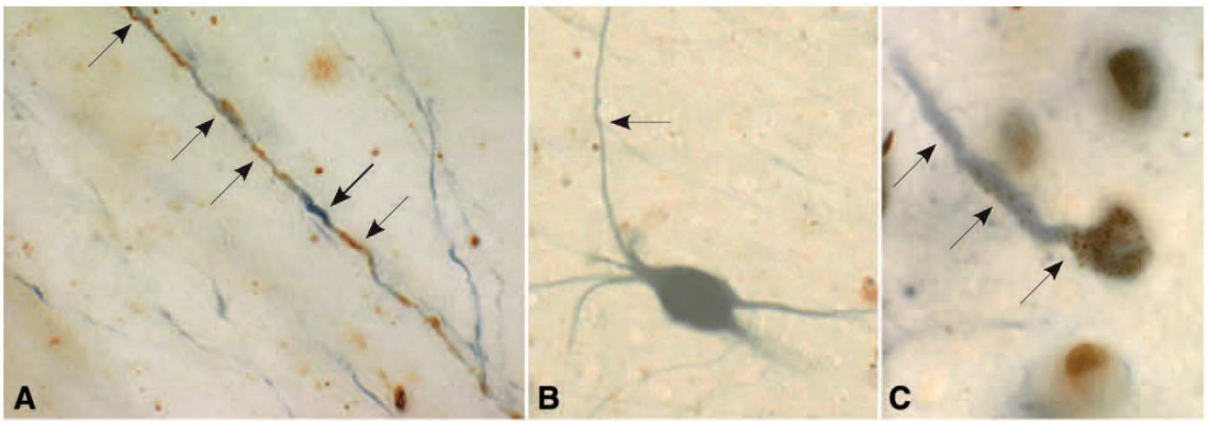

Figure 4. Immunohistochemistry of LB in non-dopaminergic neurons. (A) The thin arrows indicate LB-containing neurites (in brown) in a poorly immunoreactive axon segment for TH (the thick arrow shows a highly immunoreactive region) in the catecholaminergic tract located in the superior cerebellar peduncle. Figures (B) and (C) show TH-immunoreactive neuronal projections at the locus coeruleus. Figure B shows a healthy cell and Figure C a cell with α-synuclein aggregates. Reproduction from DEL TREDICI e BRAAK (2012).

Braak's stages propose a staging of PD based on its neuro and peripheric pathological evolution, hypothesizing that the disease would start in the periphery (olfactory bulb and / or stomach enteric plexus), progressively and stereotypically making its way to the central nervous system, from the medulla oblongata to the cortex, through the brainstem (Figure 5) (BRAAK; DEL TREDICI; RUB; DE VOS *et al.*, 2003; DEL TREDICI; BRAAK, 2012; HAWKES; DEL TREDICI; BRAAK, 2010).

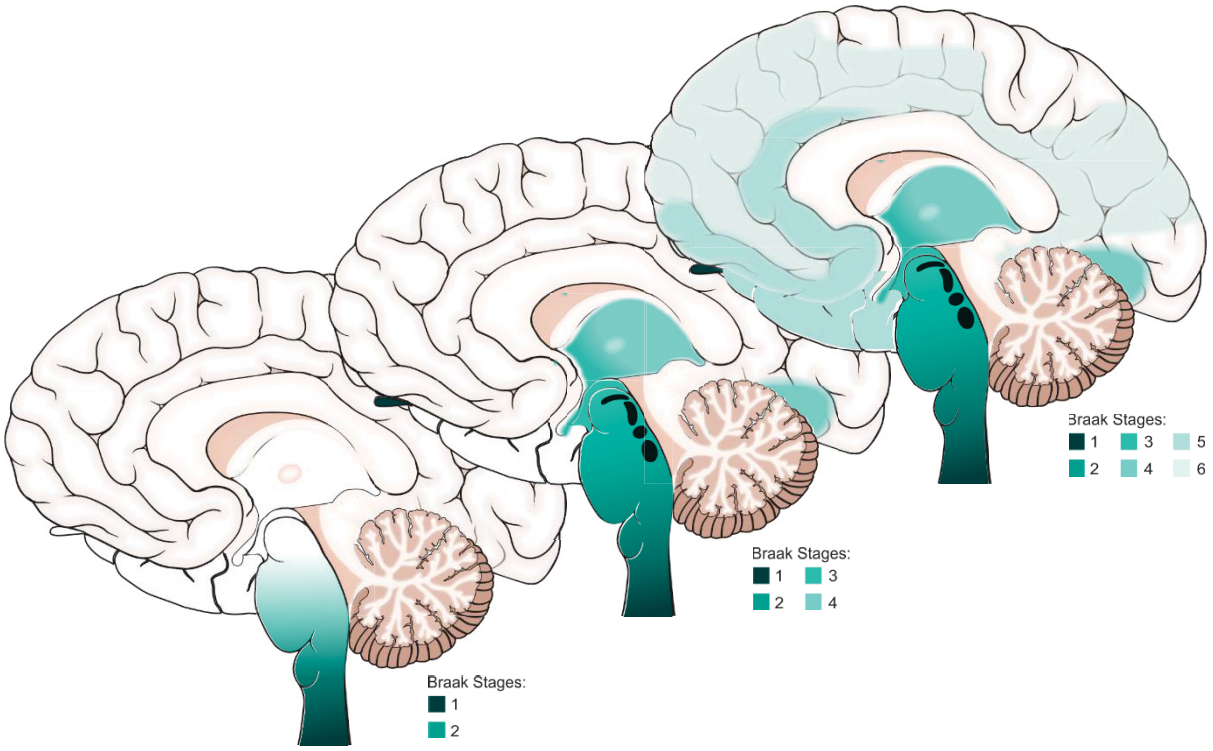

Figure 5. Staging of PD according to Braak's Theory. In stages 1 and 2, the pathology is mainly limited to the medulla oblongata; brainstem is affected in stage 3 and 4, reaching SNpc, therefore when the motor symptoms appear; and finally extending to neocortical areas in stages 5 and 6. Adapted from BRAAK; DEL TREDICI; RUB; DE VOS *et al.* (2003).

Even if Braak's work is fundamental for PD research, is noteworthy to say that James Parkinson suggested somehow a similar portrayal:

> *But of what nature that morbid change is; and **whether originating in the medulla** itself, in its membranes, or in the containing theca, is, at present, the subject of doubt and conjecture. […]*
> *It seldom happens that the agitation extends beyond the arms within the first two years; which period, therefore, **if we were disposed to divide the disease into stages**, might be said to comprise the first stage. (PARKINSON, 2002, p. 234).*
> *Although unable to trace the connection by which a **disordered state of the stomach and bowels may induce a morbid action in a part of the medulla spinalis**, yet taught by the instruction of Mr. Abernethy, little hesitation need be employed before we determine on the probability of such occurrence. (PARKINSON, 2002, p. 236).*

Besides these two cardinal elements, PD is for a fact a chronic multisystem disorder that affects multiple systems during its evolution. Other structures from the brainstem nuclei, cortical areas, spinal cord, preganglionic sympathetic and parasympathetic neurons and also portions of the peripheral and enteric nervous were already implicated in the pathology (BRAAK; DEL TREDICI, 2017; DEL TREDICI; BRAAK, 2015; LIMA; MARTINS; DELATTRE; PROENCA *et al.*, 2012; SCHAPIRA; CHAUDHURI; JENNER, 2017).

2.2 PD ETIOLOGY

> *"On the subject indeed of remote causes, no satisfactory accounts has yet been obtained from any of the sufferers. Whilst one has attributed this affliction to indulgence in spirituous liquors, and another to long lying on the damp ground; the others have been unable to suggest any circumstance whatever, which, in their opinion, could be considered as having given origin, or disposed, to the calamity under which they suffered" (PARKINSON, 2002)*

Although the pathophysiological characteristics of the disease are already well described, causes and mechanisms are not yet fully known. Several genes have been implicated in PD. Genetic forms of the disease accounts for only 5 to 10% of all cases, but many of them have also been implied in sporadic PD that cause familial as well as sporadic PD have been identified and familial aggregation studies support a genetic component (BILLINGSLEY; BANDRES-CIGA; SAEZ-ATIENZAR; SINGLETON, 2018). Converging evidence shows that the onset of α-syn aggregation occurs in the olfactory bulb and/or enteric nervous system, sites potentially exposed to hostile factors. Once formed, these aggregates appear to be able to transynaptically propagate in a virtually self-propelled process through specific pathways (DEL TREDICI; BRAAK, 2015). The protagonist role α-syn in the neurodegenerative process is still under debate, as well as the underlying pathogenic mechanisms triggering its misfolding, (RIEDERER; BERG; CASADEI; CHENG *et al.*, 2019), but mitochondrial dysfunction appears to have an intrinsic relation with α-syn (LUTH; STAVROVSKAYA; BARTELS; KRISTAL *et al.*, 2014) and PD-linked genes (HANG; THUNDYIL; LIM, 2015; ZANELLATI; MONTI; BARZAGHI; REALE *et al.*, 2015)

Mitochondrial dysfunction, in fact, is a key features of PD pathogenesis. More specifically, mitochondrial complex I of respiratory chain is strongly affected in different structures and tissues in patients (BOSE; BEAL, 2016; GRUNEWALD; KUMAR; SUE, 2019) and animals models (LANGSTON; BALLARD, 1983; SCHULER; CASIDA, 2001). This impairment leads to oxidative stress as a result of the chronic production of reactive oxygen species (ROS), which promotes α-syn misfolding (GRUNEWALD; KUMAR; SUE, 2019), and leads to neurodegeneration linked to a neuroinflammatory process (BEAL, 2003).

Inflammation seems to be the linkage between all triggering factors of PD. Apart from the relationship with ROS and mitochondrial dysfunction, inflammatory mediators are known to activate microglia and to foster α-syn aggregation, provoking dopaminergic neurodegeneration (GAO; KOTZBAUER; URYU; LEIGHT *et al.*, 2008; GARCIA-DOMINGUEZ; VESELA; GARCIA-REVILLA; CARRILLO-JIMENEZ *et al.*, 2018; RODRIGUES; FAGOTTI; A; AC *et al.*, 2019) and inflammatory genes are linked to an increase risk factor to develop PD (KRUGER; HARDT; TSCHENTSCHER; JACKEL *et al.*, 2000; WAHNER; SINSHEIMER; BRONSTEIN; RITZ, 2007).

Finally, PD presents a range of epidemiological, molecular, pathophysiological and genetic traits that mutually promotes its progression. Evidence suggests that the vast majority of cases are due to the interaction of environmental factors and genetic predisposition (SUBRAMANIAM; CHESSELET, 2013), and it probably has several components (Figure 6). Therewithal, the pathogenesis begins to be understood as a multifactorial cascade of deleterious factors, so it is difficult to assign values or proportions for each of these etiological agents.

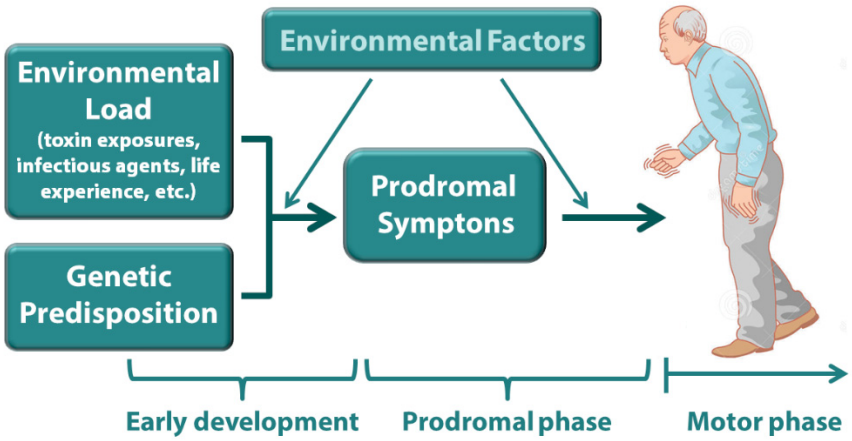

Figure 6. The etiology of PD is not entirely known: several identified environmental aspects together with genetic traits may initiate the neurodegenerative process or make the individual more susceptible to develop the PD. The progression of the disease, if nothing intervenes, would lead to the prodromal phase and continuing to the motor phase. Environmental factors once again appear, worsening symptoms or even causing new ones. This frame provides different windows for neuroprotective interventions. Adapted from CHEN; BURTON; ROSS; HUANG *et al.* (2013)

2.2.1 Environmental Causes

Several environmental factors are associated with increased risk of PD, from toxins, drugs and pollutants to pesticides (BALL; TEO; CHANDRA; CHAPMAN, 2019). A meta-analysis of 16 studies addressing different environmental factors revealed that, of these, 14 suggested an increased risk for disease occurrence in individuals who were exposed to pesticides (PRIYADARSHI; KHUDER; SCHAUB; PRIYADARSHI, 2001). Similar results were obtained in another study with 319 patients and a positive correlation was observed between PD and pesticide exposures (HANCOCK; MARTIN; MAYHEW; STAJICH *et al.*, 2008). The authors report that organochlorines, organophosphates, chlorophenyl esters / acids and rotenone are the pesticides most related to an increased risk for Parkinsonism. This environmental exposure also influences the increase in mortality within PD, demonstrated by a larger number of deaths in areas where pesticide use was higher (RITZ; YU, 2000). It has also been observed that chronic occupational exposure to heavy metals such as lead, manganese and copper is related to the onset of typical PD symptoms. Similarly, several epidemiological studies have shown that pesticide exposure is related to increased risk for disease development (GORELL; PETERSON; RYBICKI; JOHNSON, 2004; HANCOCK; MARTIN; MAYHEW; STAJICH *et al.*, 2008; PRIYADARSHI; KHUDER; SCHAUB; PRIYADARSHI, 2001; RITZ; YU, 2000).

The involvement of environmental toxins in the pathogenesis of PD has been extensively investigated, especially after the discovery that administration of 1-methyl-4-phenyl-1,2,3,6-tetrahydropyridine (MPTP) leads to the onset of Parkinsonian symptoms by nigrostriatal neurodegeneration (LANGSTON; BALLARD, 1983). Since then, toxins have been systematically used to mimic PD in animal models, which provide a better understanding of the mechanisms underlying the disease process (LE; SAYANA; JANKOVIC, 2014). Those represent an essential resource to investigate the pathogenesis of PD *in vivo* and access new potential outcomes. Hence, the right choice of the model is critical to a successful study design and depends on how trustworthy the PD features are replicated (JOHNSON; BOBROVSKAYA, 2015; LEI; POWERS, 2013). In particular, neurotoxin-based models are far-reaching in enlightening many aspects of the dopaminergic neuron cell death related to PD (DAUER; PRZEDBORSKI, 2003). Most insights into PD pathogenesis come from investigations performed in experimental models, especially those produced by neurotoxins. Although a

host of natural and synthetic molecules of exert deleterious effects on dopaminergic neurons, only a handful are used in living laboratory animals to recap some of the hallmarks of PD (BOVE; PROU; PERIER; PRZEDBORSKI, 2005)

2.2.1.1 Rotenone model of PD

In this context, the pesticide rotenone (ROT) mimics the hallmark traits of PD to various extents. ROT is a toxin that freely crosses cell membranes, accumulating in organelles such as mitochondria, where it impairs oxidative phosphorylation by inhibiting the complex I of the electron transport chain (SCHULER; CASIDA, 2001). The ROT-induced animal model of PD is one of the most recent approaches to mimic disease in rats (BETARBET; SHERER; MACKENZIE; GARCIA-OSUNA *et al.*, 2000) and has been well characterized in our laboratory (DOS SANTOS; CASTRO; JOSE; DELATTRE *et al.*, 2013; MOREIRA; BARBIERO; ARIZA; DOMBROWSKI; SABIONI; BORTOLANZA; DA CUNHA *et al.*, 2012). The toxin causes approximately 40-60% reduction in SNpc TH-immunoreactive (TH-ir) neurons, as well as, in the long term, the depletion of DA and its metabolites, producing a selective lesion (MOREIRA; BARBIERO; ARIZA; DOMBROWSKI; SABIONI; BORTOLANZA; CUNHA *et al.*, 2012).

Therefore, pathophysiologically, bilateral administration of SNpc rotenone as a model of PD corresponds to the early-stage of the disease, comparable to Braak Stages 3-4, with a time-dependent neurodegeneration associated with equivalent neurochemical, histological and cognitive changes (MOREIRA; BARBIERO; ARIZA; DOMBROWSKI; SABIONI; BORTOLANZA; DA CUNHA *et al.*, 2012). These include canonical alterations, like time-dependent reduction of dopaminergic (DA) nigrostriatal neurons, a-synuclein (PARK1) aggregation, Lewy-like body formation, oxidative stress and ultrastructural impairments in the SN mitochondria (ALAM; SCHMIDT, 2002; BETARBET; SHERER; MACKENZIE; GARCIA-OSUNA *et al.*, 2000; CANNON; TAPIAS; NA; HONICK *et al.*, 2009; CARRIERE; KANG; NILES, 2017; JOHNSON; BOBROVSKAYA, 2015; MORAIS; LIMA; MARTYNHAK; SANTIAGO *et al.*, 2012; MOREIRA; BARBIERO; ARIZA; DOMBROWSKI; SABIONI; BORTOLANZA; DA CUNHA *et al.*, 2012; VOITENKO; NIKONENKO, 2015).

In the behavioural context, animals submitted to rotenone present reduced mobility, flexed posture and even rigidity and catalepsy (ALAM; SCHMIDT, 2002; SHERER; BETARBET; TESTA; SEO *et al.*, 2003). Cognitive impairment has also been reported following intranigral administration of this neurotoxin (DOS SANTOS; CASTRO; JOSE; DELATTRE *et al.*, 2013), as well as excessive daytime sleepiness, REM sleep behaviour disorder, insomnia and deterioration of spontaneous sleep, dopamine-dependent behavioural deficits, hyposmia and gastrointestinal problems (BETARBET; SHERER; MACKENZIE; GARCIA-OSUNA *et al.*, 2000; CANNON; TAPIAS; NA; HONICK *et al.*, 2009; JOHNSON; BOBROVSKAYA, 2015; LIMA, 2013; MORAIS; LIMA; MARTYNHAK; SANTIAGO *et al.*, 2012; MOREIRA; BARBIERO; ARIZA; DOMBROWSKI; SABIONI; BORTOLANZA; DA CUNHA *et al.*, 2012; RODRIGUES; TARGA; NOSEDA; AURICH *et al.*, 2014).

Studies that take into account the extent of lesions induced by this toxin showed that its infusion through several pathways leads to a nigrostriatal dopaminergic neurodegeneration, with different degrees of severity (BETARBET; SHERER; MACKENZIE; GARCIA-OSUNA *et al.*, 2000; HOGLINGER; FEGER; PRIGENT; MICHEL *et al.*, 2003; SHERER; BETARBET; GREENAMYRE, 2002). This variation of susceptibility among individuals represents an important feature of the model, as it can represent a research landscape that takes into consideration the genetic characteristics of each individual as well as their environmental interactions in the hypothesis of the pathogenesis of PD (PERIER; BOVE; VILA; PRZEDBORSKI, 2003). Likewise, this model produces damage to protein folding in the cytoplasm of nigrostriatal dopaminergic neurons remaining in the lesion. Such conformational errors eventually generate protein inclusions comparable to LB pathology in humans (BETARBET; SHERER; MACKENZIE; GARCIA-OSUNA *et al.*, 2000; HOGLINGER; FEGER; PRIGENT; MICHEL *et al.*, 2003; SHERER; BETARBET; TESTA; SEO *et al.*, 2003). This aspect is considered an advantage over other neurotoxin-induced models, since it has predictive validity.

2.3 PD SYMPTOMS

> *"Involuntary tremulous motion, with lessened muscular power, in parts not in action and even when supported; with a propensity to bend the trunk forwards, and to pass from a walking to a running pace: the senses and intellects being uninjured."* (PARKINSON, 2002).

Clinically, the most prominent signs of Parkinsonism are progressive hypokinetic motor disorders, resulting from dopamine shortage. The cardinal motor symptoms of the disease are resting tremor, stiffness and bradykinesia (MARSILI; RIZZO; COLOSIMO, 2018), which were already described by James Parkinson in his canonical work. These signs are still the foundation of PD diagnosis with a sensitivity of 90% (HUGHES; DANIEL; LEES, 2001). Nevertheless, motor symptoms manifest when there is already a moderate to severe neuronal loss of at least 50% in the SNpc (FEARNLEY; LEES, 1991), but usually reaching 60-70% (FAHN, 2003), as they develop slowly and sometimes intermittently at the onset of PD (SHARMA; MOON; KHOGALI; HAIDOUS *et al.*, 2013).

The motor manifestations of the disease are the most known and disabling, but they are just the tip of the iceberg. Being a chronic progressive disease, PD has a preclinical period, where the pathological process has already begun, but the necessary motor manifestations for the diagnosis are not yet perceived. This prodromal period, before the occurrence of the prominent motor signs, is marked by non-motor symptoms (NMS) that precede in many years the clinical motor phase. Prodromal symptoms are less notorious, once they started to be widely studied only a decade ago, when there were only six described markers with just a few studies (POSTUMA; BERG, 2019). Some NMS are well-known, like olfactory and gastrointestinal dysfunction, sleep disorders, circadian changes and cognitive impairment (LIMA, 2013; LIMA; MARTINS; DELATTRE; PROENCA *et al.*, 2012; TOLOSA; PONT-SUNYER, 2011; VIDENOVIC; GOLOMBEK, 2013) and they affect drastically the quality of life of individuals with the disease, appearing long before motor manifestations (GRINBERG *et al.*, 2010; LIMA, 2013).

Although it is well established that nigrostriatal degeneration and balance between direct and indirect pathways are responsible for most motor impairment, it is still unclear the mechanisms that give rise to the NMS (LIMA; MARTINS; DELATTRE; PROENCA *et al.*, 2012; POSTUMA; GAGNON; MONTPLAISIR, 2010; SHARMA; MOON; KHOGALI; HAIDOUS *et al.*, 2013) Neuropathological studies support the association of these early disorders with PD by identifying LB in non-dopaminergic nuclei in preclinical Braak stages prior to significant nigral degeneration, especially in the olfactory bulb and the gut (DEL TREDICI; BRAAK, 2012). Even though, the precise neuronal processes are unclear, and many explanations arise, like cell loss and neuronal dysfunction related not only to deposits of synuclein aggregates (TOLOSA; PONT-SUNYER, 2011), but also peripheric and neuroinflammatory processes

(RODRIGUES; FAGOTTI; A; AC *et al.*, 2019). The global inflammatory state is believed to evolve together with Braak's stages and be involved in a large part of PD symptoms, being concomitantly a response to neuronal death and a triggering factor of the pathology (Figure 7) (BARNUM; TANSEY, 2012; SU; FEDEROFF, 2014).

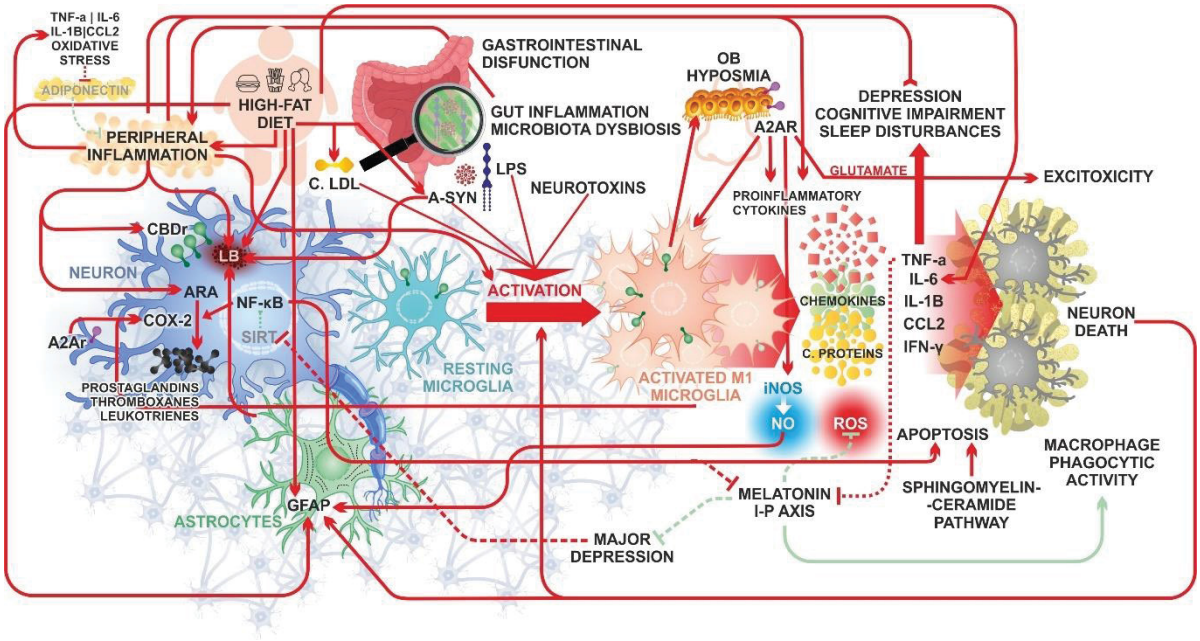

Figure 7. The complex network of inflammatory responses in PD in the context of NMS. A diversity of environmental factors is involved in activating microglia, thus initiating a neuroinflammatory process that will lead to production of inflammatory mediators and ultimately to neuronal death, via different mechanisms. In the meantime, these processes are believed to cause or modulate NMS. Red arrows: proinflammatory activation pathways/ Dashed red lines: proinflammatory inhibition pathways / Green arrows: Anti-inflammatory activation pathways in PD / Dashed green lines: Anti-inflammatory inhibition pathways. Intense and light colors represent, respectively, pathways increased and decreased in inflammatory PD context. A-syn: alpha-synuclein; LB: Lewy body; CBDr: cannabinoid receptors; A2AR: A2 adenosine receptors; LPS: lipopolysaccharides; OB: olfactory bulb; iNOS: nitric oxide synthase; NO: nitric oxide; ROS: reactive oxygen species; GFAP: Glial fibrillary acidic protein; COX-2: Cyclooxygenase 2; ARA: arachidonic acid; SIRT: sirtuins. Reproduction from (RODRIGUES; FAGOTTI; A; AC *et al.*, 2019).7

Notwithstanding the unquestionable importance of studying the NMS of PD, it has plentiful challenges. To begin, there are no robust data that reveal the sequence, prevalence and if there are additional manifestations occurring that were not characterized yet, but available epidemiological data suggest that they may appear up to 25 years before the onset of the clinical phase (TOLOSA; PONT-SUNYER, 2011) and it's well-established that patients report sleep disruption as far as a decade before the first motor symptoms (HAWKES; DEL TREDICI; BRAAK, 2010).

2.3.1 Sleep Disturbances in PD

> *"In this stage, the sleep becomes much disturbed. The tremulous motion of the limbs occur during sleep, and augment until they awaken the patient, and frequently with much agitation and alarm. (p. 224) […] but even when exhausted nature seizes a small portion of sleep, the motion becomes so violent as not only to shake the bed-hangings, but even the floor and sashes of the room. […] and at the last, constant sleepiness, with slight delirium, and other marks of extreme exhaustion, announce the wished-for release. (p. 225) […] His attendants observed, that of late the trembling would sometimes begin in his sleep, and increase until it awakened him: when he always was in a state of agitation and alarm. (p. 226-227)* (PARKINSON, 2002)

Even with the extensively description of sleep issues in the initial presentation of the disease, sleep disorders in PD started to be consistently studied only a few decades ago (ASKENASY; YAHR, 1985; FERRARI; PUCA; MARGHERITA, 1964; KALES; ANSEL; MARKHAM; SCHARF *et al.*, 1971; MOURET, 1975). Primarily, these disorders refer to insomnia, abnormal movements during sleep (e.g., periodic limb movements and RBD) and excessive daytime sleepiness (ABBOTT; ROSS; WHITE; TANNER *et al.*, 2005; COMELLA, 2006; THOLFSEN; LARSEN; SCHULZ; TYSNES *et al.*, 2015). RBD, for instance, has a prevalence ranging from 24 to more than 40 and up to 90% (ZHANG; XU; LIU, 2017; ZHANG; SUN; WANG; TANG *et al.*, 2017), and a great predictive value in PD, since approximately 50% of individuals with RBD develop dementia in 10 years (POSTUMA; GAGNON; MONTPLAISIR, 2010). However its prognostic sensitivity is still questioned, since it is not identified in all individuals with PD and the specificity of their symptoms has not yet been fully established (SHARMA; MOON; KHOGALI; HAIDOUS *et al.*, 2013). But, in general, sleeping problems can affect up to 98% of PD patients (ADLER; THORPY, 2005) and, generally, they are the most impacting of the non-motor characteristics of PD, since, in addition to negatively affecting the patient's life, they contribute to the aggravation of other cognitive signs, such as memory impairment (DOS SANTOS; CASTRO; JOSE; DELATTRE *et al.*, 2013; PUSHPANATHAN; LOFTUS; THOMAS; GASSON *et al.*, 2016).

The specific neurophysiological mechanisms of sleep disorders are far from being fully understood. Although it has an obvious dopaminergic component, its etiology is difficult to be attributed solely to dopaminergic neurodegeneration, given the variables involved in PD, such as pharmacological and cognitive (LIMA, 2013). Even if sleep disturbances have a multifactorial origin, the classical pathological degeneration is concentrated in brainstem

and thalamocortical DA pathways, which are involved in sleep regulation (LIMA, 2013). DA degeneration in the nigrostriatal pathway is primarily associated with motor PD, but patients who experience extensive loss of DA cells in SNpc usually experience greater sleepiness (LIMA; ANDERSEN; REKSIDLER; FERRAZ *et al.*, 2012). A number of studies have presented DA as a dual neurotransmitter, thus being related not only to wakefulness but also to the regulation of sleep processes (LIMA, 2013; LIMA; ANDERSEN; REKSIDLER; FERRAZ *et al.*, 2012; LIMA; ANDERSEN; REKSIDLER; SILVA *et al.*, 2008; LIMA; ANDERSEN; REKSIDLER; VITAL *et al.*, 2007). From such studies, it has been suggested that the nigrostriatal dopaminergic system plays a key role for sleep regulation, especially in a context of neurodegeneration as in the case of PD (LIMA; ANDERSEN; REKSIDLER; VITAL *et al.*, 2007) and, even more, changes in this component would have direct effects on cognitive and sleep changes found in patients with the disease (PROENCA; DOMBROWSKI; DA CUNHA; FISCHER *et al.*, 2014). Therefore, it's clear the intrinsic link between sleep and PD, suggesting a remarkable influence of the dopaminergic system on both.

It's becoming clearer that the relation between neurodegenerative diseases and sleep disturbances is bi-directional since, further than been observed before the onset of the disease, sleeping problems like insomnia also increases the risk of developing dementia (OSORIO; PIRRAGLIA; AGUERA-ORTIZ; DURING *et al.*, 2011). Specifically in PD, there is sufficient evidence to endorse possible feedback between sleep disorders and motor impairment (LIMA; ANDERSEN; REKSIDLER; FERRAZ *et al.*, 2012). In general, normal ageing is associated with inadequacy in sleep physiology, including a diminished capacity to initiate and maintain it. Above all, in the context of neurodegeneration, sleep disruption is notably piercing, ultimately leading to sleep loss, and suggests that inadequate sleep could represent a risk factor that predisposes and contributes to the decline and could even emerge as an early biomarker of abnormal ageing (MANDER; WINER; WALKER, 2017).

2.4 CHRONIC SLEEP RESTRICTION

Both sleep deprivation (an acute event that can last for hours or even uninterrupted days) and restriction (a chronic event that lasts a few hours for several days) have become increasingly common, generating a great impact on society, not just in patients with

neurodegenerative diseases. At first, many studies aimed at investigating the physiology of sleep were conducted using total deprivation protocols, but numerous experiments have been specifically designed to better mimic sleep restriction or sleep disturbance as they occur in humans, and, rather than total acute deprivation, in these models animals are subjected to chronic limitation of sleep hours (MEERLO; MISTLBERGER; JACOBS; HELLER *et al.*, 2009).

In a context of neurodegenerative diseases, the SR for 6h daily in an animal model of Alzheimer's disease promoted impairments in contextual memory and accumulation of cortical Aβ and pTau levels, also correlated with circulating levels of these metabolites (ROTHMAN; HERDENER; FRANKOLA; MUGHAL *et al.*, 2013). Moreover, Alzheimer's patients who exhibit excessive daytime sleepiness also display more parkinsonian motor signs (PARK; COMELLA; LEURGANS; FAN *et al.*, 2006). Specifically in the PD context, a 7-day SR protocol demonstrated that sleep impairment mechanisms play a crucial role in the development of levodopa-induced dyskinesia (GALATI; SALVADE; PACE; SARASSO *et al.*, 2015). Considering these results and the well-known sleep impairment of PD, is evident the need to establish possible effects of SR on PD.

2.5 PD BIOMARKERS

> *"But although, at present, uninformed as to the precise nature of the disease, still it ought not to be considered as one against which there exists no countervailing remedy.*
> *On the contrary, there appears to be sufficient reason for hoping that some remedial process may ere long be discovered, by which, at least, the progress of the disease may be stopped." (PARKINSON, 2002)*

Two centuries are gone, and PD diagnostic is still puzzling, with no current treatment to stop neuronal cell death progression or to even cure it. Thus, to find neuroprotective strategies, a clear understanding of the mechanism(s) involved in dopaminergic cell death is needed. But the data becoming available should guide the investigation of predictive biomarkers and the identification of risk or protective factors (TOLOSA; PONT-SUNYER, 2011). Like in many other neurodegenerative diseases, the list of candidates with the potential to predict the disease is well explored, but many are still

inconsistent. For this reason, an alternative approach would be screening a great number of candidates or even an unbiased methodology to assess potential biomarkers with putative biological information. This high-throughput method would require the ability to process hundreds of potential metabolites (CHEN-PLOTKIN, 2014), having a great potential for identifying reliable markers of PD, which could represent a major step towards early diagnosis, disease progression, and effective treatments (LEI; POWERS, 2013).

As a multisystemic disease, PD pathogenesis involves a plethora of molecular mechanism reflecting in a huge set of possible biochemical pathways that can be explored as a source of biomarkers. Some metabolomic studies have already shed a light in metabolic dysregulation underlying the pathological process, mostly revealing the involvement of a variety of biological categories, lipid and energy metabolism, and some amino acids, enzymes and signalling molecules (Figure 8) (SHAO; LE, 2019), showing that PD metabolomic biomarker discovery has a framework with great potential to be explored.

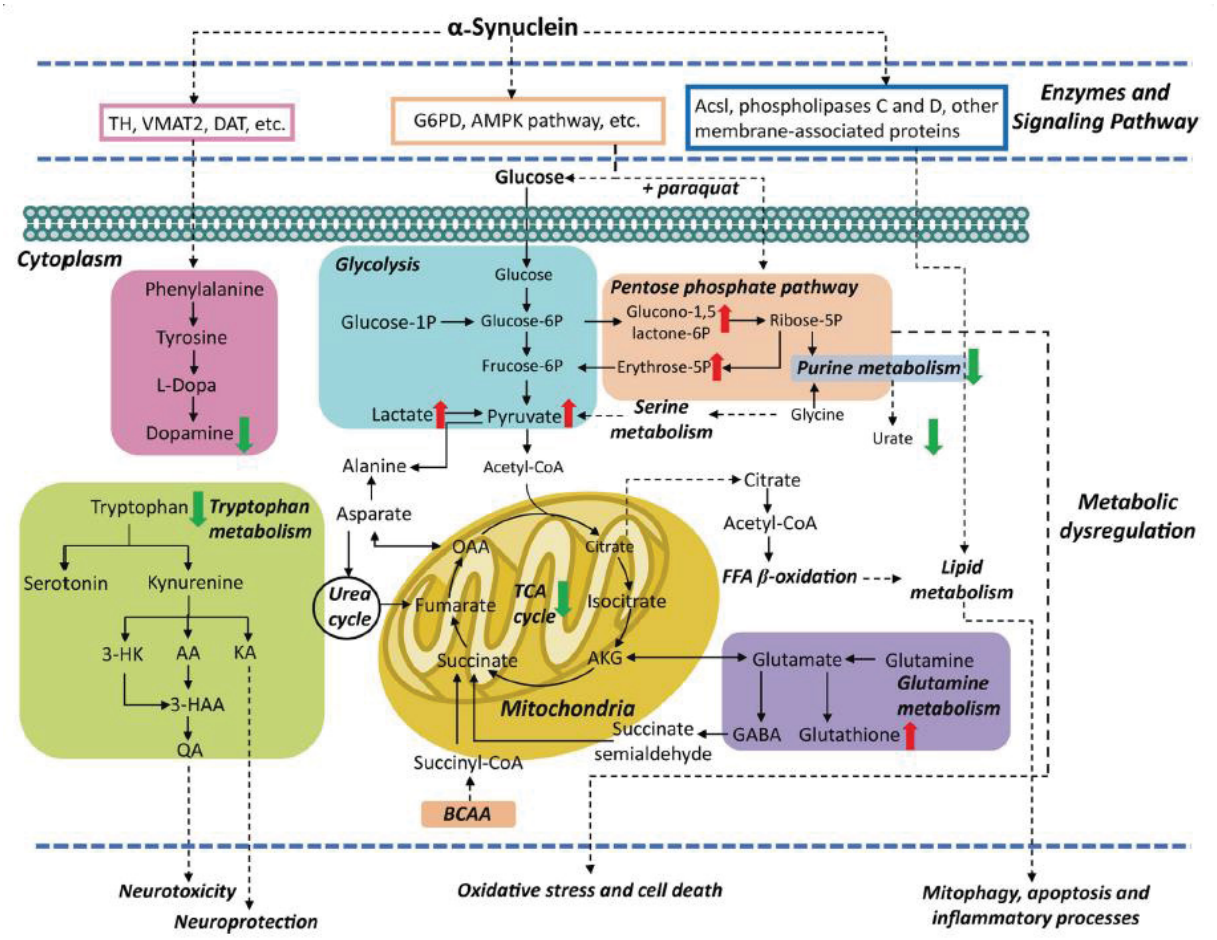

Figure 8. Representative overview of the metabolic pathway dysregulations in PD. Majorly perturbations in PD are related to fatty and bile acids, a-syn mediators, neurotransmitters, the metabolism of lipids and energy (TCA cycle, glycolysis, PPP, BCAA, acylcarnitines), and amino acids. Reproduction from SHAO e LE (2019)

2.6 METABOLIC PROFILING

The relationship between disease risk and metabolism, the set of all chemical reactions involved in maintaining the living state of a biological system, are already well-known (HOLMES; LI; MARCHESI; NICHOLSON, 2012; PEDERSEN; GUDMUNDSDOTTIR; NIELSEN; HYOTYLAINEN *et al.*, 2016). From this perspective, metabolite profiling (generally, cellular metabolism intermediates and products of less than 1kDa in size) of a given organism allows to investigate not only the systemic homeostasis but also diseases aftermath. Therefore, this systematic study of the unique metabolic profile of a cell, tissue, biofluid, organ or organism, play a key-role in life science research (HOLMES; WILSON; NICHOLSON, 2008; JOHNSON; IVANISEVIC; SIUZDAK, 2016). This profiling was originally divided in two different approaches: *metabonomics*, defined as *"the study of the metabolic response of organisms to disease, environmental change or genetic modification"* (LINDON; NICHOLSON; HOLMES; EVERETT, 2000) and *metabolomics,* the *"comprehensive analysis in which all the metabolites of a biological system are identified and quantified" (FIEHN, 2002).* As the field developed and probably because the overlap between them, these terms started to be used conversely. As a preference, in this work the term metabolomics is used.

Metabolomics is the newest addition in the *-omics* technologies and goes a step further by linking both gene and environmental interactions. Its advantage over the other "omics" technologies is the ability to directly evaluate metabolic fluctuations, and, at the same time, represents the downstream output of the genome but also the upstream input from the environment, thus providing a unique, dynamic and accurate molecular description of the functional phenotype (HOLMES; WILSON; NICHOLSON, 2008; SKENE; MIDDLETON; FRASER; PENNINGS *et al.*, 2017; WISHART, 2016). The principal metabolomics techniques include nuclear magnetic resonance (NMR) and mass spectrometry (MS)-based technologies (particularly liquid chromatography (LC) and gas chromatography). GC/MS, despite its superior chromatographic resolution and easier metabolite annotation, requires volatile and thermally stable analytes, free from water, a fact that prolongs substantially sample preparation and compromises throughput while it offers lower metabolite coverage than LC/MS (AMBERG; RIEFKE; SCHLOTTERBECK; ROSS *et al.*, 2017; WISHART, 2016)

Regardless the technique, a successful metabolomics investigation relies on following a standardized step-by-step analytical workflow which is similar in the general view (Figure 9), but with specificities depending on the adopted protocol.

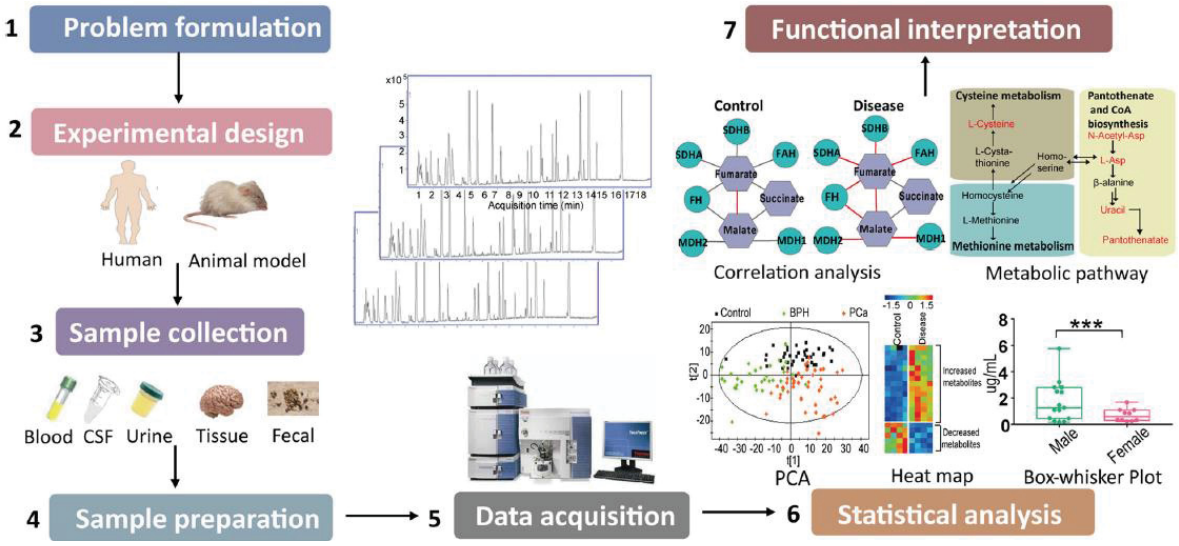

Figure 9. Schematic analytical workflow of a typical metabolomics study, including experimental design, sample collection, sample preparation, data acquisition, statistical analysis and biological interpretation. Reproduction from SHAO e LE (2019)

2.6.1 Targeted and Untargeted Metabolomics

Metabolomic experiments fall into two distinct categories: untargeted and targeted. They are generally complementary, and usually, a first exploratory analysis is performed in untargeted fashion, mainly for unbiased discovery, followed by tailored, targeted experiments which validate and expand the initial findings (Figure 10) (SCHRIMPE-RUTLEDGE; CODREANU; SHERROD; MCLEAN, 2016).

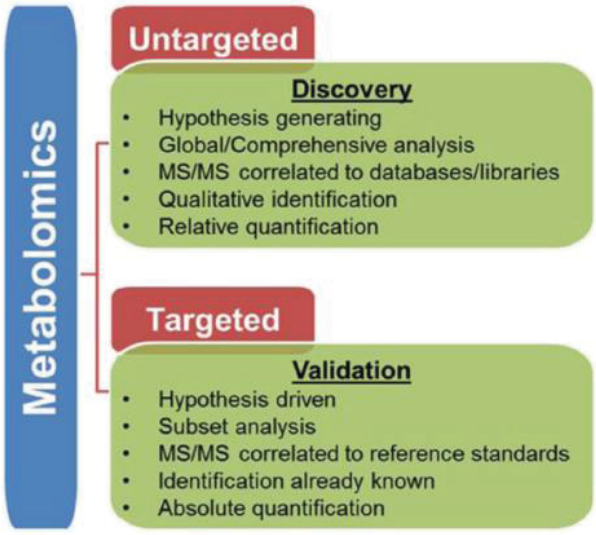

Figure 10. Untargeted and targeted metabolomics have different purposes and approaches. Untargeted focus on metabolite discovery and targeted validation and metabolite quantification. Reproduction from (SCHRIMPE-RUTLEDGE; CODREANU; SHERROD;

In untargeted approaches, regardless the analytical platform of choice, samples are minimally processed before data acquisition, to avoid alterations in the metabolome and all spectroscopic signals are recorded (e.g. mass spectrometry in full scan mode). The main advantages of untargeted assays are that they are not biased, cover a large part of the metabolome, help in building a mechanistic insight and data can be re-visited at any time and reprocessed/reannotated, depending on the biological question. However, the annotation of signals is lengthy and can become extremely complex or even practically impossible for several features. Furthermore, when taking into account the amount of acquired information from high resolution techniques (as chromatography online with high resolution MS) and the lack of authentic standards for several metabolites or the high cost for the commercially available ones, metabolite annotation can become very challenging and in best case scenario, is considered tentative. Additionally, a universal analytical method exhibits worse analytical characteristics since it is not optimised to maximise these in a small set of metabolites, but it is a compromise to achieve a wide metabolome coverage. Finally, since no calibration curves are analysed, the results are expressed in arbitrary units and can be used only for relative comparisons within groups pf the same study (AMBERG; RIEFKE; SCHLOTTERBECK; ROSS *et al.*, 2017; SCHRIMPE-RUTLEDGE; CODREANU; SHERROD; MCLEAN, 2016)}.

On the other hand, in a targeted assay, a method is developed and optimised around a small predefined set of compounds (usually, chemical class- or metabolic pathway-based), with the use of authentic and potentially isotopically labelled internal standards (for mass spectrometry). Targeted methods, except their superior analytical performance (detection limits, linearity, reproducibility etc), generate validated data. Sample preparation is tailored for the target analytes, contaminating compounds from the sample matrix are eliminated and the spectrometers are tuned in order to maximise their response for those specific compounds. The use of standard compounds and internal standards adds confidence to the target analyte data and since the measurements are quantitative, can be compared with other studies and not only relatively between groups of the same analytical run. Finally, targeted data analysis is straight-forward and does not require advanced computational methods. However, analytical method development is a lengthy, challenging and expensive procedure, requires strong background in analytical chemistry and can provide answers only for the levels of specific pre-selected metabolites, whose number in generally limited. Thus,

a wrong choice of targets, can lead a project to a dead end. To conclude, the most common approach generally, is to initially apply untargeted assays for discovery purposes and validate the untargeted findings, with quantitative and validated methods (ROBERTS; SOUZA; GERSZTEN; CLISH, 2012).

The most widely used analytical techniques for metabolic profiling, are nuclear magnetic resonance (NMR) spectroscopy and mass spectrometry (MS) (AMBERG; RIEFKE; SCHLOTTERBECK; ROSS *et al.*, 2017). NMR is probably the most powerful approach for metabolite identification and it generally does not require coupling with other techniques to enhance its selectivity. It is extremely reproducible, non-destructive and the sample preparation is simple and quick. Biofluids (tissue samples have to be homogenised) are centrifuged, diluted, buffered and analysed directly while they remain intact after the analysis and they can be reused. Also, data pre-processing is simpler compared to MS-based assays since NMR is affected much less from batch and signal drift effects compared to MS and requires less maintenance. The major drawback of NMR though is its sensitivity which is approximately limited in the low ppm levels and covers only a small fraction of the metabolome. Additionally, the cost of an NMR instrument is also generally much higher than a mass spectrometer (AMBERG; RIEFKE; SCHLOTTERBECK; ROSS *et al.*, 2017; LARIVE; BARDING; DINGES, 2015).

On the other hand, MS, regardless its lower robustness and the complexity of the generated data, shows a series of advantages. It is more sensitive and can acquire data for thousands of metabolites in a single run with much lower sample volumes than NMR. Furthermore, it is often coupled with chromatography, either liquid (LC) or gas (GC) and ion mobility spectrometry (IMS) in order to enhance its selectivity by adding extra dimensions of metabolite separation (DUMAS; KINROSS; NICHOLSON, 2014). LC/MS requires minimal sample preparation (still longer than NMR) where protein removal is necessary in order to avoid chromatographic column blockages and furthermore, depending on the approach, salts and other interfering compounds are removed from the samples in order to minimise matrix effects (AMBERG; RIEFKE; SCHLOTTERBECK; ROSS *et al.*, 2017; GARCIA; BARBAS, 2011; ZHOU; XIAO; TULI; RESSOM, 2012).

2.6.2 Data pre-processing/ Data analysis/ Biological interpretation

Data pre-processing in metabolomics aims to prepare the dataset to be analysed and to reduce biological variability of no interest, instrument instability, and inconsistency in sample handling and preparation, which could interfere with data analysis.

Data pre-processing is straightforward in LC/MS, since acquired spectra are usually processed with the instrument's vendor software for integration and quantification. But straightforward doesn't mean simpler: in several cases, it has to be corrected for variances due to nonlinear shifts in retention time, peak overlap, and *m/z* shifts. Also, quality control (QC) is very crucial aspect and usually pooled QC samples, dilution series of pooled QCs and blanks are analysed, interspaced in the analytical run. The quality of the data is assessed, in terms of reproducibility (CV% in pooled QCs), linearity (1-tailed Spearman correlation coefficients in dilution series of pooled QCs), contaminations (blank subtraction) and low-quality samples/outliers are removed. With use of unsupervised multivariate statistics and more specifically, Principal Component Analysis (PCA), the size of analytical variability (expressed by the clustering of pooled QCs and the distance from the centre of PCA plot) is compared versus the size of biological variability (expressed by the spread of study samples in the PCA plot). Furthermore, a second inspection is taking place with the use of PCA for outliers and with the above-mentioned analytical corrections. Finally, pooled QC samples are removed from the fully pre-processed dataset, which is ready for detection and quantification of significant peaks – a process that may or may not be automatized –, followed by statistical and biological interpretation (AMBERG; RIEFKE; SCHLOTTERBECK; ROSS *et al.*, 2017).

For untargeted, in order to obtain an accurate and reliable spectrum for statistical analysis, after spectra extraction it must be (1) phase and baseline corrected, (2) aligned, (3) deconvolved, (4) normalized, (5) identified, and (6) integrated. The first step is to correct NMR-specific effects, like incorrect phases of the spectra or shifting baselines, and alignment aims to correct variations in the chemical shifts of the peaks. Deconvolution is used to remove instrumental distortion by deconvolving the spectrum using a chemical shift reference signal, as glucose or an internal standard. Normalisation is a crucial step, especially for the quantitative analysis, since it adjusts variations in the overall concentration of samples. Different normalisation methods can be used, like the median quotient normalisation, which

accounts for dilution considering that it affects all metabolites evenly, but metabolic responses affect just a few ones. At this point, the dataset is ready for data analysis. The identification and integration of chemical shifts is usually performed after peaks of interest be identified in multivariate statistical analysis (AMBERG; RIEFKE; SCHLOTTERBECK; ROSS *et al.*, 2017).

Metabolomics generate a large and valuable number of signals, which require multivariate statistical analysis to extract useful information and to identify patterns of metabolite level changes. Methods such as PCA and partial least square analysis with discriminant analysis projection (PLS-DA) allow the visualization of similarities and differences between samples and spectral data; PCA is an unbiased approach, since it is group blind, and PLS is a supervised method, which is more powerful but more biased at the same time, requiring strong validation methods. Orthogonal partial least squares discriminant analysis (OPLS-SA) analysis is used to statistically correlate data, and allows for a deeper insight into the metabolites that are likely to be associated with a condition, generating important statistical models for discrimination between groups (LI; SWANN; MARCHESI, 2017; WORLEY; POWERS, 2013). Finally, univariate approaches are also applied to investigate differences in individual metabolite levels, followed by false discovery rate (FDR) correction to avoid false positives.

3 METODOLOGIA

3.1 ANIMAIS

Os experimentos foram realizados de acordo com as diretrizes estabelecidas pelo CEUA/BIO da Universidade Federal do Paraná (nº #858), que visam à aplicação dos princípios de ética e cuidados no uso de animais de experimentação (SBCAL). Os protocolos de pesquisa foram revisados pelo *Animal Welfare Ethical Review Body (AWERB)* e pelo Cirurgião Veterinário Nomeado *(NVS)* da Universidade de Surrey, UK, antes de qualquer trabalho, de acordo com os princípios da legislação do Reino Unido (Lei de Animais [Procedimentos Científicos], 1986).Foram utilizados ratos Wistar machos saudáveis de 3 meses de idade, pesando entre 280-330g, com sistema imune normal, que não foram envolvidos em nenhum teste ou tratamento anterior. Os animais foram mantidos em grupos (4 por gaiola) em gaiolas de polipropileno com cepilho descartável em ciclo claro-escuro (L / D) padrão (12 h: 12 h ciclo, luzes acesas às 07:00 h = ZT 0) em uma sala com temperatura controlada (22 ± 2 ºC). Água e comida foram fornecidas à vontade aos animais durante todo o experimento.

3.2 DELINEAMENTO EXPERIMENTAL

A Figura 11 traz o desenho experimental e a distribuição dos animais anos grupos. O delineamento foi for executado em 6 replicatas, com 4 animais por grupo experimental ao início de replicata. Os procedimentos estão detalhados nos tópicos subsequentes.

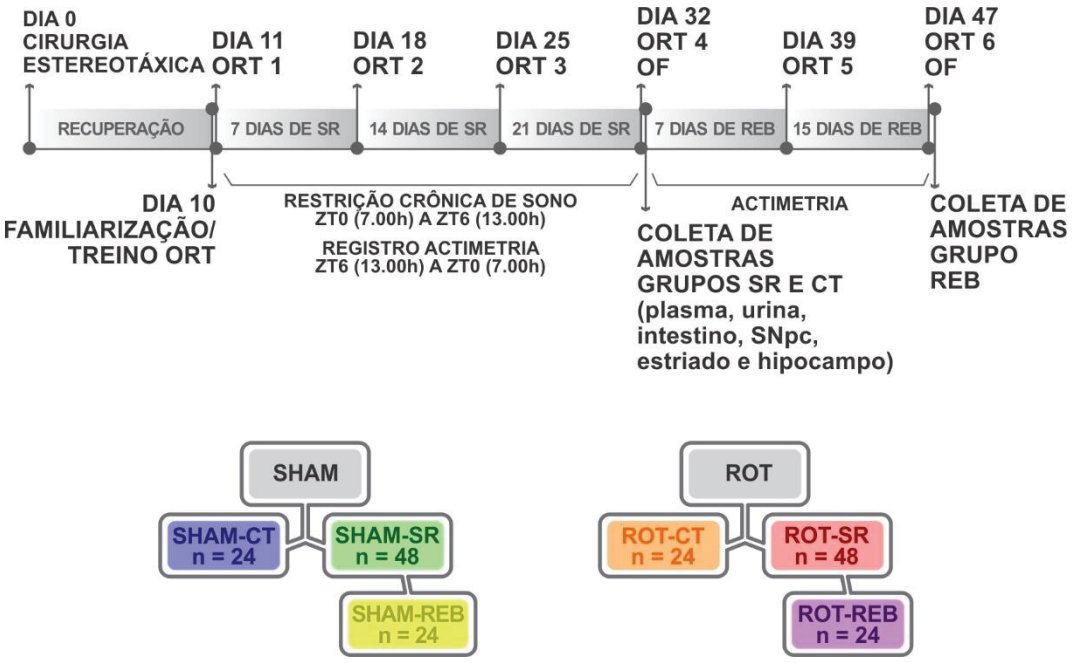

Figura 11. Desenho experimental fora de escala e distribuição dos animais nos grupos. ORT – Teste de Reconhecimento de Objetos, OF – Teste do Campo Aberto, ZT – Hora Zeitgeber (início do estímulo sincronizador - luz). SHAM – veículo; ROT – lesão com rotenona; CT – Controle; SR – Restrição Crônica de Sono; REB – Rebote.

3.3 CIRURGIA ESTEREOTÁXICA

Os animais foram sedados injetados com xilasina (10 mg/kg, i.p.; Syntec do Brasil Ltda, Brazil) e anestesiados com quetamina (90 mg/kg, i.p.; Syntec do Brasil Ltda, Brazil). Para a infusão bilateral de rotenona na SNpc as coordenadas, a partir do bregma, são: (AP) = - 5,0 mm, (ML) = ± 2,1 mm e (DV) = - 8,0 mm (Paxinos and Watson, 2005). Agulhas foram guiadas até a região de interesse e foi feita a infusão bilateral de 1 µL da neurotoxina (12 µg/µl; Sigma-Aldrich®, St. Louis, MO, United States) utilizando micro seringa de 10 µL (Hamilton Apparatus) com auxílio de uma bomba de infusão eletrônica (Insight Instruments, Ribeirão Preto, Brasil), a uma taxa de 0,33 µL/min, durante 3 minutos. Os animais do grupo SHAM foram injetados apenas com veículo (DMSO – dimetilsulfóxido, Sigma-Aldrich®, St. Louis, MO, United States), nas mesmas condições. Após as cirurgias, os animais ficaram acomodados nas caixas de manutenção durante um período de 10 dias para recuperação antes dos testes.

3.4 PRIVAÇÃO CRÔNICA DE SONO

Foi realizada através do método *gentle handling/stimulation*, que consiste em manter os animais acordados através de leve intervenção em suas caixas de contenção (pequenas batidas ou sacudir a caixa gentilmente) e, se não fosse suficiente para manter os animais acordados, as grades da caixa de contenção eram retiradas ou então o ninho de sono era perturbado. Durante 21 dias os animais foram submetidos a 6 horas diárias de restrição, iniciando às 7 horas (início da fase clara) até as 13 horas, sendo esse o período em que o animal dorme durante mais tempo (van der Borght et al, 2006). Os animais do grupo controle foram mantidos em suas caixas de contenção no mesmo ambiente sem serem perturbados. Após o período de restrição de sono, os animais permaneceram no aparato de actimetria.

3.5 TESTE DO CAMPO ABERTO

O campo aberto consiste em uma arena circular de metal com 1 metro de diâmetro e 50 cm de altura. O teste se inicia quando os animais são colocados sobre o círculo central, para que seus comportamentos motores sejam avaliados por um período pré-determinado de 5 minutos. Todas as análises foram registradas e realizadas por meio de câmera digital acoplada ao sistema Smart Junior (Panlab, - Harvard Apparatus Espanha) (Noseda et al, 2014).

3.6 TESTE DE RECONHECIMENTO DE OBJETOS

O aparato execução reconhecimento de objetos consiste em um campo aberto retangular (80cm (comprimento) x 80cm (largura) x 50cm (altura)), feito de madeira e com o fundo coberto com um filme plástico opaco preto, em ambiente com iluminação fraca. Os objetos-estímulo utilizados a serem reconhecidos na tarefa foram todos previamente cobertos por uma camada de verniz não tóxico, e de tamanho suficiente que impedisse de serem movidos na arena pelos animais. Os objetos são biologicamente neutros, ou seja, não

possuem significância comportamental para os animais experimentais, de maneira que nunca foram associados a um reforço (Ennaceur and Delacour 1988). A cada passagem de animal, a arena, assim como os objetos estímulo, foram desinfetados com uma solução de etanol a 70% para garantir a ausência de pistas olfativas. A exploração foi definida como cheirar ou tocar os objetos com o focinho ou as patas dianteiras; sentar no objeto ou permanecer ao redor dele não foi considerado comportamentos exploratórios.

O teste consiste em 2 fases: uma de aquisição e uma de escolha. Na fase de aquisição (treino), o animal foi exposto 4 vezes durante 3 minutos, com um intervalo de 15 minutos entre cada exposição, a 2 objetos idênticos, posicionados a 10 cm das paredes lateral e de trás da arena. Os animais foram colocados na arena virados de costas para os objetos em todas as sessões. Vinte e quatro horas após o treino, o primeiro teste de escolha foi realizado, onde um dos objetos familiares foi substituído por outro objeto novo para o animal. O teste se repetiu a cada sete dias durante o período de experimentação, onde o objeto novo foi novamente substituído por outro objeto não-familiar ao animal, totalizando quatro testes para os animais que passaram apenas pela restrição de sono (ORT 2: 7 dias após ORT 1; ORT 3: 14 dias após ORT 1; ORT 4: 21 dias após ORT 1) e seis para os animais que permaneceram no rebote após o término do período de restrição (ORT 5: 28 dias após ORT 1; ORT 6: 36 dias após ORT 1). A localização (lado direito ou esquerdo da arena) dos objetos familiar e não-familiar foram contrabalanceados a cada animal e a cada experimento. Todos os testes, para um mesmo grupo, foram executados pelo mesmo experimentador para evitar viés de operação. A atividade dos animais na exploração foi filmada e posteriormente avaliada por observação manual por um único experimentador que não teve conhecimento do grupo (ROT ou SHAM) ou tratamento (CT ou SD) dos animais. O resultados foram calculados utilizando a diferença de tempo explorando o objeto familiar (a') e o não-familiar (b) (Δ = b-a') (Ennaceur and Delacour, 1988).

3.7 ACTIMETRIA

A atividade motora dos animais foi mensurada por actimetria em suas caixas de contenção diariamente após a restrição de sono e durante todo o período rebote. O actímetro, manufaturado no próprio laboratório, consiste em um sensor de movimento

infravermelho, conectada a um computador que registra as interrupções em seu feixe de luz. O programa registra a quantidade de atividade em segundos em intervalos de 5 minutos. Os dados brutos foram primariamente processados com o software CTools 8.0 (desenvolvido pelos colaboradores na Universidade de Surrey).

3.8 COLETA DE AMOSTRAS

3.8.1 Imunohistoquímica, urina e intestino

Para obtenção das amostras de cérebro fixadas para imuno-histoquímica (n = 30, 5 por grupo), os animais foram anestesiados com quetamina. Em seguida, o abdômen cada animal foi exposto cirurgicamente para retirada de urina (n = 60, 10 por grupo). direto da bexiga por punção e obtenção de uma porção inferior do intestino com conteúdo fecal (n = 60, 10 por grupo). Os animais foram então perfundidos transcardialmente com solução salina (120 mL/6 min), seguida de solução fixadora de formaldeído a 4% em tampão fosfato 0,1 M (pH 7,4) (120 mL/6 min). Em seguida, os cérebros foram removidos dos crânios e imersos em solução fixadora a 4ºC. Quarenta e oito horas depois, o material foi imerso em solução de sacarose a 30% por três dias e, finalmente, armazenados em freezer -80ºC para posterior análise. As amostras de urina e intestino foram também armazenadas freezer -80 ºC até serem transportadas em gelo seco para o Reino Unido (Imperial College) para análise metabolômica por ou NMR.

3.8.2 Plasma, SNpc, estriado e hipocampo

As amostras de plasma (n = 60, 10 por grupo).) foram coletadas imediatamente após a decapitação através de sangria em tubos de heparina de lítio, que foram invertidos suavemente de 5 a 8 vezes após obtenção do volume desejado (10 mL). As amostras foram prontamente centrifugadas a 3200 rpm (1620 g) por 10 minutos a 4° C e divididas em alíquotas de 1 mL e 25 µl. Concomitantemente, os cérebros foram removidos dos crânios e as estruturas de interesse (SNpc (n = 32, 8 por grupo), estriado (n = 32, 8 por grupo) e

hipocampo (n = 32, 8 por grupo)) rapidamente dissecadas. As estruturas encefálicas e as alíquotas de plasma foram então armazenadas freezer -80 ºC até serem transportadas em gelo seco para o Reino Unido (Universidade de Surrey/Imperial College) para análise metabolômica por LC/MS ou NMR.

3.9 TH-IMUNO-HISTOQUÍMICA

Para quantificação dos neurônios imunorreativos a TH, os cortes foram obtidos dos cérebros fixados após a perfusão. Nove seções de 40 µm correspondentes à SNpc (- 4,92 mm e - 5,28 mm) foram coletadas de 5 animais de cada grupo (coordenadas obtidas de (Paxinos e Watson, 2005). Três fatias foram escolhidas aleatoriamente de cada animal e incubadas com anticorpo primário (camundongo) para TH primário (1: 500; Chemicon, Rolling Meadows, IL, EUA). O anticorpo secundário conjugado à biotina (1: 200 anti-camundongo; Vector Laboratories, Burlingame, CA, EUA) foi localizado usando o sistema ABC (Vectastain ABC Kit Elite, Vector Laboratories, Burlingame, CA, EUA), seguido da reação de 3,30-diaminobenzidina com níquel para intensificação. A determinação da densidade neuronal foi realizada com o programa Image J (National Institutes of Health, Rockville, MD, EUA). Para cada grupo, calculou-se um valor médio e converteu-se em uma porcentagem em relação ao grupo controle e para fins de comparação. As imagens foram obtidas utilizando um microscópio motorizado Axio Imager Z2 (Carl Zeiss, Jena, Alemanha), equipado com um escaneamento automático VSlide (Me tasystems, Altlussheim, Alemanha).

3.10 ANÁLISE METABOLÔMICA

3.10.1 Direcionada (LC / MS)

As amostras de plasma foram medidas usando o kit de metabolômica direcionada AbsoluteIDQ® p180 (Biocrates Life Sciences AG, Innsbruck, Áustria) e um espectrômetro de massa Waters Xevo TQ-S acoplado a um sistema UPLC Acquity (Waters Corporation, Milford, MA, EUA) semelhante ao nossos estudos anteriores (Davies et al., 2014, Isherwood et al.,

2017, Skene et al., 2017). As amostras de plasma (10 µL) foram preparadas de acordo com as instruções do fabricante, adicionando vários padrões estáveis marcados com isótopos às amostras antes das etapas de derivação e extração. Utilizando LC/MS ou análise de injeção de fluxo (FIA) /MS, até 183 metabólitos de 5 classes de compostos diferentes (acilcarnitinas, aminoácidos, aminas biogênicas, glicerofosfolípides e esfingolípidos) podem ser quantificados. Todas as amostras de plasma e 3 níveis de controle de qualidade (QC) foram processados em uma única placa de 96 poços, com ordem de processamento randomizada. Os níveis de metabólitos presentes em cada CQ foram comparados com os valores esperados e o coeficiente de variação percentual (CV%) calculado. Metabólitos em que concentrações (> 25%) estavam abaixo do limite de detecção (<LOD), ou abaixo do limite inferior de quantificação (≪LLOQ), ou acima do limite de quantificação (> LOQ), ou amostra em branco fora da faixa, ou o coeficiente de variação QC2 > 30 %, foram excluídos (n = 50) (Isherwood et al., 2017, Skene et al., 2017). Os 133 metabólitos quantificados restantes compreendiam 10 acilcarnitinas, 21 aminoácidos, 12 aminas biogênicas, 76 glicerofosfolípides e 14 esfingolípidos.

3.10.2 Não-direcionada (^{1}H NMR)

3.10.2.1 Preparo das amostras

Plasma

As amostras de plasma foram preparadas como descrito por Beckonert et al. (2007). Foram obtido espectros bidimensionais (2D) a partir de amostras agrupadas para cada tipo de amostra para garantir a captura abrangente de metabólitos. Uma alíquota de 300 µL de plasma foi reunida de cada rato com a adição de 300 µL de tampão (NaHPO4 0,142 M, NaN3 2 mM, TSP a 0,08%) e 550 µL do volume resultante foram adicionados ao tubo de NMR de 5 mm. A espectroscopia de ^{1}H RMN foi realizada a 300 K (26,85ºC) em um espectrômetro Bruker 600 MHz (Bruker Biospin, Karlsruhe, Alemanha) usando a seguinte sequência de pulso unidimensional padrão com saturação da ressonância da água: atraso de relaxamento (RD)-90°-t1-90°-tm-90°- aquisição decaimento de indução livre (FID), em que 90° representa o pulso de radiofrequência aplicado a 90 ° (rf), t1 é um atraso de interpulsão definido para

um intervalo fixo de 3 ms, RD foi 2 s e tm (tempo de mistura) foram de 100 ms. A supressão da água foi alcançada por irradiação do sinal de água durante RD e tm (Escalona et al., 2015, Swann et al., 2017).

Urina

Antes da preparação, as amostras foram descongeladas à temperatura ambiente. Em seguida, 540 µL da amostra foram misturados com 60 µL de tampão fosfato ^{1}H NMR (pH 7,4 em D2O) contendo 1 mM de padrão interno, 3- (trimetilsilil) - [2,2,3,3, -2H4] -propiônico ácido (TSP) como referência de mudança química. As amostras foram agitadas em vórtex e as partículas foram removidas por centrifugação (16.000 g por 10 min) antes de transferir 550 µL para um tubo de NMR de ^{1}H de 5 mm.

Conteúdo intestinal

As amostras foram descongeladas completamente em temperatura ambiente e o conteúdo intestinal foi separado da parede intestinal. Pesaram-se 50 mg de fezes e adicionou-se 1 mL de água para HPLC. As amostras foram homogeneizadas com um batedor de contas por 40s a 6.500 rpm, depois centrifugadas por 20 minutos a 13.000 g e 400 µL de sobrenadante (água fecal) foram combinados com 200 µL de tampão fosfato ^{1}H NMR (pH 7,4 em D2O) contendo 1 mM de padrão interno (TSP). A água fecal foi agitada no vórtex e centrifugada a 16.000 g por 10 min, antes de 550 µL do sobrenadante ser transferido para um tubo de NMR de ^{1}H de diâmetro externo de 5 mm.

SNpc, estriado e hipocampo

Os metabólitos aquosos foram extraídos das amostras usando um lisador de tecidos, onde tecido cerebral foi homogeneizado em 300 µL de clorofórmio: metanol (2: 1 v / v). O homogenato foi combinado com 300 µL de água, agitadas com vortéx e centrifugado a 13.000 g por 10 min. A fase aquosa superior foi separada da fase orgânica inferior e a água: metanol foi removida usando um concentrador de vácuo (SpeedVac). A fase aquosa foi reconstituída em 550 µL de tampão fosfato (pH 7,4 em D2O) contendo 1 mM de TSP. Os extratos aquosos foram agitados no vórtex e centrifugados a 16.000 g por 10 min, antes que 550µL do sobrenadante fossem transferidos para um tubo de RMN de ^{1}H de diâmetro externo de 5 mm.

3.10.2.2 Aquisição e Pré-processamento - espectroscopia de NMR de ^{1}H

Os espectros de NMR de ^{1}H dos extratos de urina e tecido cerebral foram adquiridos a 300 K em um espectrômetro Bruker 600 MHz (Bruker Biospin, Karlsruhe, Alemanha) e os espectros de água fecal foram obtidos em um espectrômetro Bruker 600 MHz AVANCE III HD de sonda BBI de 600 MHz (Rheinstetten, Alemanha), usando a seguinte sequência de pulso unidimensional padrão com supressão de pico de água usando uma sequência de pulso padrão: atraso de relaxamento (RD) -90◦-t-90◦-tm − 90◦-aquisição decaimento de indução livre (FID), em que 90◦ representa o pulso de radiofrequência de 90◦ aplicado, r é um atraso de interpulsão definido para um intervalo fixo, RD foi de 2 s e tm (tempo de mistura) foi de 100 ms. Para cada amostra, oito exames fictícios foram seguidos por 128 exames e coletados em pontos de dados de 64 K usando uma largura espectral de 12 partes por milhão (ppm) para urina e tecido cerebral e 16 ppm para água fecal. Antes da análise dos dados, os espectros foram corrigidos manualmente para distorções de fase e de linha de base, se necessário, usando o TSP padrão de referência.

Os espectros de 1H RMN (δ 0 · 2–10 · 0) foram digitalizados em regiões espectrais integradas consecutivas de igual largura usando MATLAB (versão R2018b, The Mathworks, Inc.; Natwick, MA) usando um script interno (https: / /csmsoftware.github.io/docs/impacts/ index.html). Os espectros brutos foram referenciados ao singuleto TSP em δ 0,0 usando TOPSPIN (versão 3.1, Bruker BioSpin). As regiões contendo sinais de ureia (δ 5,5-6,0), água residual (δ 4,7-5,5) e TSP (δ -0,2-0,2) foram removidas para minimizar os efeitos da linha de base. Os espectros foram então alinhados manualmente para ajustar a variação no desvio químico e a normalização do quociente probabilístico foi aplicada aos espectros para controlar a variabilidade entre amostras e desvios de resposta do instrumento (DIETERLE; ROSS; SCHLOTTERBECK; SENN, 2006).

3.11 ESTATÍSTICA

Os animais foram divididos aleatoriamente em grupos experimentais sem estratégia específica de randomização. Os critérios para o cálculo do tamanho da amostra foram

estabelecidos a partir da fórmula que estabelece o tamanho da amostra para uma população finita: $n= [N. \sigma^2. (Z_{\alpha/2})^2]/[(N-1).E^2+\sigma^2. (Z_{\alpha/2})^2]$, onde n = número de indivíduos; $Z\alpha/2$ = valor crítico que corresponde ao intervalo de confiança desejado; E = o erro máximo da estimativa; N = tamanho da população; σ = desvio padrão da população. Assim, a seguinte equação foi usada para este estudo: N = 10. 52. (1,96) 2 / (10-1) .052 + 52. (1,96) 2 = 9,99 ± 10 (número da amostra por grupo / parâmetro). Consequentemente, foi estipulado que cada grupo deveria incluir um número amostral de 10 ratos para cada análise.

Para cada experimento comportamental, o teste estatístico correspondente é indicado na legenda da figura. O número de amostras para cada grupo também é sempre mostrado na legenda da figura. A análise estatística dos dados comportamentais foi realizada utilizando o GraphPad Prism Versão 6.0 (GraphPad Software, La Jolla, CA, EUA) e Statistica Versão 12 (StatSoft Inc, Tulsa, OK, EUA). Os valores foram apresentados como média ± EPM. A homogeneidade da variância foi avaliada pelo teste de Bartlett e a distribuição normal dos dados foi avaliada pelo teste de Kolmogorov-Smirnov. A significância estatística para os resultados comportamentais foi estabelecida em $P < 0,05$. A inclusão dos dados foi determinada pelo método ROUT de identificação de valores discrepantes (Q = 10%) para o Open Field Test e pelo Box Plot Diagram para identificar valores discrepantes da Tarefa de Reconhecimento de Objetos, onde um discrepante era aquele com um valor mais de 1,5 vezes o intervalo interquartil acima do terceiro quartil ou abaixo do primeiro quartil (animais com 3 ou mais valores excluídos dos testes ORT, problemas extremos ou de aquisição de dados tiveram todos os valores excluídos).

3.11.1 Modelagem Quimiométrica e Análise Estatística

3.11.1.1 Análise direcionada (LC/MS)

A análise multivariada foi realizada por análise de componentes principais (PCA) e análise discriminante dos mínimos quadrados ortogonais parciais (OPLS-DA), utilizando o software SIMCA-P v12.0 (Umetrics, Umeå, Suécia) com configurações padrão. O algoritmo PCA transforma os dados em um número menor de componentes para que a principal variação nos dados possa ser visualizada em uma figura com um número menor de

dimensões. Enquanto o PCA analisa a variação geral (não supervisionada), o OPLS-DA distingue entre variação preditiva de classe (discriminante) (supervisionada) e variação não preditiva (ortogonal). O uso combinado desses métodos permite a compreensão da extensão e dos padrões subjacentes da variação preditiva de classe no conjunto de dados como um todo. As diferenças nos níveis individuais de metabólitos foram analisadas na versão R 3.1.2 (R Foundation for Statistical Computing, Viena, Áustria) usando os modelos lineares e os métodos ANOVA no pacote de estatísticas. Modelos lineares foram ajustados ao tratamento e procedimento. Diferenças significativas para todos os parâmetros e sua interação foram determinadas usando ANOVA multivariada. Os valores de p foram corrigidos para comparações múltiplas de acordo com a taxa de falsas descobertas de Benjamini-Hochberg (FDR). Os metabólitos foram considerados significativos com um ponto de corte de FDR <0,05. Para testar a significância estatística, os valores ausentes (15) não foram levados em consideração. Para visualização dos dados, utilizamos um mapa de calor combinado ao agrupamento hierárquico (distância euclidiana e ligação de Ward). Modelos de previsão baseados em combinações de metabólitos foram feitos por modelagem logística no software estatístico R. Primeiro, foram selecionados metabólitos que atendiam aos seguintes critérios: diferença significativa (FDR <0,05) entre o controle e o grupo de interesse no modelo ANOVA; uma área (não validada cruzada) sob a curva (AUC) que foi significativamente maior do que para valores permutados aleatoriamente (p <0,05, determinado por 10.000 permutações); e uma diferença na concentração plasmática de mais de 5% entre os grupos. Para os marcadores que atenderam a esses critérios, foram feitos modelos logísticos usando valores transformados em log. Os valores ausentes foram imputados como o valor médio em todas as amostras para esse metabólito. O desempenho preditivo dos modelos foi testado através da determinação da AUC usando validação cruzada de sobreaquecimento (LOOCV), na qual um modelo foi treinado usando dados de todos menos um e testado no rato restante. Usando essa abordagem, os modelos foram desenvolvidos testando passo a passo o resultado da adição de outro metabólito ao modelo atual e selecionando o metabólito com o maior ganho em AUC a ser incluído no modelo para a próxima etapa. Isso foi repetido até que nenhuma melhoria adicional na AUC pudesse ser alcançada. Para os modelos obtidos, as previsões foram mostradas pela visualização ROC (Receiver Operating Characteristic). Finalmente, para determinar a sensibilidade e a especificidade dos modelos de RS, as amostras com uma probabilidade prevista de mais de

50% foram consideradas como SR, enquanto as amostras com uma probabilidade prevista de menos de 50% foram consideradas como não-SR.

3.11.1.1 Análise não-direcionada (NMR)

Os dados foram importados para o SIMCA-P 16.0.1 (Umetrics, Umea, Suécia), centralizados em média e em escala de Pareto. Estatísticas multivariadas não supervisionadas e, mais especificamente, Análise de Componentes Principais (PCA) foram realizadas para identificar fontes de variação nos dados metabólicos, a fim de garantir que a variabilidade observada tenha origem biológica e não analítica / técnica (lote, peso da amostra) e criar um visão geral e mostrando tendências, agrupamentos e discrepâncias nos dados. Qualquer discrepância excepcional foi removida, se necessário (efeitos de diluição, contaminantes, etc.).

Após a remoção de valores extremos, foram aplicadas estatísticas multivariadas supervisionadas e Análise Ortogonal de Mínimos Quadrados Parciais (OPLS-DA), em particular, com análise de validação cruzada de 7 vezes (padrão), a fim de identificar variáveis de separação de classes e encontrar diferenças entre pares entre grupos. Os parâmetros Q2 (variação prevista; “qualidade da previsibilidade”) e R2 (variação explicada; “qualidade do ajuste”) foram utilizados para avaliar os modelos, seguidos pelo teste de permutação de 100 para validação e pCV-ANOVA para significância. Os resultados foram visualizados usando as pontuações do OPLS-DA produzidas no SIMCA e as plotagens de carregamento por um script desenvolvido internamente no MATLAB (https://csmsoftware.github.io/docs/impacts/index.html).

As atribuições correspondentes das regiões de deslocamento químico foram baseadas no Human Metabolome Database (HMDB, http://www.hmdb.ca), uma lista interna de atribuições de deslocamentos químicos e o software Chenomx Profiler - Chenomx NMR Suite 8.4 (Chenomx Inc. , Edmonton, Canadá) e confirmado por Espectroscopia Estatística de Correlação Total (STOCSY) em MATLAB (HOLMES; CLOAREC; NICHOLSON, 2006).

- CHAPTER 1 -

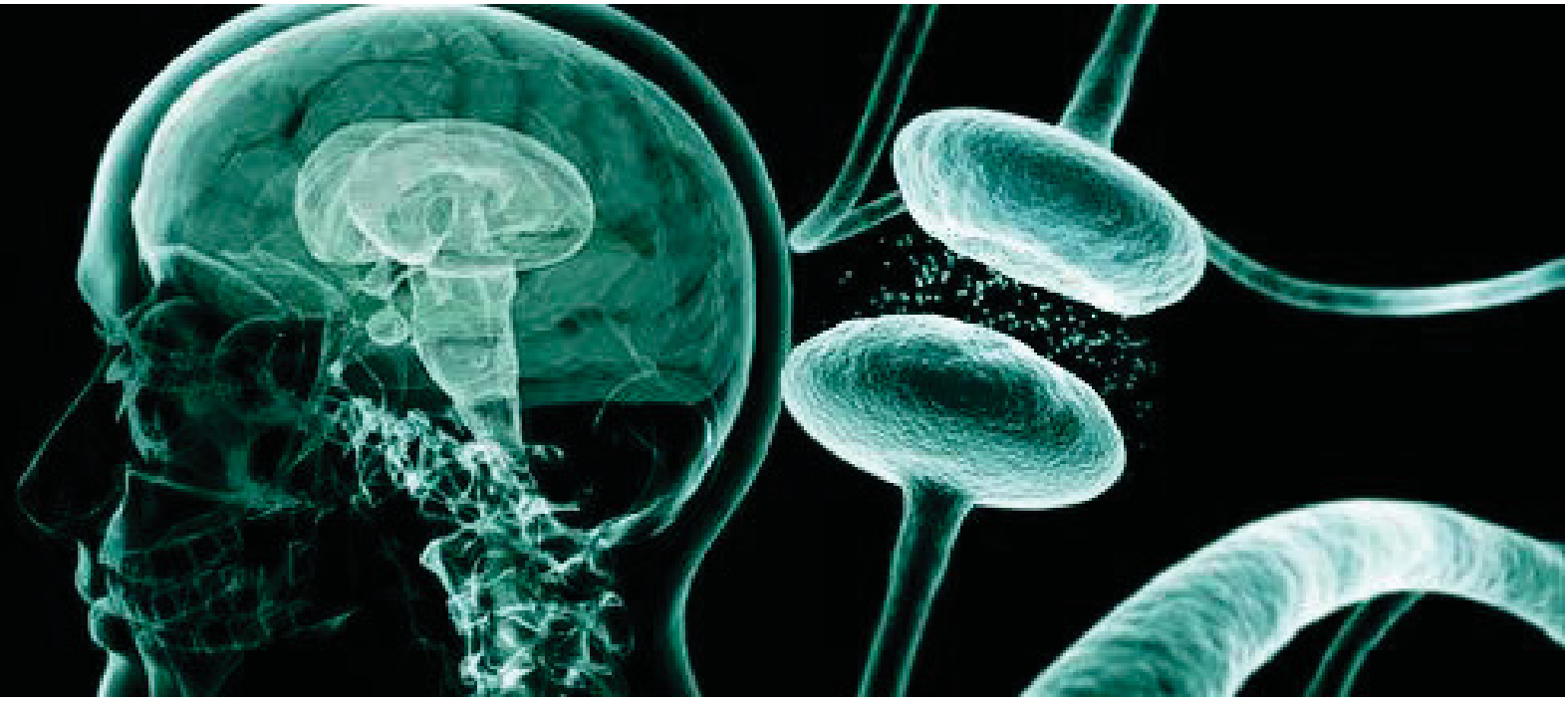

Behavioural analysis and Plasma metabolomics

Article published in Scientific Reports, February 2019.

Available at:

https://www.nature.com/articles/s41598-018-37657-6

www.nature.com/scientificreports

OPEN

Chronic sleep restriction in the rotenone Parkinson's disease model in rats reveals peripheral early-phase biomarkers

Received: 12 July 2018
Accepted: 6 December 2018
Published online: 13 February 2019

Juliane Fagotti[1], Adriano D. S. Targa[1], Lais S. Rodrigues[1], Ana Carolina D. Noseda[1], Flávia W. C. Dorieux[1], Franciele F. Scarante[1], Jessica L. Ilkiw[1], Fernando M. Louzada[1], Namrata R. Chowdhury[2], Daan R. van der Veen[2], Benita Middleton[2], Jeroen L. A. Pennings[3], Jonathan R. Swann[4], Debra J. Skene[2] & Marcelo M. S. Lima[1]

Parkinson's disease (PD) is a chronic disorder that presents a range of premotor signs, such as sleep disturbances and cognitive decline, which are key non-motor features of the disease. Increasing evidence of a possible association between sleep disruption and the neurodegenerative process suggests that sleep impairment could produce a detectable metabolic signature on the disease. In order to integrate neurocognitive and metabolic parameters, we performed untargeted and targeted metabolic profiling of the rotenone PD model in a chronic sleep restriction (SR) (6 h/day for 21 days) condition. We found that SR combined with PD altered several behavioural (reversal of locomotor activity impairment; cognitive impairment; delay of rest-activity rhythm) and metabolic parameters (branched-chain amino acids, tryptophan pathway, phenylalanine, and lipoproteins, pointing to mitochondrial impairment). If combined, our results bring a plethora of parameters that represents reliable early-phase PD biomarkers which can easily be measured and could be translated to human studies.

Parkinson's disease (PD) is a chronic neurodegenerative disease that typically affects dopaminergic neurons in the substantia nigra pars compacta (SNpc). However, other regions such as brainstem nuclei, cortical areas, spinal cord, preganglionic sympathetic/parasympathetic neurons, as well as portions of the peripheral and enteric nervous systems are involved in the pathophysiology[1–4]. Before occurrence of the prominent motor signs, PD presents a range of non-motor symptoms (NMS) that precede the clinical motor phase by many years. Some are well-known, such as olfactory and gastrointestinal dysfunction, sleep disorders, circadian changes and cognitive impairment[3,5–7]. Moreover, neuropathological studies support the association of these early-phase disturbances based on the identification of Lewy bodies in non-dopaminergic nuclei in early Braak stages, prior to significant SNpc degeneration and motor signs[2]. Recent epidemiological studies propose that NMS can appear up to 25 years before the onset of clinical PD[6], and it is well-established that patients report sleep disruption at least a decade before the first motor symptoms[8]. In animal models, the SNpc was shown to regulate sleep patterns[9] and recently it was found that sleep-wake disturbance can predispose the brain to PD neuropathology[10]. Undoubtedly, sleep disorders represent an essential part of PD progression, once brain structures affected in the first stages of the disease[11] and correspondent neurotransmitter systems are involved in sleep regulation[12], but they are poorly investigated in the diagnosis.

Reduced total sleep time, sleep efficiency and sleep fragmentation, all leading to sleep loss, consistently emerge as sleep issues in PD[13,14], but it is unclear if sleep loss constitutes a risk-factor for PD due to the lack of more specific prospective studies[15]. In general, these sleep alterations are one of the premotor features that most affect the patients' quality of life, and could contribute to worsening cognitive abilities, such as memory impairment[16,17],

[1]Department of Physiology, Federal University of Paraná, Curitiba, PR, Brazil. [2]Chronobiology, Faculty of Health and Medical Sciences, University of Surrey, Guildford, UK. [3]RIVM - National Institute for Public Health and the Environment, Bilthoven, The Netherlands. [4]Division of Computational and Systems Medicine, Department of Surgery and Cancer, Faculty of Medicine, Imperial College London, South Kensington, London, UK. Correspondence and requests for materials should be addressed to M.M.S.L. (email: mmslima@ufpr.br)

apart from having a direct association with the motor impairment[18]. In this context, PD-related sleep disturbances[5] and society-imposed sleep restrictions[19] may contribute to cognitive decline, and even emerge as an early biomarker of abnormal aging[20], perhaps producing detectable changes in peripheral tissues in addition to behavioural parameters, like memory deficits and circadian shifts. Despite much effort, there is as yet no reliable way to identify those individuals that will develop PD. Failure to establish the pathological process is the main obstacle to find a cure or treatment that alters the course of the disease, but our inability to diagnose it early enough hinders a better approach or improvement of the existing treatments. Therefore, the identification of risk factors and detection of early symptoms are a priority, since no approach to date has identified specific or sensitive signs that have a practical application in diagnosis[21,22]. Metabolic phenotyping (metabonomics/metabolomics) using high resolution analytical chemistry platforms coupled with multivariate statistics provides great potential for identifying reliable biomarkers of PD. The elucidation of such biochemical signatures could represent a major step towards early diagnosis, disease progression, and effective treatments[23,24].

Here we investigated, in the rotenone (ROT) animal model of PD, chronic sleep restriction (SR) as a possible triggering factor for peripheral metabolic changes, cognitive impairment and circadian alterations. Rotenone, a mitochondrial complex I activity inhibitor pesticide, mimics the hallmark traits of early-phase PD (equivalent to Braak stages 2–3) extending to NMS such as excessive daytime sleepiness, REM sleep behaviour disorder, insomnia and deterioration of spontaneous sleep, dopamine-dependent behavioural deficits, hyposmia and gastrointestinal problems, as well as canonical pathological alterations, such as time-dependent reduction of dopaminergic nigrostriatal neurons, α-synuclein (PARK1) aggregation, Lewy-like body formation, oxidative stress and ultrastructural impairments in the SNpc mitochondria[5,25–35]. To identify the biochemical perturbations associated with SR in this model, two metabolic profiling platforms were applied to characterize the plasma metabolic signatures: global ^{1}H nuclear magnetic resonance (NMR) spectroscopy and targeted liquid chromatography/mass spectrometry (LC/MS).

Methods

Ethics Approval. All animal procedures were approved by the Ethics Committee of the Federal University of Paraná (approval ID #858) and conducted according to the guidelines of ethics and experimental care and use of laboratory animals (SBCAL). The research protocols were reviewed by The University of Surrey Animal Welfare Ethical Review Body (AWERB) and by the Named Veterinary Surgeon (NVS) prior to any work, in accordance with the principles of UK legislation (Animals [Scientific Procedures] Act 1986).

Experimental design. The experiments were performed on healthy male Wistar rats, 90 days old, weighing 280–330 g, with normal immune status. Experimental animals were not involved in any previous test or drug treatment. The animals were group housed (4 per cage) in polypropylene cages with disposable bedding on a standard light-dark (L/D) cycle (12 h:12 h cycle, lights on at 07.00 h = ZT0) in a temperature controlled room (22 ± 2 °C). Food and water were provided *ad libitum* throughout the experiment.

Figure 1A shows the group distribution flowchart and a timeline diagram of the study design. The animals were randomly distributed in one of the groups: SHAM-CT (vehicle infusion and control for sleep restriction)/SHAM-SR (vehicle infusion and sleep restriction condition)/SHAM-REB (vehicle infusion and sleep restriction condition followed by sleep recovery)/ROT-CT (rotenone infusion and control for sleep restriction)/ROT-SR (rotenone infusion and sleep restriction condition)/ROT-REB (rotenone infusion and sleep restriction condition followed by sleep recovery). Total of 6 groups, n = 24 animals per group, total number of 144 animals. The experimental design was performed in 6 cohorts (6 groups with 4 animals each, total number of 24 animals per cohort).

One week before the experiments began, the animals were maintained in the room described above for habituation. On day 0, the animals underwent stereotaxic surgery. After a 10 day interval for recovery, the animals were trained for the Object Recognition Task (ORT) and the following day the basal test (ORT 1) was performed prior to 21 days of sleep restriction (commencing on day 11). Every week, ORT was repeated on the same weekday (ORT 2 = 7 days of SR; ORT 3 = 14 days of SR) until the end of sleep restriction (day 32 = 21 days of SR). On day 32, another ORT (ORT 4) was carried out, followed by an Open Field Test and then the control (CT) groups (SHAM-CT; ROT-CT) and half of the animals from the SR groups (SHAM-SR, n = 24, and ROT-SR, n = 24) were sacrificed. The other half of the SHAM-SR (n = 24) and ROT-SR (n = 24) groups were allowed sleep recovery for 15 days (Rebound group (REB) – SHAM-REB and ROT-REB) at the end of the sleep restriction period. Throughout the experiment, animals' activity was recorded daily for 21 days by infrared motion sensors after the 6 h of sleep restriction and throughout the rebound period.

Stereotaxic surgery. The animals were initially sedated with intraperitoneal xylazine (10 mg/kg; Syntec do Brasil Ltda, Brazil) and anaesthetized with ketamine (90 mg/kg, i.p.; Syntec do Brasil Ltda, Brazil). For ROT (3 groups, 24 animals per group, total number of 72 animals) or vehicle (dimethylsulfoxide - SHAM) (3 groups, 24 animals per group, total number of 72 animals) infusion within the SNpc, the following coordinates was used, bregma as a reference: (AP) −5.0 mm, (ML) ± 2.1 mm and (DV) −8.0 mm[36]. Rotenone (12 μg/μl; Sigma-Aldrich®, St. Louis, MO, United States) or DMSO (Sigma-Aldrich®, St. Louis, MO, United States) infusions of 1 μL into each hemisphere were made at a rate of 0.33 μL/min for 3 min[32,33,37]. These infusions were made using an electronic infusion pump (Insight Instruments, Ribeirão Preto, SP, Brazil).

Sleep restriction procedure. SR (4 groups, 24 animals per group, total number of 96 animals) was performed using a gentle handling/stimulation protocol, which consisted of soft tapping on the cage, gently shaking the cage or, when this was not sufficient to keep animals awake, gently disturbing the sleeping nest[38]. CT animals (2 groups, 24 animals per group, total number of 48 animals) were left undisturbed.

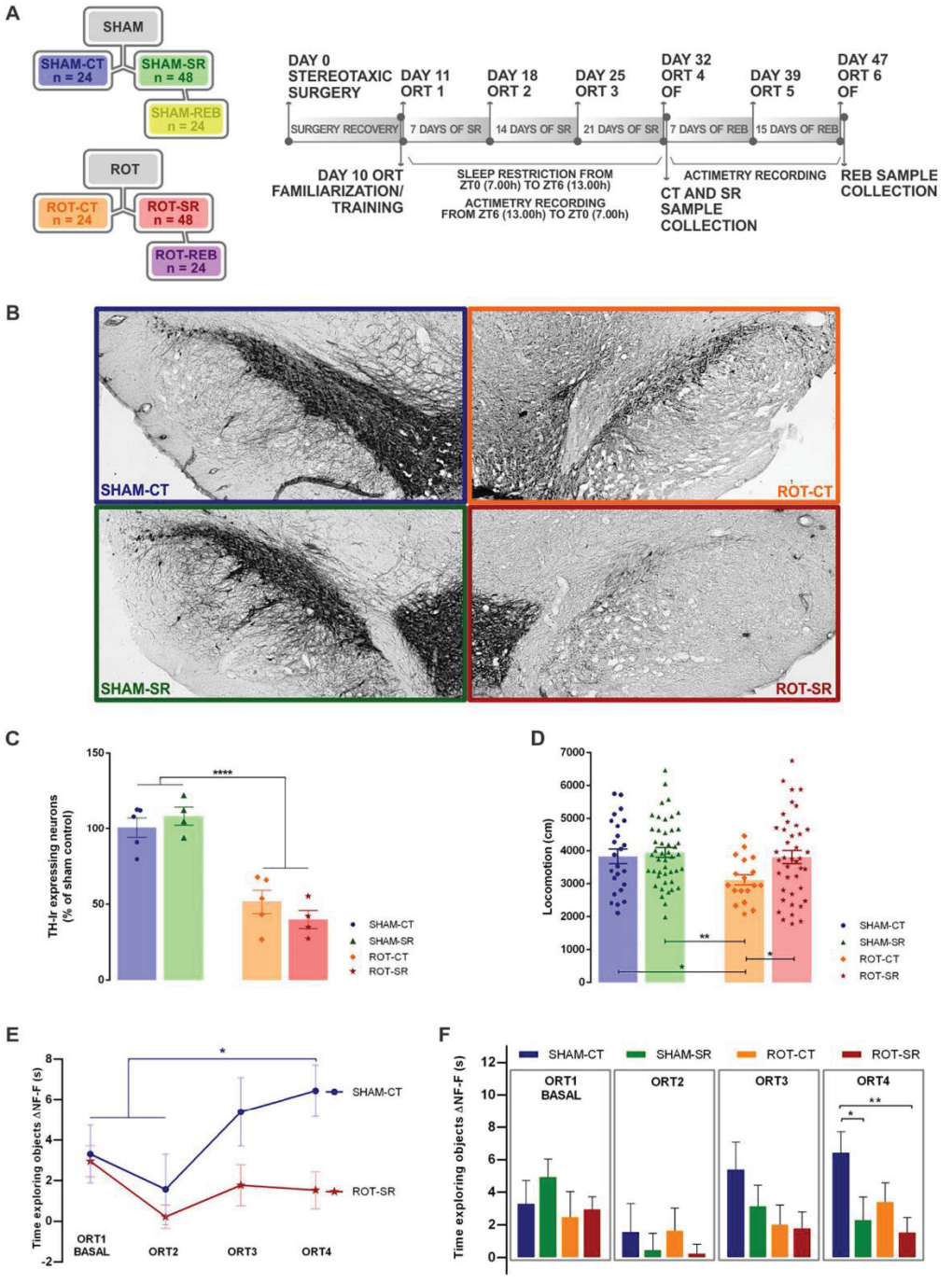

Figure 1. Sleep restriction in the rotenone model of PD. (**A**) Group distribution and timeline diagram. Colours are representative of groups throughout the results. SR = Sleep Restriction; REB = Rebound sleep; SHAM = vehicle; ROT = rotenone; SHAM-CT = sham control for SR (blue); ROT-CT = rotenone control for SR (orange); SHAM-SR = vehicle SR (green); ROT-SR = rotenone SR (red); SHAM-REB = SHAM-SR after 15 days of REB (yellow); ROT-REB = ROT-SR after 15 days of REB (purple); ORT = Object Recognition Task; OF = Open Field. (**B**) Representative immunohistochemistry labelling of TH-ir neurons at the end of SR for SHAM-CT, ROT-CT, SHAM-SR and ROT-SR. (**C**) Percentage of TH-ir expressing neurons in the SNpc in relation to the SHAM-CT group. Individual data are shown as a scatter plot with bar of mean ± standard error of the mean (SEM), n = 4 per group for CT (SHAM-CT and ROT-CT) and n = 5 per group for SR (SHAM-SR and ROT-SR). ****$P \leq 0.0001$ sham compared to rotenone treated (two-way ANOVA followed by Fisher's LSD test). (**D**) Locomotion parameter obtained from the open field test. Individual data (cm) are shown as a scatter plot with bar of mean ± SEM. *$P < 0.05$; **$P \leq 0.01$ (two-way ANOVA followed by Fisher's LSD test). n = 24 SHAM-CT; n = 46 SHAM-SR; n = 20 ROT-CT; n = 41 ROT-SR. (**E**) Exploration index (ΔNF–F). Bars represent

the mean (±SEM) time exploring objects (s). *P < 0.05 (two-way ANOVA followed by Fisher's LSD test). ORT 1 = First test, before SR; ORT 2 = second test (SR = 7 days); ORT 3 = third test (SR = 14 days); ORT 4 = fourth test (SR = 21 days). n = 24 SHAM-CT; n = 24 SHAM-SR; n = 20 ROT-CT; n = 20 ROT-SR. NF = non-familiar object; F = familiar object. (**F**) Learning curve comparing SHAM-CT and ROT-SR during the SR protocol. Time exploring objects (ΔNF–F) values (s) are expressed as mean ± SEM. *P < 0.05; **P ≤ 0.01 (one-way repeated-measures ANOVA followed by Fisher's LSD test). n = 24 SHAM-CT; n = 20 ROT-SR.

Open Field (OF) Test. The OF test apparatus consisted of a circular arena (1 m diameter) limited by a 50 cm high wall. The animals were placed in the centre of the arena and allowed to freely explore the area for 5 min. The animals' distance travelled was recorded by a digital camera coupled to the Smart Junior system (Panlab, Harvard Apparatus Spain, Barcelona, Spain)[39].

Object Recognition Task. The ORT was performed in an open box (80 cm (W) × 80 cm (L) × 50 cm (H)) made of wood and covered with a black, opaque plastic film in dim light conditions. The objects to be discriminated were made of different materials, all of them previously covered with non-toxic varnish, so that the animals could not move them around in the arena. The objects are not known to have any ethological significance for the rats and had never been associated with reinforcement[40]. The first day of the experiment consisted of 4 familiarization/training trials (3 min each, 15–20 min apart), in which two identical objects (familiar objects) were placed in the back corners of the open box, 10 cm away from the sidewall. The rat was placed in the open box facing away from the objects. Twenty-four hours after training, the first test of choice was performed (ORT 1), where one of the familiar objects was replaced by a new object (non-familiar for the animal). The test was repeated every seven days, when the non-familiar object was always replaced and the familiar one remained the same, totalling four tests for the animals that experienced daily sleep restriction only or control (ORT 2: 7 days after ORT 1; ORT 3: 14 days after ORT 1; ORT 4: 21 days after ORT 1) and six ORT tests for the animals that remained in rebound after the end of the sleep restriction period (ORT 5: 28 days after ORT 1; ORT 6: 36 days after ORT 1). The time spent exploring each object was analysed by the same experimenter, blind to animal condition, to avoid operator bias. Exploration was defined as only occurring when the rat touched the object with its nose or the rat's nose was directed towards an object at a distance ≤2 cm. The familiar/non-familiar object locations (left or right side of the arena) were counterbalanced within each experiment, as well as within-subject for subsequent experiments. The arena and objects were cleaned between each trial with 70% ethanol[41]. The results were calculated using the time spent by rats exploring the familiar (a′) and the non-familiar object (b) (Δ = b-a′)[40].

Diurnal activity measurement. Overall activity of all animals in a cage was measured continuously after the sleep restriction and throughout the rebound period. Home cage activity was continuously recorded by passive infrared detectors connected to a computer that registered the motion (in-house apparatus). The device recorded the amount of activity in seconds in 5-minutes bins. Raw data were primarily analysed with the in-house software CTools 8.0.

TH-immunohistochemistry. For TH-immunoreactive (TH-ir) neurons quantification, the animals were anaesthetized with ketamine. Then, each animal was transcardially perfused with a saline solution, followed by a fixative solution of formaldehyde 4% in 0.1 M phosphate buffer (pH 7.4). After that, brains were removed from the skulls and were immersed in the fixative solution at 4 °C. Forty-eight hours later, the material was immersed in a 30% sucrose solution for three days and finally stored in a −80 °C freezer before sectioning. Nine 40 µm sections corresponding to SNpc (−4.92 mm and −5.28 mm/coordinates obtained from Paxinos and Watson[36]) were collected from 5 animals of each group. Three slices were randomly chosen from each animal and incubated with primary mouse anti-TH antibody (1:500; Chemicon, Rolling Meadows, IL, USA). Biotin-conjugated secondary antibody (1:200 anti-mouse; Vector Laboratories, Burlingame, CA, USA), was localized using the ABC system (Vectastain ABC Elite kit, Vector Laboratories, Burlingame, CA, USA), followed by 3,30-diaminobenzidine reaction with nickel enhancement. Neuronal density determination was conducted using the software Image J (National Institutes of Health, Rockville, MD, USA). For each group, a mean value was calculated and converted to a percentage relative to the sham control group and compared with the other groups (data not shown for REB groups, which had no statistical differences to the correspondent SR group). The images were obtained using a motorized Axio Imager Z2 microscope (Carl Zeiss, Jena, Germany), equipped with an automated scanning VSlide (Metasystems, Altlussheim, Germany).

Sample collection for metabolomics. For metabolomics analyses, plasma samples were collected after decapitation. At this stage, brains were also removed from the skulls and structures of interest (SNpc, striatum and hippocampus) were dissected for later analysis. Following this, 10 mL of blood was placed into lithium heparin tubes, which were gently inverted 5–8 times. The samples were centrifuged immediately at 3200 rpm (1620 g) for 10 minutes at 4 °C and split into aliquots (1 mL and 25 µl). The plasma aliquots were placed immediately into a −80 °C freezer. The samples were stored at −80 °C prior to being shipped on dry ice to the UK (University of Surrey/Imperial College) for LC/MS or NMR metabolomics analysis.

Targeted metabolomics analysis (LC/MS). Plasma samples were measured using the AbsoluteIDQ® p180 targeted metabolomics kit (Biocrates Life Sciences AG, Innsbruck, Austria), and a Waters Xevo TQ-S mass spectrometer coupled to an Acquity UPLC system (Waters Corporation, Milford, MA, USA) similar to our previous studies[42–44]. Plasma samples (10 µl) were prepared according to the manufacturer's instructions adding several stable isotope–labelled standards to the samples prior to the derivatization and extraction steps. Using

either LC/MS or flow injection analysis/MS up to 183 metabolites from 5 different compound classes (namely acylcarnitines, amino acids, biogenic amines, glycerophospholipids and sphingolipids) can be quantified. All the plasma samples and 3 levels of quality control (QC) were processed on a single 96-well plate, sample order being randomised. The levels of metabolites present in each QC were compared to the expected values and the percent coefficient of variation (CV%) calculated. Metabolites where >25% concentrations were below the limit of detection (<LOD) or below lower limit of quantification (≪LLOQ) or above limit of quantification (>LOQ) or blank out of range, or the QC2 coefficient of variance was >30%, were excluded (n = 50)[43,44]. The remaining 133 quantified metabolites comprised 10 acylcarnitines, 21 amino acids, 12 biogenic amines, 76 glycerophospholipids and 14 sphingolipids.

^{1}H NMR spectroscopy. Plasma samples were prepared as described by Beckonert, *et al.*[45]. ^{1}H NMR spectroscopy was performed at 310 K on a Bruker 600 MHz spectrometer (Bruker Biospin, Karlsruhe, Germany). For each sample, water-suppressed Carr-Purcell-Meiboom-Gill spin-echo spectra were recorded. In this experiment, eight dummy transients were followed by 64 transients and collected in 64 K data points. NMR spectra were manually corrected for phase and baseline distortions and referenced to the anomeric proton of β-glucose at δ 5.223.

Quantification and Statistical Analysis. Animals were randomly assigned to experimental groups, with no specific randomization strategy. The criteria for calculating the sample size was established from the formula that establishes the sample size for a finite population: $n = [N.\ \sigma^2.\ (Z_{\alpha/2})^2]/[(N\text{-}1).E^2 + \sigma^2.\ (Z_{\alpha/2})^2]$, where n = number of individuals; Zα/2 = critical value that corresponds to the desired confidence interval; E = the maximum error of the estimate; N = population size; σ = population standard deviation. Thus, the following equation was used for this study: $N = 10.\ 52.\ (1.96)\ 2/(10\text{-}1)\ 0.052 + 52.\ (1.96)\ 2 = 9.99 \cong 10$ (sample number per group/parameter). Consequently, it was stipulated that each group should comprise a sample number of 10 rats for each analysis.

For behavioural data, statistical analysis was performed using GraphPad Prism Version 6.0 (GraphPad Software, La Jolla, CA, USA) and Statistica Version 12 (StatSoft Inc, Tulsa, OK, USA). Values were presented as mean ± SEM. Homogeneity of variance was assessed by the Bartlett test and normal distribution of the data was assessed by the Kolmogorov-Smirnov test. Statistical significance for behavioural results was set at $P < 0.05$. Data inclusion was determined by The ROUT method of identifying outliers (Q = 10%) for the Open Field Test and by the Box Plot Diagram to identify outliers for the Object Recognition Task, where an outlier was that with a value more than 1.5 times the interquartile range above the third quartile or below the first quartile (animals with 3 or more values excluded from the ORT tests, outlier or data acquisition issues, had all values excluded).

Statistical analysis of TH-immunohistochemistry, Open Field Test, Object Recognition Test and Rest-activity pattern was performed using two-way ANOVA followed by Fisher's LSD test, using treatment (SHAM/ROT) and procedure (CT/SR/REB) as independent variables. For the learning curve of Object Recognition Test, a one-way repeated-measures ANOVA followed by Fisher's LSD test was performed using the Δ (Δ = b-a′) of each group.

LC/MS metabolomics analysis: multivariate analysis was performed by principal component analysis (PCA) and orthogonalized partial least squares discriminant analysis (OPLS-DA), using SIMCA-P v13.0 software (Umetrics, Umeå, Sweden) and default software settings. Whereas PCA looks at overall variation (unsupervised), OPLS-DA distinguishes between class-predictive (discriminating) variation (supervised) and non-predictive (orthogonal) variation. The use of these methods allows insight into the extent and underlying patterns of class-predictive variation within the data set as a whole. Differences in individual metabolite levels were analysed in R version 3.1.2 (R Foundation for Statistical Computing, Vienna, Austria) using the linear models and ANOVA methods in the stats package. Linear models were fitted to the treatment (SHAM/ROT) and procedure (CT/SR/REB). Significant differences for all parameters and their interaction were determined using multivariate ANOVA. P-values were corrected for multiple comparisons according to the Benjamini-Hochberg False Discovery Rate (FDR). Metabolites were considered as significant at an FDR cutoff < 0.05. For testing statistical significance, missing values (n = 15) were not taken into account. For data visualisation, we used a heat map combined with hierarchical clustering (Euclidean distance and Ward linkage). Prediction models based on combinations of metabolites were made by logistic modelling in R statistical software. First, metabolites were selected that met the following criteria: a significant (FDR < 0.05) difference between the control and group of interest in the ANOVA model; a (non-cross-validated) Area Under the Curve (AUC) that was significantly higher than for randomly permutated values ($P < 0.05$, determined by 10,000 permutations); and a difference in plasma concentration of more than 5% between groups. For the markers that met these criteria, logistic models were made using log-transformed values. The predictive performance of the models was tested by determining the AUC using leave-one-out cross-validation, in which a model was trained using data of all-but-one and tested on the remaining rat. Using this approach, models were developed by stepwise testing the result of adding another metabolite to the current model and selecting the metabolite with the highest gain in AUC to be included in the model for the next step. This was repeated until no further improvement in AUC could be achieved. For the models obtained, predictions were shown by Receiver Operating Characteristic (ROC) visualisation. Finally, for determining sensitivity and specificity of the SR models, samples with a predicted probability of more than 50% were considered predicted as SR, whereas samples with a predicted probability of less than 50% were considered predicted as not-SR.

NMR spectroscopy: Spectra were digitized using an in-house MATLAB (version R2009b, The Mathworks, Inc.; Natick, MA, USA) script. The spectral region containing the water resonance was excised from the spectra. PCA was then performed with Pareto scaling in Matlab[46]. Overview PCA analysis identified 4 outliers in the data set (1 due to high plasma lactate; 3 had high plasma glucose). These samples were removed from subsequent analyses, including OPLS-DA analysis performed using in-house scripts in Matlab.

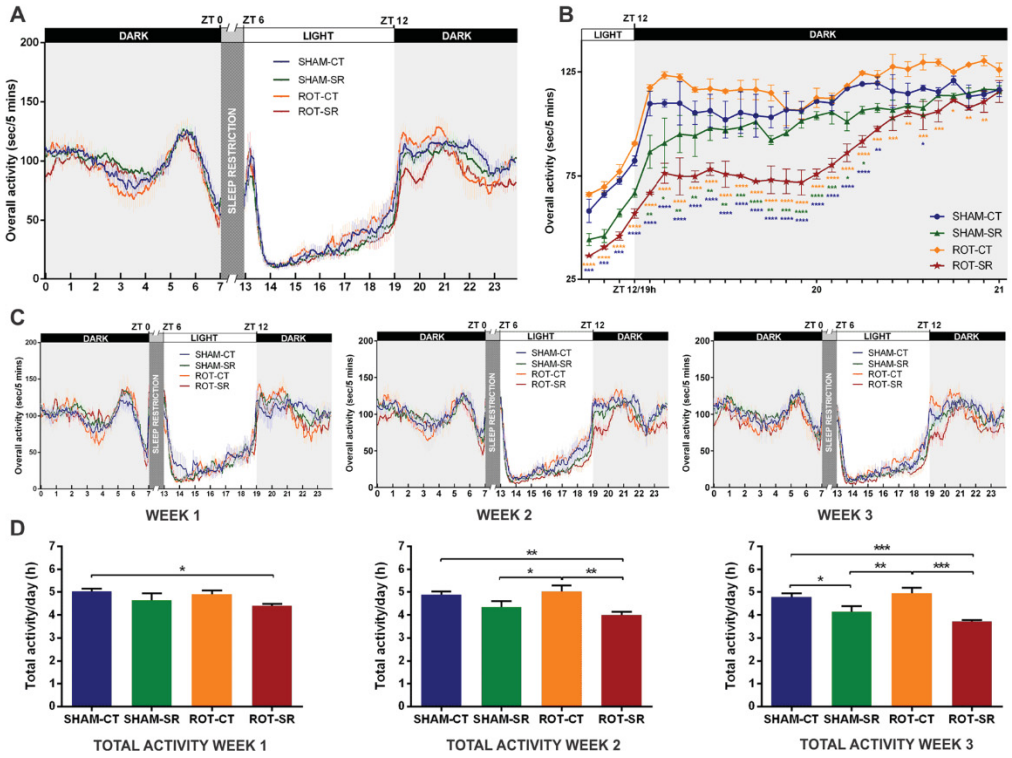

Figure 2. Rest-activity parameters. (**A**) Daily activity pattern of each group (seconds/5 minutes) during the sleep restriction (SR) period. Each line represents the mean activity (±SEM) across the 21 days of SR. ZT0 = lights on and the beginning of gentle handling until ZT6 when recording started. n = 6 per group for CT (SHAM-CT and ROT-CT) and n = 12 per group for SR (SHAM-SR and ROT-SR). (**B**) Activity profile 15 minutes before and 2 hours after the onset of darkness (ZT12) during weeks 2 and 3 after the start of SR. Each line represents the mean activity (seconds/5 minutes) of the 14 days (±SEM). Ticks on x axis represent 5-minutes blocks. *$P < 0.05$; **$P \leq 0.01$; ***$P \leq 0.001$; ****$P \leq 0.0001$ (two-way ANOVA followed by Fisher's LSD test). Orange (*) = ROT-CT compared to ROT-SR; Blue (*) = ROT-SR compared to SHAM-SR; Green (*) = ROT-SR compared to SHAM-SR. n = 6 per group for CT (SHAM-CT and ROT-CT) and n = 12 per group for SR (SHAM-SR and ROT-SR). (**C**) Daily activity pattern each week of the 3 weeks of SR. Each line represents the mean activity (seconds/5 minutes) of 7 days ± SEM. ZT0 - lights on and the beginning of gentle handling until ZT6 when recording started. n = 6 per group for CT (SHAM-CT and ROT-CT) and n = 12 per group for SR (SHAM-SR and ROT-SR). (**D**) Total activity/day (h) in each of the 3 weeks of SR. The bars represent the mean ± SEM. *$P < 0.05$; **$P \leq 0.01$; ***$P \leq 0.001$ (two-way ANOVA followed by Fisher's LSD test). n = 24 SHAM-CT; n = 24 SHAM-SR; n = 20 ROT-CT; n = 20 ROT-SR.

Results

Rotenone lesion combined with Sleep Restriction altered locomotor activity, lead to cognitive impairment and delay of rest-activity rhythm. Characterization of dopaminergic neuronal loss by TH immunohistochemistry in the SNpc (representative photomicrographs Fig. 1B) showed that Rotenone (ROT) (12 µg/µl) infusion (1 µl at 0.33 µl/min) induced a decrease of TH-ir neurons when compared to the sham groups (SHAM-CT vs. ROT-CT = 49% reduction; SHAM-CT vs. ROT-SR = 61% reduction; SHAM-SR vs. ROT-CT = 57% reduction; SHAM-SR vs. ROT-SR = 69% reduction), [$F(1,14) = 74.58$; $P < 0.0001$] (Fig. 1C). SR did not have a significant effect overall. The percentage reduction of TH-ir neurons was maintained after 15 days of sleep recovery (REB) (Fig. S1A).

In order to evaluate the integrity of the locomotor activity we analysed the animals' performance on Open Field Test. As can be seen in Fig. 1D, the ROT-CT group, on day 32, exhibited a decrease in the distance travelled in the OF compared with all other groups on the same day, with an effect both of the lesion [$F(1,125) = 4.415$; $P < 0.05$] and of the sleep restriction [$F(1,125) = 3.964$; $P < 0.05$]. After REB, there was no statistical difference between the groups (Fig. S1B).

We used the Object Recognition Test – a measure where the time spent on a new object presented to the animal permits to evaluate recognition memory – to estimate the cognition status. The sham CT group exhibited a significant learning curve as shown by the memory improvement over subsequent tasks [$F(83.544) = 3.129$; $P < 0.05$], with a marked difference between ORT1/2 and ORT4 ($P < 0.05$) (Fig. 1E). In each test, a two-way ANOVA followed by Fisher's LSD test between groups was performed revealing that in the last test (ORT4) SR impaired both SHAM ($P < 0.05$) and ROT ($P < 0.01$) groups compared to SHAM-CT (Fig. 1F), which was

the only group that explored the non-familiar object significantly more after ORT2 (Fig. S2). Moreover, in the first week of sleep rebound, significant memory impairment in the ROT-REB group compared to SHAM-REB ($P < 0.05$) was observed. However, after 15 days of sleep rebound, this difference between the groups disappeared (Fig. S1C).

The assessment of the activity pattern to observe possible rest-activity alterations was performed using an infrared beam-break system. The two-way ANOVA analysis revealed that there was a statistical difference in the diurnal activity profile among groups [$F(3,6912) = 38.56$; $P < 0.0001$] at several time-points [$F(215,6912) = 87.72$; $P < 0.0001$] over the 21 days of SR (Fig. 2A). There was a consistent diminished activity level in the ROT-SR group starting at ZT12 (lights-off; 19:00 h clock time) that remained lower for at least 1 hour after the onset of darkness. This difference was not seen in the first week but emerged and became statistically significant in weeks 2 and 3 (Fig. 2C). We investigated the first 2 hours of the dark phase in the course of weeks 2 and 3 in more detail, and this analysis showed that the ROT-SR group exhibited significantly reduced activity [$F(3,100) = 220.4$; $P < 0.0001$] during the 75 minutes after lights-off, suggesting reduced behavioural arousal (Fig. 2B). Total activity also showed a progressive decline each week in the SR groups: in week 1 [$F(1,83) = 4.753$; $P < 0.05$] only ROT-SR showed a significant difference from SHAM-CT ($P < 0.05$); in the second week both SR groups showed reduced activity [$F(1,83) = 12.94$; $P < 0.001$] that was even more evident in week 3 [$F(1,83) = 19.46$; $P < 0.0001$] (Fig. 2D). On the first day after SR ended, both SHAM and ROT groups exhibited a disturbed rest-activity rhythm throughout the day, which recovered over time (Fig. S3).

Plasma metabolic profiling. Targeted LC/MS-based metabolic profiling was used to examine the effect of phenotype (ROT vs SHAM) and sleep condition (CT vs SR) on plasma metabolite concentrations. A pair-wise orthogonal partial least-squares discriminant analysis (OPLS-DA) model was obtained comparing the plasma metabolic profiles of SHAM-CT animals with ROT-CT animals (Fig. 3A); $R^2X = 0.636$; $R^2Y = 0.996$; $Q^2Y = 0.312$; $n = 1 + 5$ components. This model was not significant (CV ANOVA $P > 0.05$). The corresponding p(corr) loading plot is shown in Fig. 3B and the p(corr) values for each metabolite are presented in Supplementary Table S1A. ROT treatment was associated with increased plasma branched-chain amino acids (BCAA) (leucine (LEU), isoleucine (ILE), valine (VAL)), ornithine and 33 phospholipids ($p(corr) > 0.3$) and decreased circulating alpha-aminoadipic acid (α-AAA) and propionylcarnitine (AC-C3) ($p(corr) < -0.3$) (Fig. 3B; Table S1A). By contrast a significant difference was observed in the SHAM-SR group compared to SHAM-CT. A significant pair-wise OPLS-DA model comparing SHAM-CT with SHAM-SR ($R^2X = 0.421$; $R^2Y = 0.934$; $Q^2Y = 0.525$; $n = 1 + 2$ components; CV ANOVA $P = 0.04$; validated by permutation analysis) is shown in Fig. 3C, the p(corr) loading plot is shown in Fig. 3D and the p(corr) values for each metabolite are presented in Supplementary Table S1B. Sleep restriction in control animals increased plasma concentrations of the BCAAs (LEU, ILE, VAL), ornithine, arginine, lysine, alanine, proline, phenylalanine (PHE), carnitine (AC-C0), and phospholipids ($n = 15$) ($p(corr) > 0.3$) and decreased creatinine, putrescine, symmetric dimethylarginine, kynurenine (KYN), α-AAA, trans-4-hydroxyproline, acetylcarnitine (AC-C2), tetradecenoylcarnitine (AC-C14:1) and glutaconylcarnitine (AC-C5:1-DC) ($p(corr) < -0.3$) compared to controls. A significant pair-wise comparison OPLS-DA model was also obtained comparing SHAM-CT with ROT-SR ($R^2X = 0.499$; $R^2Y = 0.920$; $Q^2Y = 0.566$; $n = 1 + 2$ components; CV ANOVA $P = 0.03$; validated by permutation analysis; Fig. 3E). The p(corr) loading plot is shown in Fig. 3F and the p(corr) values of the metabolites are presented in Supplementary Table S1C. Sleep restriction with ROT increased plasma concentrations of the BCAAs (LEU, ILE, VAL), ornithine, arginine, lysine, proline, PHE, serine, spermidine, the sphingolipid (SM C16:1) and many phospholipids ($n = 54$) ($p(corr) > 0.3$) and decreased creatinine, trans-4-hydroxyproline, acetylcarnitine (AC-C2) and tetradecenoylcarnitine (AC-C14:1) ($p(corr) < -0.3$) compared to controls (SHAM-CT). After rebound, the effects of SR and ROT were lost (SHAM-CT vs ROT-REB) (OPLS-DA model $R^2X = 0.350$, $R^2Y = 0.348$, $Q^2Y = 0.216$; $n = 1 + 0$ components; CV ANOVA $P = 0.113$).

ANOVA analysis was performed to assess differences in metabolite concentration ratios. Before this analysis, a heat map combined with hierarchical clustering was performed (Fig. S4A). Statistical analysis with one-way ANOVA (simple six-group - SHAM/ROT - CT, SR and rebound group- comparison, straightforward approach) identified 10 metabolites that were significantly different between the study groups when compared to SHAM-CT ($FDR < 0.05$): ILE, LEU, VAL, alpha-AAA, KYN, PC aa C30:0, PC aa C34:1, PC aa C40:2, PC aa C42:4, and PC ae C38:3 (shown in Table 1 with FDR values). Multivariate ANOVA including all groups showed 3 significant metabolites (ILE, LEU – increased; KYN – decreased) due to SR if compared to SHAM-CT and no differences for the rotenone lesion. Table 1 shows the metabolite ratios compared to control (SHAM-CT) and FDR values per comparison. Models including interactions did not present any metabolites with $FDR < 0.10$. Results after rebound show different metabolites altered, either if compared to SR or CT. Supplementary Fig. S4B shows the hits from one-way and multivariate ANOVA combined for all groups, including rebound. Using logistic prediction modeling, models were built to predict whether samples were exposed to ROT, SR or rebound. Starting from no model, models were developed by adding one metabolite at a time to an existing model until no further improvement in AUC was obtained. For ROT, since no metabolites were significant, the best model was only with PC aa C40:2 ($FDR = 0.072$; $AUC = 0.669$), adding other metabolites did not improve AUC. For SR, the simplest model was based on KYN and stepwise improvement combined with leave-one-out cross-validation resulted in a final model with KYN and ILE ($AUC = 0.845$) (Fig. 4A). This model allowed 80% accuracy, 70% sensitivity and 86% specificity. ROT animals were more often correctly predicted as SR (ROT-SR $n = 11$; $n = 9$ predicted as SR) than SHAM (SHAM-SR $n = 12$; $n = 7$ predicted as SR).

We also performed a correlations analysis (Fig. 5) to see if any of the parameters could be associated, considering only the correlation with an $r > 0.4$ or < -0.4, since this value is approximately the threshold where the tested correlations become significant with $FDR < 0.05$. For illustration purposes, we show the correlation between sleep condition and total activity on day killed, with $r = -0.57$. For metabolite concentrations, there was

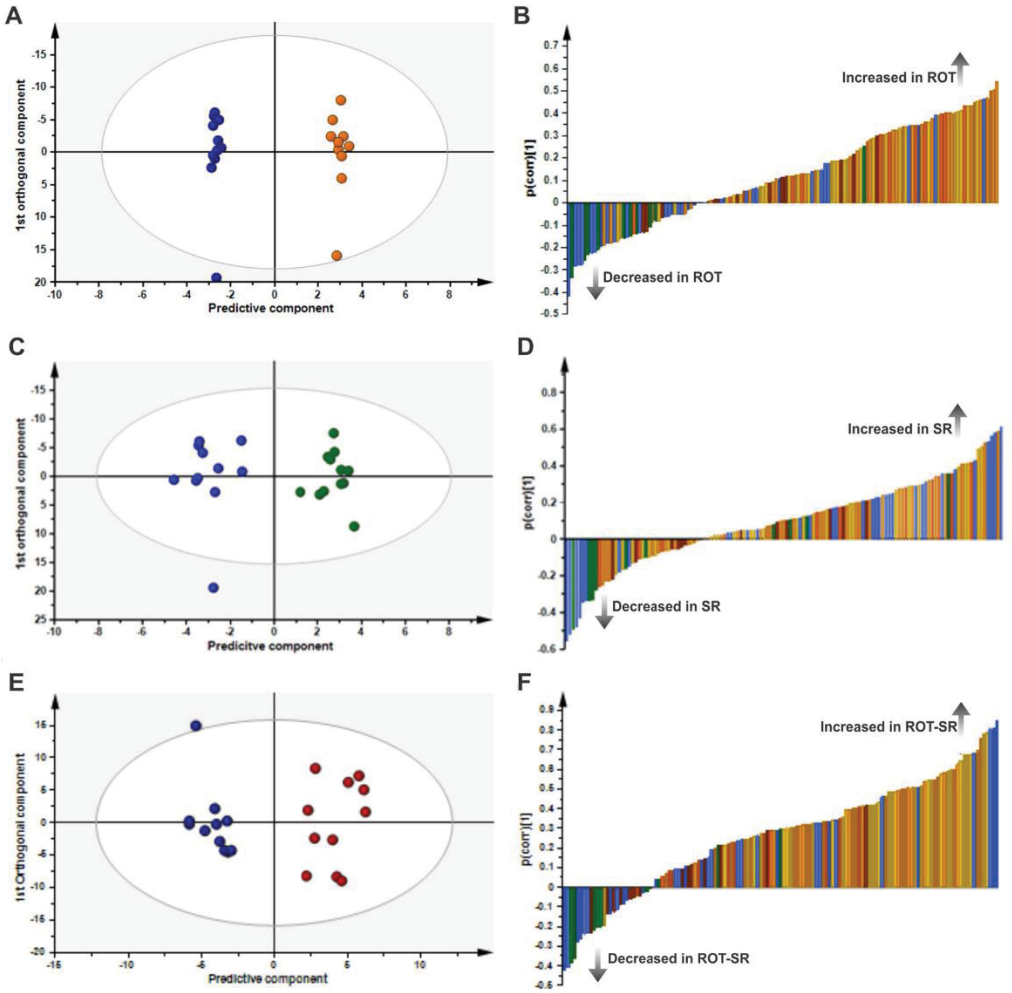

Figure 3. OPLS-DA plots in LC/MS targeted metabolomics data. (**A**) OPLS-DA scores plot showing separation by phenotype between the sham control group (SHAM-CT, dark blue, n = 11) and the rotenone control (ROT-CT, orange, n = 10); R^2X 0.636; R^2Y 0.996; Q^2Y 0.312; $P < 0.05$. (**B**) OPLS-DA loading plot of SHAM-CT vs ROT-CT. Negative p(corr) values represent decreased and positive p(corr) values represent increased metabolite concentrations in the rotenone group (ROT-CT) compared to sham group (SHAM-CT). The metabolite bars are colour coded according to metabolite class as follows: amino acids and biogenic amines (blue); acylcarnitines (green); lysophosphatidylcholine acyl (lyso PC a) (dark orange); phosphatidylcholine diacyl (PC aa) (yellow); phosphatidylcholine acyl-alkyl (PC ae) (light orange); sphingolipids (SM) (brown). (**C**) OPLS-DA scores plot showing separation by sleep restriction alone (blue, SHAM-CT, n = 11; green, SHAM-SR, n = 12); R^2X 0.421; R^2Y 0.934; Q^2Y 0.525; P = 0.04. (**D**) OPLS-DA loading plot of SHAM-CT vs SHAM-SR. Negative p(corr) values represent decreased and positive p(corr) values represent increased metabolite concentrations in sleep restriction (SR) compared to control. (**E**) OPLS-DA scores plot for SHAM-CT vs ROT-SR (dark blue, SHAM-CT, n = 11; dark red, ROT-SR, n = 11); R^2X 0.499; R^2Y 0.920; Q^2Y 0.566; P = 0.03. (**F**) OPLS-DA loading plot of SHAM-CT vs ROT-SR. Negative p(corr) values represent decreased and positive p(corr) values represent increased metabolite concentrations in rotenone and SR compared to sham control.

a correlation between SR and KYN (r = −0.51), ILE (r = 0.41) and LEU (r = 0.42). Considering the behavioural and metabolomics data, a correlation between total activity on day killed and methionine (MET) concentrations was demonstrated (r = 0.41). All the other correlations found were between metabolite concentrations, all increased in the model: LEU × ILE (r = 0.90); PHE × ILE (r = 0.50); VAL × ILE (r = 0.94); PHE × LEU (r = 0.52); VAL × LEU (r = 0.89); PHE × MET (r = 0.73); tryptophan (TRP) × MET (r = 0.64); MET × VAL (r = 0.41); PHE × VAL (r = 0.55); PHE × TRP (r = 0.58).

^{1}H NMR spectroscopy was used for untargeted metabolic profiling of the plasma samples. A significant OPLS-DA model was obtained comparing the plasma metabolic profiles between SHAM-CT and ROT-CT groups ($R^2X = 0.56$, $R^2Y = 0.75$, $Q^2Y = 0.35$; P = 0.027 following 999 permutations). The corresponding coefficient plot is shown in Fig. 6A. Plasma from the ROT-CT group contained lower amounts of dimethylsulfone and pyruvate compared to the SHAM-CT group, but the most evident differences were associated with higher

Ratios to CT	SHAM CT	SHAM SR	ROT CT	ROT SR	FDR		
					one-way ANOVA	Multivariate ANOVA	
						SR	Rotenone
Isoleucine	1.00	1.22	1.12	1.35	0.021	**0.039**	0.300
Leucine	1.00	1.26	1.18	1.40	0.021	**0.039**	0.261
Valine	1.00	1.21	1.12	1.33	0.014	0.061	0.285
Alpha-AAA	1.00	0.87	0.72	0.92	0.032	0.432	0.862
Kynurenine	1.00	0.79	1.15	0.72	0.028	**0.014**	0.799
PCaaC30:0	1.00	1.19	1.17	1.36	0.021	0.622	0.275
PCaaC34:1	1.00	1.21	1.17	1.43	0.049	0.529	0.275
PCaaC40:2	1.00	1.02	1.13	1.48	0.028	0.771	0.072
PCaaC42:4	1.00	1.01	1.00	1.26	0.028	0.871	0.489
PCaaC38:3	1.00	1.10	1.27	1.49	0.034	0.357	0.128

Table 1. Metabolite concentration ratios compared to control (SHAM-CT) and FDR values per comparison. Statistical analysis with one-way ANOVA showed 10 metabolites with significant differences (FDR < 0.05) listed here. Multivariate ANOVA showed 3 metabolites significantly altered (highlighted in bold) due to SR in comparison to SHAM-CT and no differences for rotenone lesion.

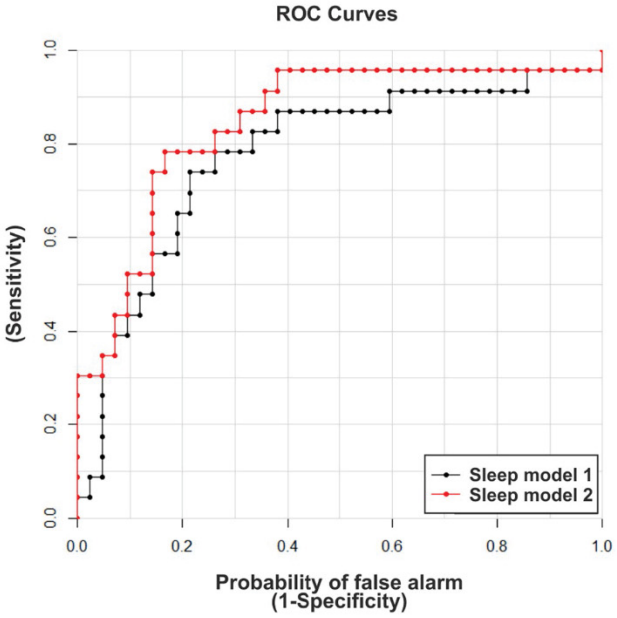

Figure 4. Receiver operating characteristic (ROC) plots of SR prediction models. Models were improved stepwise by including an additional metabolite until no more gain in AUC could be obtained during cross-validation. Model 1: kynurenine (KYN) (black); AUC = 0.777. Model 2: kynurenine and isoleucine (ILE) (red); AUC = 0.845.

circulating amounts of triglycerides and lipoproteins (specifically, low density lipoproteins (LDL) and very-low density lipoproteins (VLDL) in the ROT-CT group). Consistent with the targeted LC/MS metabolomics, there was an increase in all BCAAs in the ROT-CT compared to the SHAM-CT group. However, a comparison between the sham groups (SHAM-CT vs SHAM-SR) did not reveal any significant difference produced by sleep restriction itself, in contrast to LC/MS analysis. Nevertheless, when comparing the additive effects of ROT and SR (ROT-SR) with SHAM-CT, the predictive ability of the OPLS-DA model was stronger ($R^2X = 0.59$, $R^2Y = 0.91$, $Q^2Y = 0.70$, $P = 0.001$ following 999 permutations; Fig. 6B) than ROT alone (SHAM-CT vs ROT-CT; $Q^2Y = 0.35$). While the increase in lipoproteins observed in the ROT-CT group remained, the increase in BCAAs was more pronounced with additional increases in TRP, PHE and glycerophosphocholine (GPC). After rebound, the additive effects produced by SR in ROT were lost (SHAM-CT vs ROT-REB) (OPLS-DA model $R^2X = 0.27$, $R^2Y = 0.40$, $Q^2Y = 0.19$; $P = 0.068$).

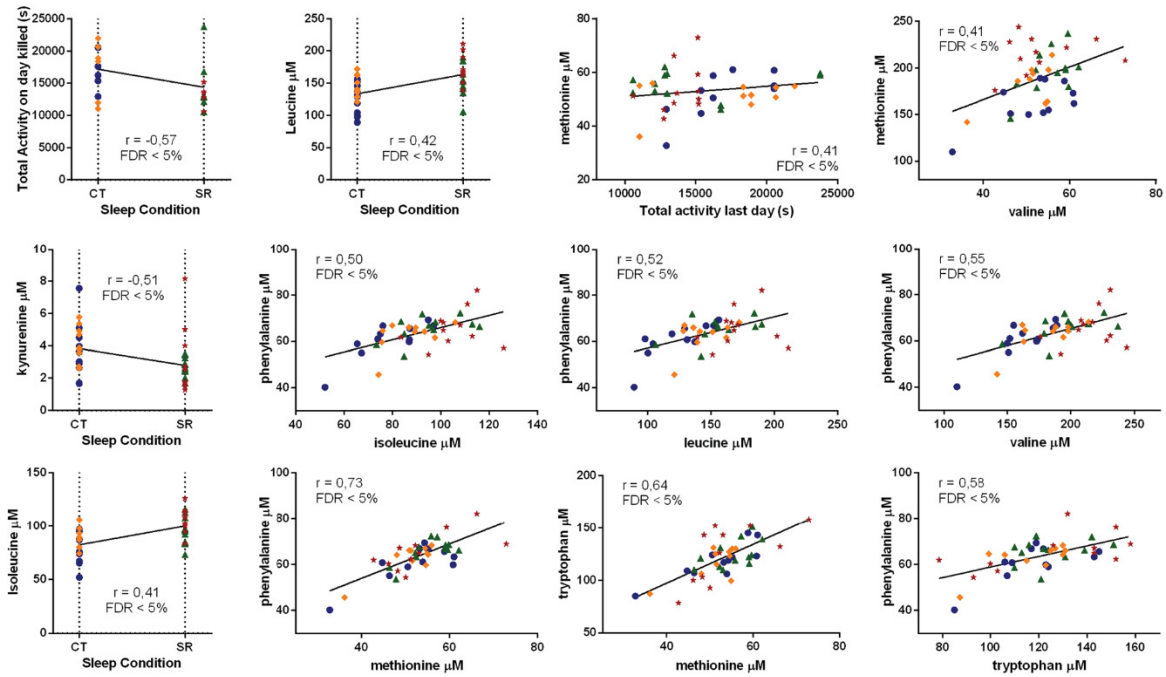

Figure 5. Behavioural and neurochemical correlations. Correlations with an $r > 0.4$ or < -0.4 were considered since this value is approximately the threshold where the tested correlations become significant with $FDR < 0.05$. From the top left to the bottom right: total activity on day killed × Sleep Condition ($r = -0.57$); LEU × Sleep Condition ($r = 0.42$); total activity on day killed × MET ($r = 0.41$); MET × VAL ($r = 0.41$); KYN × Sleep Condition ($r = -0.51$); PHE × ILE ($r = 0.50$); PHE × LEU ($r = 0.52$); PHE × VAL ($r = 0.55$); ILE × Sleep Condition ($r = 0.41$); PHE × MET ($r = 0.73$); TRP × MET ($r = 0.64$); PHE × TRP ($r = 0.58$). Colour code: dark blue, SHAM-CT, n = 11; green, SHAM-SR, n = 12; orange, ROT-CT, n = 10; dark red, ROT-SR, n = 11.

Discussion

Using the established ROT rodent model of PD, we have shown that chronic SR can affect the behavioural and metabolic characteristics in this model consistent with PD. Collectively, these data reinforce the concept that SR in PD contributes to the development of metabolic shifts early in the disease (equivalent to Braak stages 2–3) that could aggravate its progression and be established as reliable early-phase predictive biomarkers. In addition, our work contributes to the consolidation of the ROT-PD model as a reliable model to study PD features. The ROT-PD has established itself more and more as a prototypical model to study sleep aspects related to the SNpc dopaminergic lesion. Previous studies have shown that both chronic systemic administration and stereotaxic injection of ROT were associated with sleep alterations, as long-term and progressive deterioration of spontaneous sleep[35] and decrease of the time in NREM sleep[33].

In the ROT-treated compared to the SHAM animals a selective reduction in the percentage of TH-ir neurons within the SNpc, which is related to several NMS that are landmarks of early-phase features of PD, was observed[9,32,33,37]. Dopamine depletion within the SNpc leads to an increase in striatal D2 receptors, increasing activity of the nigrostriatal indirect-pathway resulting in movement impairment[47]. In addition, a dopaminergic lesion selectively decreases the synaptic strength of thalamic inputs into the direct-pathway, suggesting that motor impairments occur as a result of an imbalanced activation of basal ganglia circuitry by the thalamus, which can be reversed with thalamic inhibition[48]. The reduction in motor activity seen in the ROT-CT group, also observed in other ROT-PD models[39,49], was reversed in the ROT-SR group, indicating that SR triggers a dopaminergic compensatory mechanism. This is in agreement with Ramanathan, *et al.*[50], who showed that a 6 h SR protocol of gentle handling produced an increase in exploratory behaviour. Similarly, 24 h of total sleep deprivation produced the same outcome, without changes in plasma corticosterone, suggesting that the increase in locomotor activity was not a consequence of the hypothalamic-pituitary-adrenal stress response[51]. REM sleep deprivation is also able to augment locomotion[39] and counterbalance PD model-induced hypokinesia[52], a compensatory effect considered to be due to supersensitivity of brain dopamine receptors[53], specifically, through D2 receptor up-regulation[54]. Therefore, total SR can lead to a substantial loss of REM sleep, enough to compensate for the motor impairment produced by ROT lesion.

Substantial evidence supports the idea that sleep deprivation or SR impairs memory processes[55–59] as a result of different mechanisms: (i) reduction of thalamic activity[60]; (ii) decline of hippocampal long-term potentiation[61]; (iii) decrease of hippocampal AMPA receptor function[62]; (iv) brain inflammation and increasing susceptibility to toxins[63]. Therefore, our ORT findings, showing that the ROT-SR group was not able to remember the familiar object, are aligned with the results of Dos Santos, *et al.*[39], showing that ROT can impair object recognition, but,

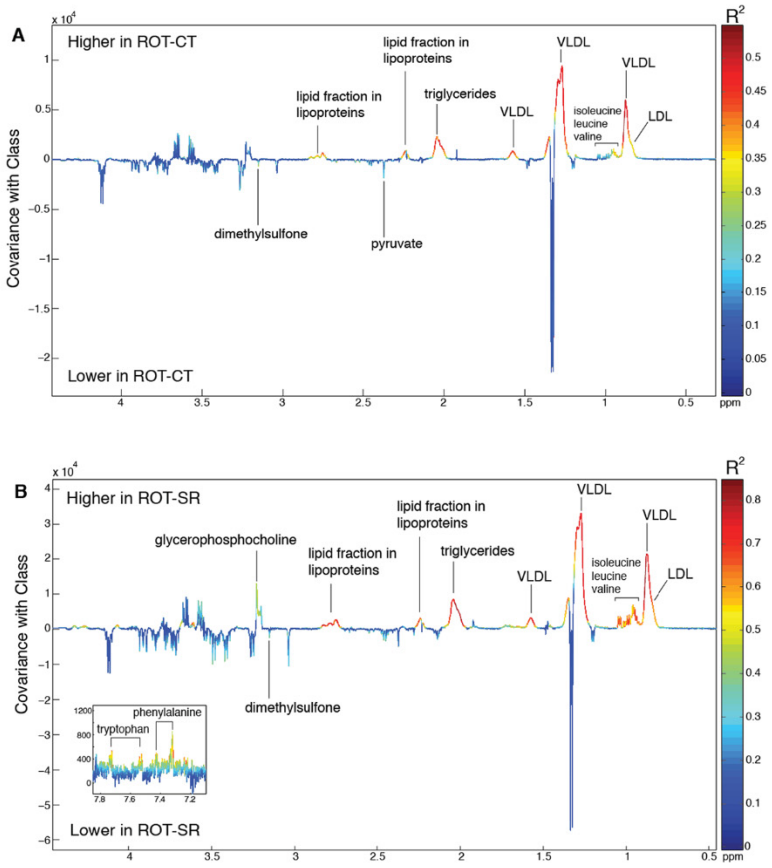

Figure 6. OPLS-DA models comparing the plasma ^{1}H NMR spectral profiles. (**A**) OPLS-DA from SHAM-CT versus ROT-CT ($Q^2Y = 0.35$, $P = 0.027$). LDL = Low density lipoproteins; VLDL = very low density lipoproteins (dark blue, SHAM-CT, n = 10; orange, ROT-CT, n = 9; dark red, ROT-SR, n = 6). (**B**) OPLS-DA from SHAM-CT versus ROT-SR ($Q^2Y = 0.70$, $P = 0.001$).

unlikely the acute REM sleep deprivation which improved memory, our chronic protocol suggest a significant synergistic effect of SR and the dopaminergic ROT lesion in the maintenance of cognitive impairment. It is noteworthy that ORT is a familiarity-based memory task, which is correlated to human episodic-like memory and spatial learning, both impaired in early-stage PD, suggesting that the basal ganglia interact with the prefrontal cortex to mediate high-level cognition[64,65]. Basal ganglia influence cortical learning-dependent synaptic plasticity by selectively modulating corticostriatal inputs; in a dopamine depletion background, this plasticity is altered due to unsuitable filtering by the basal ganglia, resulting in abnormal learning[66]. It is known that significant areas for object recognition in rats are cortical association areas, the mediodorsal thalamic nucleus, the rhinal cortices, especially the perirhinal, and the prefrontal cortical areas[67,68]. These structures have primary projections to the striatum and there is evidence that the striatum modulates information flow to the prefrontal cortex[69], providing the background for cognitive impairment.

There is also evidence for effects of circadian disruption in long-term object recognition, independent of sleep[70]. The observed rest-activity patterns revealed that the ROT-SR group showed significantly reduced arousal during the first hour of night-time activity (their active phase), suggesting attenuated behavioural arousal and an association between sleep and circadian changes in a PD context. Circadian disruption in PD could reflect not only sleep disturbances but also autonomic, cognitive, psychiatric and motor impairments, further endorsed by the role that dopamine has in sleep regulation and circadian homeostasis[5,7,71]. Lastly, it is plausible that the mechanisms that affect the circadian system in PD could influence sleep/wake processing. Therefore, the occurrence of one reinforces the progression of the other, potentially involving a feedback mechanism[72], predisposing the brain to neurodegeneration through a number of key mechanisms[73].

To elucidate the biochemical processes through which chronic SR can enhance the PD phenotype in the ROT model, we combined behavioural testing with targeted LC/MS and untargeted NMR spectroscopy based metabolic profiling. Targeted metabolomics quantifies a large number of known metabolites, enabling the detailed characterization of changes in specific metabolic pathways in response to stimuli (ROT and/or SR)[44]. Untargeted ^{1}H NMR spectroscopy-based metabolic profiling is complementary to the targeted approach, measuring an extensive range of metabolites, both endogenous and exogenous, providing a holistic overview of the metabolic system and how it is modulated by different exposures[46]. This dual approach provides wide metabolome coverage

and, in this study, significant metabolic alterations were observed in the animals, mainly due to SR associated with the ROT-induced dopaminergic lesion.

ROT treatment was observed to increase the plasma lipoproteins, LDL and VLDL. This occurred both in the presence and absence of SR. VLDL is responsible for transporting energy-rich triacylglycerol to cells in the body while LDL is responsible for delivering cholesterol. Hypercholesterolemia has become a prognostic risk factor for neurodegenerative diseases, even contributing to PD onset[74]. Indeed, elevated cholesterol is associated with the loss of dopaminergic neurons in the SNpc, followed by a reduction in striatal dopamine levels, as a product of mitochondrial dysfunction, that leads to motor impairment[75]. Lipoprotein lipase (LPL) is the enzyme that removes triacylglycerol from VLDL transforming it into LDL. LPL is highly expressed in hippocampal neurons. Additionally, LPL is involved in the pathogenesis of dementia[76–78] and LPL-deficient mice have been shown to have presynaptic dysfunction and impaired memory function[79]. Interestingly, ROT lesion was already linked to lipid impairment, with alterations in polyunsaturated fatty acid cardiolipin in the SNpc and plasma in rats[80].

A family of metabolites suggested to be involved in lipid metabolism, implicated in insulin resistance and obesity, are the BCAAs[81], which were found to be significantly elevated in our model. In SR rats compared to non-SR controls, LEU, ILE and KYN were significantly altered, with a statistical correlation for the sleep condition. Although LEU and ILE were increased in all groups in comparison with SHAM-CT, the most prominent increment was in the ROT-SR group. The remaining BCAA, VAL, showed a non-significant trend ($P = 0.061$) to increase (measured by targeted metabolomics), which was corroborated by the untargeted approach with all BCAAs showing increased plasma levels in the ROT-SR condition (there was also a slight increase in ROT-CT only, but SR appears to enhance this effect). These findings are in accordance with previous studies that have shown increased BCAA levels in PD patients, notably ILE and LEU[82,83], and in PD animal models[84]. The pathophysiological significance of these changes is still unclear, but it is known that impaired BCAA metabolism results in greater circulation of these BCAAs, and consequent mitochondrial dysfunction[85]. They are also transported into the brain via the large neutral amino acid transporter, which also transports TRP, PHE and tyrosine (TYR). Increased plasma BCAA levels reduce TRP and TYR transport into the brain due to competition for the carrier at the blood-brain barrier, influencing synthesis and release of serotonin and catecholamines (most notably dopamine, by reducing tyrosine available for hydroxylation) within the brain[86]. TRP is the precursor of serotonin, which is involved in sleep/wake regulation, functioning primarily to promote wakefulness and closely related to memory and emotional processes in PD[37,87]. Competition between BCAA and TRP/TYR for brain uptake could, therefore, negatively impact serotonin and dopamine metabolism, contributing to the occurrence of NMS in PD.

Interestingly, TRP was also found to be higher in the plasma of the ROT-SR group compared to the SHAM-CT group (measured by NMR). TRP metabolism was found to be altered in early-stage PD patients in the study of Luan, *et al.*[82], with TRP catabolites increased in the urine compared to healthy subjects, particularly KYN. There are some studies showing the involvement of KYN metabolism in PD[88–90], and in our plasma samples, KYN was found to be decreased as a result of SR but not ROT. The KYN pathway, after its conversion from TRP by indoleamine 2,3-dioxygenase, produces three metabolites that have important roles in the brain: two of them, quinolinic acid and 3-hydroxyl-kynurenine, are NMDA receptor agonists and have neurotoxic effects, producing progressive mitochondrial dysfunction; the other one, kynurenic acid (KYNA), has a neuroprotective effect, acting as a free radical scavenger and glutamate antagonist[91]. In mammals, about 40% of KYN is produced in the brain, whereas 60% of it is taken up from the periphery[92]. Therefore, if there is a transport impairment of TRP in the blood-brain barrier due to competition with BCAA, it could reflect in an increased uptake of KYN from the periphery. On the other hand, TRP pathway could be shifted towards serotonin synthesis, since, as previously mentioned, it is known to promote wakefulness[87]. Beyond that, LEU, ILE, MET and PHE have been shown to reduce tissue KYN concentrations and suppress KYNA synthesis in a dose-dependent manner[93]. Since these metabolites were found to be significantly increased in the SR group and even more increased in the ROT-SR group, they could be modulating KYNA formation and therefore KYN metabolism. In addition, using logistic regression prediction, a model with 80% accuracy, 70% sensitivity and 86% specificity was obtained for SR using KYN and ILE (i.e. 70% of SR animals were predicted correctly based on their plasma KYN and ILE abundance), corroborating a relationship between both metabolites.

The other amino acids that were altered in our PD model were PHE and MET, with a positive correlation with BCAA and TRP levels in the LC/MS analysis; likewise, PHE was increased in the ROT-SR group in the untargeted NMR analysis. PHE is the precursor of DA, reported to be altered in PD[82,94], and has been associated with alterations in sleep patterns[95]. MET levels on day killed had a positive correlation with the total activity on the last day. The administration of MET, an acetylcholine precursor, was found to increase diurnal activity in birds, an effect supposed to be due acetylcholine stimulation[96]; MET is also implicated in PD, mainly through its metabolite homocysteine, since elevated plasma levels of homocysteine have been observed in PD[97]. The observed increase in ornithine and arginine levels could be indicative of impairment in the urea cycle; ornithine has previously been reported to be increased in PD, purportedly due to a reduction in the ability of mitochondria to transport ornithine for conversion in the urea cycle[83] and also as a consequence of ROT exposure, which inhibits the activity of ornithine decarboxylase (Rhee *et al.*, 2016). Arginine, in turn, is also part of the nitric oxide pathway, which has already been implicated in PD through nitrosative stress[98], reported to be higher in PD patients[99], and in the initial phase of PD animal models, being inversely correlated with TH immunolabeling[100].

ROT exposure in combination with sleep deprivation also resulted in an increase in plasma GPC. GPC, a cholinergic precursor, is one of the major phosphorus containing-choline components[101], and is a precursor of acetylcholine, a neurotransmitter necessary for normal cognitive function, including learning and memory[102]. In PD patients with mild cognitive impairment, brain GPC abundance has also been found to be increased[103], although it was decreased in cerebrospinal fluid in idiopathic PD[104]. In addition, thalamic GPC spectroscopy analysis has been shown to be useful in differentiating tremor-dominant PD patients from those with resting tremor in essential tremor[105]. In the SR context, it has previously been reported that GPC concentrations were

increased following recovery from a night of sleep deprivation[101]. It is known that choline transport through the blood-brain barrier decreases with age contributing to degenerative processes[106]; therefore, the findings observed here could be related to a reduction in choline transport, with a consequent increase in plasma GPC levels.

Although one can arguably question the validity of the rotenone model, in fact our work contributes to understand the underlying pathophysiology of the SNpc dopaminergic neurodegeneration. Still, some limitations of the study should be highlighted: sleep measurement was limited to behavioural rest-activity analysis and lacked a physiological measure of sleep (i.e., EEG) to determine the impact of the sleep restriction on the sleep architecture; the absence of quantification of proteins, for example, indoleamine 2,3-dioxygenase, quinolinic acid and 3-hydroxyl-kynurenine, from TRP and KYN pathway, or lipoprotein lipase, to correlate with the lipid alterations, in order to better understand the mechanism underlying the observed alterations; failure to establish the extent of the lesion in each animal to compare with the variation in the measured parameters. Nevertheless, these limitations open a research agenda to keep investigating these findings and fully understand the role of these metabolites and metabolic pathways in PD pathophysiology.

In conclusion, in our model, we have observed that chronic SR produces behavioural and metabolic alterations that reveal for the first time to our knowledge a novel set of metabolic pathways, which are involved in PD pathophysiology. Sleep restriction in the early-phase of PD can exacerbate and modulate the biochemical changes associated with disease progression. These metabolic alterations could represent reliable and sensitive markers of early-phase PD and may help track progression of the disease before the appearance of motor signs. Identification of such individuals has the potential to improve therapeutic strategies and possibly delay or attenuate the onset of symptoms which amplify the behavioural and metabolic characteristics in this model consistent with PD. Collectively, our findings reinforce the concept that SR in PD contributes to the development of metabolic shifts early in the disease (parallel to the non-motor phase) that could aggravate its progression and be established as reliable early-phase predictive biomarkers.

Data Availability

The datasets used and/or analysed during the current study are included in this published article [and its supplementary information files]. If any additional information is required, it is available from the corresponding author on request.

References

1. Braak, H. & Del Tredici, K. Neuropathological staging of brain pathology in sporadic Parkinson's disease: separating the wheat from the chaff. *Journal of Parkinson's disease* **7**, S73–S87, https://doi.org/10.3233/JPD-179001 (2017).
2. Del Tredici, K. & Braak, H. Review: sporadic Parkinson's disease: development and distribution of alpha-synuclein pathology. *Neuropathology and applied neurobiology* **42**, 33–50, https://doi.org/10.1111/nan.12298 (2016).
3. Lima, M. M. *et al.* Motor and non-motor features of Parkinson's disease - a review of clinical and experimental studies. *CNS & neurological disorders drug targets* **11**, 439–449 (2012).
4. Schapira, A. H. V., Chaudhuri, K. R. & Jenner, P. Non-motor features of Parkinson disease. *Nature reviews. Neuroscience* **18**, 509, https://doi.org/10.1038/nrn.2017.91 (2017).
5. Lima, M. M. Sleep disturbances in Parkinson's disease: the contribution of dopamine in REM sleep regulation. *Sleep medicine reviews* **17**, 367–375, https://doi.org/10.1016/j.smrv.2012.10.006 (2013).
6. Tolosa, E. & Pont-Sunyer, C. Progress in defining the premotor phase of Parkinson's disease. *Journal of the neurological sciences* **310**, 4–8, https://doi.org/10.1016/j.jns.2011.05.027 (2011).
7. Videnovic, A. & Golombek, D. Circadian and sleep disorders in Parkinson's disease. *Exp Neurol* **243**, 45–56, https://doi.org/10.1016/j.expneurol.2012.08.018 (2013).
8. Hawkes, C. H., Del Tredici, K. & Braak, H. A timeline for Parkinson's disease. *Parkinsonism & related disorders* **16**, 79–84, https://doi.org/10.1016/j.parkreldis.2009.08.007 (2010).
9. Lima, M. M., Andersen, M. L., Reksidler, A. B., Vital, M. A. & Tufik, S. The role of the substantia nigra pars compacta in regulating sleep patterns in rats. *PLoS One* **2**, e513, https://doi.org/10.1371/journal.pone.0000513 (2007).
10. Lauretti, E., Di Meco, A., Merali, S. & Pratico, D. Circadian rhythm dysfunction: a novel environmental risk factor for Parkinson's disease. *Molecular psychiatry* **22**, 280–286, https://doi.org/10.1038/mp.2016.47 (2017).
11. Braak, H. *et al.* Staging of brain pathology related to sporadic Parkinson's disease. *Neurobiol Aging* **24**, 197–211 (2003).
12. French, I. T. & Muthusamy, K. A. A Review of Sleep and Its Disorders in Patients with Parkinson's Disease in Relation to Various Brain Structures. *Frontiers in aging neuroscience* **8**, 114, https://doi.org/10.3389/fnagi.2016.00114 (2016).
13. Tandberg, E., Larsen, J. P. & Karlsen, K. A community-based study of sleep disorders in patients with Parkinson's disease. *Movement disorders: official journal of the Movement Disorder Society* **13**, 895–899, https://doi.org/10.1002/mds.870130606 (1998).
14. Garcia-Borreguero, D., Larrosa, O. & Bravo, M. Parkinson's disease and sleep. *Sleep medicine reviews* **7**, 115–129 (2003).
15. Palma, J. A., Urrestarazu, E. & Iriarte, J. Sleep loss as risk factor for neurologic disorders: a review. *Sleep medicine* **14**, 229–236, https://doi.org/10.1016/j.sleep.2012.11.019 (2013).
16. Adler, C. H. & Thorpy, M. J. Sleep issues in Parkinson's disease. *Neurology* **64**, S12–20 (2005).
17. Pushpanathan, M. E., Loftus, A. M., Thomas, M. G., Gasson, N. & Bucks, R. S. The relationship between sleep and cognition in Parkinson's disease: A meta-analysis. *Sleep medicine reviews* **26**, 21–32, https://doi.org/10.1016/j.smrv.2015.04.003 (2016).
18. Lima, M. M. *et al.* Paradoxical sleep deprivation modulates tyrosine hydroxylase expression in the nigrostriatal pathway and attenuates motor deficits induced by dopaminergic depletion. *CNS & neurological disorders drug targets* **11**, 359–368 (2012).
19. Meerlo, P., Mistlberger, R. E., Jacobs, B. L., Heller, H. C. & McGinty, D. New neurons in the adult brain: the role of sleep and consequences of sleep loss. *Sleep medicine reviews* **13**, 187–194, https://doi.org/10.1016/j.smrv.2008.07.004 (2009).
20. Mander, B. A., Winer, J. R. & Walker, M. P. Sleep and human aging. *Neuron* **94**, 19–36, https://doi.org/10.1016/j.neuron.2017.02.004 (2017).
21. Miller, D. B. & O'Callaghan, J. P. Biomarkers of Parkinson's disease: present and future. *Metabolism: clinical and experimental* **64**, S40–46, https://doi.org/10.1016/j.metabol.2014.10.030 (2015).
22. Silveira-Moriyama, L. & Lees, A. J. Parkinson disease: how reliable are prodromal indicators of Parkinson disease? *Nature reviews. Neurology* **11**, 5–6, https://doi.org/10.1038/nrneurol.2014.235 (2015).
23. Lei, S. & Powers, R. NMR metabolomics analysis of Parkinson's disease. *Current Metabolomics* **1**, 191–209, https://doi.org/10.2174/2213235X113019990004 (2013).
24. Sharma, S. *et al.* Biomarkers in Parkinson's disease (recent update). *Neurochemistry international* **63**, 201–229, https://doi.org/10.1016/j.neuint.2013.06.005 (2013).

25. Alam, M. & Schmidt, W. J. Rotenone destroys dopaminergic neurons and induces parkinsonian symptoms in rats. *Behav Brain Res* **136**, 317–324 (2002).
26. Betarbet, R. *et al.* Chronic systemic pesticide exposure reproduces features of Parkinson's disease. *Nature neuroscience* **3**, 1301–1306, https://doi.org/10.1038/81834 (2000).
27. Cannon, J. R. *et al.* A highly reproducible rotenone model of Parkinson's disease. *Neurobiology of disease* **34**, 279–290 (2009).
28. Carriere, C. H., Kang, N. H. & Niles, L. P. Bilateral upregulation of alpha-synuclein expression in the mouse substantia nigra by intracranial rotenone treatment. *Experimental and toxicologic pathology: official journal of the Gesellschaft fur Toxikologische Pathologie* **69**, 109–114, https://doi.org/10.1016/j.etp.2016.12.007 (2017).
29. Johnson, M. E. & Bobrovskaya, L. An update on the rotenone models of Parkinson's disease: their ability to reproduce the features of clinical disease and model gene-environment interactions. *Neurotoxicology* **46**, 101–116, https://doi.org/10.1016/j.neuro.2014.12.002 (2015).
30. Morais, L. H. *et al.* Characterization of motor, depressive-like and neurochemical alterations induced by a short-term rotenone administration. *Pharmacological reports: PR* **64**, 1081–1090 (2012).
31. Moreira, C. G. *et al.* Behavioral, neurochemical and histological alterations promoted by bilateral intranigral rotenone administration: a new approach for an old neurotoxin. *Neurotoxicity research* **21**, 291–301, https://doi.org/10.1007/s12640-011-9278-3 (2012).
32. Rodrigues, L. S. *et al.* Olfactory impairment in the rotenone model of Parkinson's disease is associated with bulbar dopaminergic D2 activity after REM sleep deprivation. *Front Cell Neurosci* **8**, 383, https://doi.org/10.3389/fncel.2014.00383 (2014).
33. Targa, A. D. *et al.* Unraveling a new circuitry for sleep regulation in Parkinson's disease. *Neuropharmacology* **108**, 161–171, https://doi.org/10.1016/j.neuropharm.2016.04.018 (2016).
34. Voitenko, L. P. & Nikonenko, A. G. [Modification of experimental rotenone model of Parkinson's disease]. *Fiziolohichnyi zhurnal* **61**, 83–90 (2015).
35. Garcia-Garcia, F., Ponce, S., Brown, R., Cussen, V. & Krueger, J. M. Sleep disturbances in the rotenone animal model of Parkinson disease. *Brain Res* **1042**, 160–168, https://doi.org/10.1016/j.brainres.2005.02.036 (2005).
36. Paxinos, G. & Watson, C. *The rat brain in stereotaxic coordinates*. (Elsevier Academic Press, 2005).
37. Noseda, A. C. *et al.* Putative role of monoamines in the antidepressant-like mechanism induced by striatal MT2 blockade. *Behav Brain Res* **275**, 136–145, https://doi.org/10.1016/j.bbr.2014.09.007 (2014).
38. van der Borght, K. *et al.* Hippocampal cell proliferation across the day: increase by running wheel activity, but no effect of sleep and wakefulness. *Behav Brain Res* **167**, 36–41, https://doi.org/10.1016/j.bbr.2005.08.012 (2006).
39. Dos Santos, A. C. *et al.* REM sleep deprivation generates cognitive and neurochemical disruptions in the intranigral rotenone model of Parkinson's disease. *Journal of neuroscience research* **91**, 1508–1516, https://doi.org/10.1002/jnr.23258 (2013).
40. Ennaceur, A. & Delacour, J. A new one-trial test for neurobiological studies of memory in rats. 1: Behavioral data. *Behav Brain Res* **31**, 47–59 (1988).
41. Moore, S. J., Deshpande, K., Stinnett, G. S., Seasholtz, A. F. & Murphy, G. G. Conversion of short-term to long-term memory in the novel object recognition paradigm. *Neurobiology of learning and memory* **105**, 174–185, https://doi.org/10.1016/j.nlm.2013.06.014 (2013).
42. Davies, S. K. *et al.* Effect of sleep deprivation on the human metabolome. *Proceedings of the National Academy of Sciences of the United States of America* **111**, 10761–10766, https://doi.org/10.1073/pnas.1402663111 (2014).
43. Isherwood, C. M., Van der Veen, D. R., Johnston, J. D. & Skene, D. J. Twenty-four-hour rhythmicity of circulating metabolites: effect of body mass and type 2 diabetes. *FASEB journal: official publication of the Federation of American Societies for Experimental Biology*, https://doi.org/10.1096/fj.201700323R (2017).
44. Skene, D. J. *et al.* Metabolic profiling of presymptomatic Huntington's disease sheep reveals novel biomarkers. *Scientific reports* **7**, 43030, https://doi.org/10.1038/srep43030 (2017).
45. Beckonert, O. *et al.* Metabolic profiling, metabolomic and metabonomic procedures for NMR spectroscopy of urine, plasma, serum and tissue extracts. *Nature protocols* **2**, 2692–2703, https://doi.org/10.1038/nprot.2007.376 (2007).
46. Swann, J. R. *et al.* Application of 1H NMR spectroscopy to the metabolic phenotyping of rodent brain extracts: A metabonomic study of gut microbial influence on host brain metabolism. *Journal of pharmaceutical and biomedical analysis* **143**, 141–146, https://doi.org/10.1016/j.jpba.2017.05.040 (2017).
47. Albin, R. L., Young, A. B. & Penney, J. B. The functional anatomy of basal ganglia disorders. *Trends in neurosciences* **12**, 366–375 (1989).
48. Parker, P. R., Lalive, A. L. & Kreitzer, A. C. Pathway-specific remodeling of thalamostriatal synapses in parkinsonian mice. *Neuron* **89**, 734–740, https://doi.org/10.1016/j.neuron.2015.12.038 (2016).
49. von Wrangel, C., Schwabe, K., John, N., Krauss, J. K. & Alam, M. The rotenone-induced rat model of Parkinson's disease: behavioral and electrophysiological findings. *Behav Brain Res* **279**, 52–61, https://doi.org/10.1016/j.bbr.2014.11.002 (2015).
50. Ramanathan, L., Hu, S., Frautschy, S. A. & Siegel, J. M. Short-term total sleep deprivation in the rat increases antioxidant responses in multiple brain regions without impairing spontaneous alternation behavior. *Behavioural Brain Research* **207**, 305–309, https://doi.org/10.1016/j.bbr.2009.10.014 (2010).
51. Tartar, J. L. *et al.* Experimental sleep fragmentation and sleep deprivation in rats increases exploration in an open field test of anxiety while increasing plasma corticosterone levels. *Behav Brain Res* **197**, 450–453, https://doi.org/10.1016/j.bbr.2008.08.035 (2009).
52. Andrade, L. A., Lima, J. G., Tufik, S., Bertolucci, P. H. & Carlini, E. A. Rem sleep deprivation in an experimental model of Parkinson's disease. *Arquivos de neuro-psiquiatria* **45**, 217–223 (1987).
53. Tufik, S., Lindsey, C. J. & Carlini, E. A. Does REM sleep deprivation induce a supersensitivity of dopaminergic receptors in the rat brain? *Pharmacology* **16**, 98–105 (1978).
54. Lima, M. M. *et al.* Blockage of dopaminergic D(2) receptors produces decrease of REM but not of slow wave sleep in rats after REM sleep deprivation. *Behav Brain Res* **188**, 406–411, https://doi.org/10.1016/j.bbr.2007.11.025 (2008).
55. Alzoubi, K. H., Khabour, O. F., Tashtoush, N. H., Al-Azzam, S. I. & Mhaidat, N. M. Evaluation of the effect of pentoxifylline on sleep-deprivation induced memory impairment. *Hippocampus* **23**, 812–819, https://doi.org/10.1002/hipo.22135 (2013).
56. Diekelmann, S. & Born, J. The memory function of sleep. *Nature reviews. Neuroscience* **11**, 114–126, https://doi.org/10.1038/nrn2762 (2010).
57. Estrada, C. *et al.* Cognitive impairment after sleep deprivation rescued by transcranial magnetic stimulation application in octodon degus. *Neurotoxicity research* **28**, 361–371, https://doi.org/10.1007/s12640-015-9544-x (2015).
58. Graves, L., Pack, A. & Abel, T. Sleep and memory: a molecular perspective. *Trends in neurosciences* **24**, 237–243 (2001).
59. Tononi, G. & Cirelli, C. Sleep and the price of plasticity: from synaptic and cellular homeostasis to memory consolidation and integration. *Neuron* **81**, 12–34, https://doi.org/10.1016/j.neuron.2013.12.025 (2014).
60. Goel, N., Rao, H., Durmer, J. S. & Dinges, D. F. Neurocognitive consequences of sleep deprivation. *Seminars in neurology* **29**, 320–339, https://doi.org/10.1055/s-0029-1237117 (2009).
61. Prince, T. M. *et al.* Sleep deprivation during a specific 3-hour time window post-training impairs hippocampal synaptic plasticity and memory. *Neurobiology of learning and memory* **109**, 122–130, https://doi.org/10.1016/j.nlm.2013.11.021 (2014).
62. Hagewoud, R. *et al.* Sleep deprivation impairs spatial working memory and reduces hippocampal AMPA receptor phosphorylation. *J Sleep Res* **19**, 280–288, https://doi.org/10.1111/j.1365-2869.2009.00799.x (2010).

63. Kincheski, G. C. *et al.* Chronic sleep restriction promotes brain inflammation and synapse loss, and potentiates memory impairment induced by amyloid-beta oligomers in mice. *Brain, behavior, and immunity* **64**, 140–151, https://doi.org/10.1016/j.bbi.2017.04.007 (2017).
64. Postle, B. R., Locascio, J. J., Corkin, S. & Growdon, J. H. The time course of spatial and object learning in Parkinson's disease. *Neuropsychologia* **35**, 1413–1422 (1997).
65. Souchay, C., Isingrini, M. & Gil, R. Metamemory monitoring and Parkinson's disease. *Journal of clinical and experimental neuropsychology* **28**, 618–630, https://doi.org/10.1080/13803390590935453 (2006).
66. Beeler, J. A., Petzinger, G. & Jakowec, M. W. The enemy within: propagation of aberrant corticostriatal learning to cortical function in Parkinson's disease. *Frontiers in neurology* **4**, 134, https://doi.org/10.3389/fneur.2013.00134 (2013).
67. Aggleton, J. P., Albasser, M. M., Aggleton, D. J., Poirier, G. L. & Pearce, J. M. Lesions of the rat perirhinal cortex spare the acquisition of a complex configural visual discrimination yet impair object recognition. *Behavioral neuroscience* **124**, 55–68, https://doi.org/10.1037/a0018320 (2010).
68. Steckler, T., Drinkenburg, W. H., Sahgal, A. & Aggleton, J. P. Recognition memory in rats–II. Neuroanatomical substrates. *Progress in neurobiology* **54**, 313–332 (1998).
69. Pasupathy, A. & Miller, E. K. Different time courses of learning-related activity in the prefrontal cortex and striatum. *Nature* **433**, 873–876, https://doi.org/10.1038/nature03287 (2005).
70. Ruby, N. F. *et al.* Hippocampal-dependent learning requires a functional circadian system. *Proceedings of the National Academy of Sciences of the United States of America* **105**, 15593–15598, https://doi.org/10.1073/pnas.0808259105 (2008).
71. Cho, J. R. *et al.* Dorsal raphe dopamine neurons modulate arousal and promote wakefulness by salient stimuli. *Neuron* **94**, 1205–1219 e1208, https://doi.org/10.1016/j.neuron.2017.05.020 (2017).
72. Willison, L. D., Kudo, T., Loh, D. H., Kuljis, D. & Colwell, C. S. Circadian dysfunction may be a key component of the non-motor symptoms of Parkinson's disease: insights from a transgenic mouse model. *Exp Neurol* **243**, 57–66, https://doi.org/10.1016/j.expneurol.2013.01.014 (2013).
73. Musiek, E. S. & Holtzman, D. M. Mechanisms linking circadian clocks, sleep, and neurodegeneration. *Science* **354**, 1004–1008, https://doi.org/10.1126/science.aah4968 (2016).
74. Paul, R. *et al.* Hypercholesterolemia causes psychomotor abnormalities in mice and alterations in cortico-striatal biogenic amine neurotransmitters: Relevance to Parkinson's disease. *Neurochemistry international* **108**, 15–26, https://doi.org/10.1016/j.neuint.2017.01.021 (2017).
75. Paul, R. *et al.* Cholesterol contributes to dopamine-neuronal loss in MPTP mouse model of Parkinson's disease: Involvement of mitochondrial dysfunctions and oxidative stress. *PLoS One* **12**, e0171285, https://doi.org/10.1371/journal.pone.0171285 (2017).
76. Gong, H. *et al.* Lipoprotein lipase (LPL) is associated with neurite pathology and its levels are markedly reduced in the dentate gyrus of Alzheimer's disease brains. *The journal of histochemistry and cytochemistry: official journal of the Histochemistry Society* **61**, 857–868, https://doi.org/10.1369/0022155413505601 (2013).
77. Scacchi, R. *et al.* The H+ allele of the lipoprotein lipase (LPL) HindIII intronic polymorphism and the risk for sporadic late-onset Alzheimer's disease. *Neuroscience letters* **367**, 177–180, https://doi.org/10.1016/j.neulet.2004.05.111 (2004).
78. Vespa, G. N. *et al.* Galectin-1 specifically modulates TCR signals to enhance TCR apoptosis but inhibit IL-2 production and proliferation. *Journal of immunology* **162**, 799–806 (1999).
79. Liu, X. *et al.* Impaired synaptic vesicle recycling contributes to presynaptic dysfunction in lipoprotein lipase-deficient mice. *Neuroscience* **280**, 275–281, https://doi.org/10.1016/j.neuroscience.2014.07.080 (2014).
80. Tyurina, Y. Y. *et al.* LC/MS analysis of cardiolipins in substantia nigra and plasma of rotenone-treated rats: Implication for mitochondrial dysfunction in Parkinson's disease. *Free radical research* **49**, 681–691, https://doi.org/10.3109/10715762.2015.1005085 (2015).
81. Newgard, C. B. Interplay between lipids and branched-chain amino acids in development of insulin resistance. *Cell metabolism* **15**, 606–614, https://doi.org/10.1016/j.cmet.2012.01.024 (2012).
82. Luan, H. *et al.* Comprehensive urinary metabolomic profiling and identification of potential noninvasive marker for idiopathic Parkinson's disease. *Scientific reports* **5**, 13888, https://doi.org/10.1038/srep13888 (2015).
83. Wuolikainen, A. *et al.* Multi-platform mass spectrometry analysis of the CSF and plasma metabolomes of rigorously matched amyotrophic lateral sclerosis, Parkinson's disease and control subjects. *Molecular bioSystems* **12**, 1287–1298, https://doi.org/10.1039/c5mb00711a (2016).
84. Lu, Z. *et al.* (1)H NMR-based metabolomics study on a goldfish model of Parkinson's disease induced by 1-methyl-4-phenyl-1,2,3,6-tetrahydropyridine (MPTP). *Chemico-biological interactions* **223**, 18–26, https://doi.org/10.1016/j.cbi.2014.09.006 (2014).
85. Lynch, C. J. & Adams, S. H. Branched-chain amino acids in metabolic signalling and insulin resistance. *Nature reviews. Endocrinology* **10**, 723–736, https://doi.org/10.1038/nrendo.2014.171 (2014).
86. Fernstrom, J. D. Large neutral amino acids: dietary effects on brain neurochemistry and function. *Amino acids* **45**, 419–430, https://doi.org/10.1007/s00726-012-1330-y (2013).
87. Maturana, M. J. *et al.* REM sleep deprivation reverses neurochemical and other depressive-like alterations induced by olfactory bulbectomy. *Molecular neurobiology*. https://doi.org/10.1007/s12035-014-8721-x (2014).
88. Maddison, D. C. & Giorgini, F. The kynurenine pathway and neurodegenerative disease. *Seminars in cell & developmental biology* **40**, 134–141, https://doi.org/10.1016/j.semcdb.2015.03.002 (2015).
89. Havelund, J. F. *et al.* Changes in kynurenine pathway metabolism in Parkinson patients with L-DOPA-induced dyskinesia. *Journal of neurochemistry*, https://doi.org/10.1111/jnc.14104 (2017).
90. Lewitt, P. A. *et al.* 3-hydroxykynurenine and other Parkinson's disease biomarkers discovered by metabolomic analysis. *Movement disorders: official journal of the Movement Disorder Society* **28**, 1653–1660, https://doi.org/10.1002/mds.25555 (2013).
91. Vecsei, L., Szalardy, L., Fulop, F. & Toldi, J. Kynurenines in the CNS: recent advances and new questions. *Nature reviews. Drug discovery* **12**, 64–82, https://doi.org/10.1038/nrd3793 (2013).
92. Nemeth, H., Toldi, J. & Vecsei, L. Role of kynurenines in the central and peripheral nervous systems. *Current neurovascular research* **2**, 249–260 (2005).
93. Sekine, A. *et al.* Amino acids inhibit kynurenic acid formation via suppression of kynurenine uptake or kynurenic acid synthesis in rat brain *in vitro*. *SpringerPlus* **4**, 48, https://doi.org/10.1186/s40064-015-0826-9 (2015).
94. LeWitt, P. A. *et al.* Metabolomic biomarkers as strong correlates of Parkinson disease progression. *Neurology* **88**, 862–869, https://doi.org/10.1212/WNL.0000000000003663 (2017).
95. Barratt, E. S., Adams, P. M., Poffenbarger, P. L., Fritz, R. R. & Abell, C. W. Effects of rapid depletion of phenylalanine and tyrosine on sleep and behavior. *Pharmacology, biochemistry, and behavior* **5**, 47–53 (1976).
96. Sanchez Lopez, C. L. *et al.* Effects of oral administration of L-methionine on activity/rest rhythm. *Acta physiologica Hungarica* **97**, 224–233, https://doi.org/10.1556/APhysiol.97.2010.2.9 (2010).
97. Ansari, R., Mahta, A., Mallack, E. & Luo, J. J. Hyperhomocysteinemia and neurologic disorders: a review. *Journal of clinical neurology* **10**, 281–288, https://doi.org/10.3988/jcn.2014.10.4.281 (2014).
98. Gupta, S. P. *et al.* Does restraining nitric oxide biosynthesis rescue from toxins-induced parkinsonism and sporadic Parkinson's disease? *Molecular neurobiology* **49**, 262–275, https://doi.org/10.1007/s12035-013-8517-4 (2014).
99. Kirbas, S. *et al.* Serum levels of homocysteine, asymmetric dimethylarginine and nitric oxide in patients with Parkinson's disease. *Acta clinica Belgica* **71**, 71–75, https://doi.org/10.1080/17843286.2016.1138592 (2016).

100. Singh, S. *et al.* Involvement of nitric oxide in neurodegeneration: a study on the experimental models of Parkinson's disease. *Redox report: communications in free radical research* **10**, 103–109, https://doi.org/10.1179/135100005X38842 (2005).
101. Dorsey, C. M. *et al.* Phosphorous31 magnetic resonance spectroscopy after total sleep deprivation in healthy adult men. *Sleep* **26**, 573–577 (2003).
102. Tayebati, S. K. *et al.* Effect of choline-containing phospholipids on brain cholinergic transporters in the rat. *Journal of the neurological sciences* **302**, 49–57, https://doi.org/10.1016/j.jns.2010.11.028 (2011).
103. Nie, K. *et al.* Marked N-acetylaspartate and choline metabolite changes in Parkinson's disease patients with mild cognitive impairment. *Parkinsonism & related disorders* **19**, 329–334, https://doi.org/10.1016/j.parkreldis.2012.11.012 (2013).
104. Manyam, B. V., Giacobini, E. & Colliver, J. A. Cerebrospinal fluid choline levels are decreased in Parkinson's disease. *Annals of neurology* **27**, 683–685, https://doi.org/10.1002/ana.410270616 (1990).
105. Barbagallo, G. *et al.* Thalamic neurometabolic alterations in tremulous Parkinson's disease: A preliminary proton MR spectroscopy study. Parkinsonism & related disorders, https://doi.org/10.1016/j.parkreldis.2017.07.028 (2017).
106. Cohen, B. M. *et al.* Decreased brain choline uptake in older adults. An *in vivo* proton magnetic resonance spectroscopy study. *Jama* **274**, 902–907 (1995).

Acknowledgements

We thank the support of Dr Ricardo Fernandez Perez from Physiology Department of UFPR for the facility availability. We wish to express our sincere gratitude to the LC/MS technical support staff, and the Metabolomics Core Facility at the University of Surrey. The Cross-Faculty NMR Centre at Imperial College London and its staff are gratefully acknowledged. This work was supported by the Newton Fund, the Research Councils UK (RCUK), the Conselho Nacional das Fundações de Amparo à Pesquisa (CONFAP) and Fundação Araucária, Research Grant MR/N006321/1 (D.J.S.), Fundação Araucária (Programa de Apoio a Núcleos de Excelência – PRONEX) and in part by the Conselho Nacional de Desenvolvimento Científico e Tecnológico – CNPq. M.M.S.L. is the recipient of a CNPq fellowship, Research Grants 431279/2016-0, 305986/2016-3.

Author Contributions

Conceptualization, M.M.L., D.J.S. and F.M.L.; Methodology, M.M.L., N.R.C, B.M., J.R.S.; Software, D.R.V.D.V. and J.L.A.P.; Validation, M.M.L., B.M., J.L.A.P. and J.R.S.; Formal Analysis, J.F., B.M., J.L.A.P and J.R.S. Investigation, J.F., F.F.S., F.W.C.D., A.D.S.T., A.C.D.N., L.S.R., J.L.I., N.R.C, J.R.S.; Resources, M.M.L., F.M.L., B.M., J.R.S. and D.J.S.; Data Curation, J.F., D.R.V.D.V., J.R.S. N.R.C, B.M. and J.L.A.P.; Writing – Original Draft, J.F.; Writing – Review & Editing, M.M.L., A.D.S.T., A.C.D.N., L.S.R., D.R.V.D.V., B.M., J.L.A.P., J.R.S. and D.J.S.; Visualization, J.F., B.M., J.P., J.R.S. and M.M.L.; Supervision, M.M.L. and D.J.S.; Project Administration, J.F., D.J.S. and M.M.L.; Funding Acquisition, D.J.S., M.M.L., F.M.L., B.M. and J.R.S. All authors read and approved the final manuscript.

Additional Information

Supplementary information accompanies this paper at https://doi.org/10.1038/s41598-018-37657-6.

Competing Interests: The authors declare no competing interests.

Publisher's note: Springer Nature remains neutral with regard to jurisdictional claims in published maps and institutional affiliations.

Chronic sleep restriction in the rotenone Parkinson's disease model in rats reveals peripheral early-phase biomarkers

Juliane Fagotti[1], Adriano D S Targa[1], Lais S Rodrigues[1], Ana Carolina D Noseda[1], Flávia W C Dorieux[1], Franciele F Scarante[1], Jessica L Ilkiw[1], Fernando M Louzada[1], Namrata R Chowdhury[2], Daan R van der Veen[2], Benita Middleton[2], Jeroen L A Pennings[3], Jonathan R Swann[4], Debra J Skene[2] and Marcelo M S Lima[1*]

Supplementary Information

SI Figures and Tables

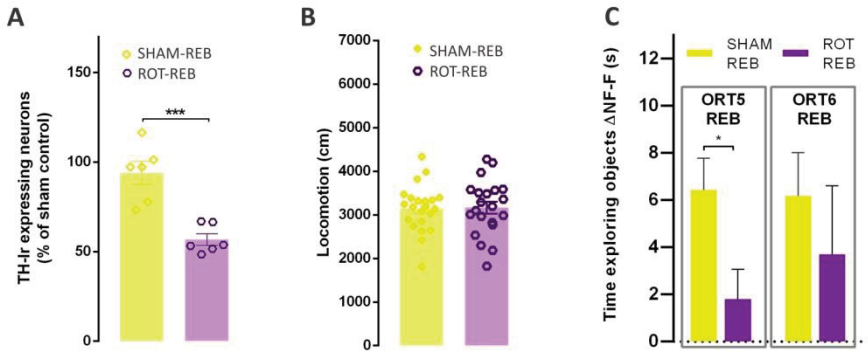

Figure S1. Immunohistochemistry and behavioural parameters after rebound (REB).
(A) Percentage of TH-ir expressing neurons in the SNpc in relation to the SHAM-CT group. Individual data are shown as a scatter plot with bar of mean ± standard error of the mean (SEM n = 6 per group. ***P ≤ 0.001 (Unpaired t-test).
(B) Locomotion parameter obtained from the open field test. Individual data (cm) are shown as a scatter plot with bar of mean ± SEM. Unpaired t-test shows no significant differences. n = 22 SHAM-REB; n = 21 ROT-REB.
(C) Exploration index (ΔNF – F). The bars represent the mean time exploring objects (s) ± SEM one (ORT5) and two weeks (ORT6) after sleep restriction. *P < 0.05 (two-way ANOVA followed by Fisher's LSD test). n = 22 SHAM; n = 21 ROT. NF = non-familiar object; F = familiar object.

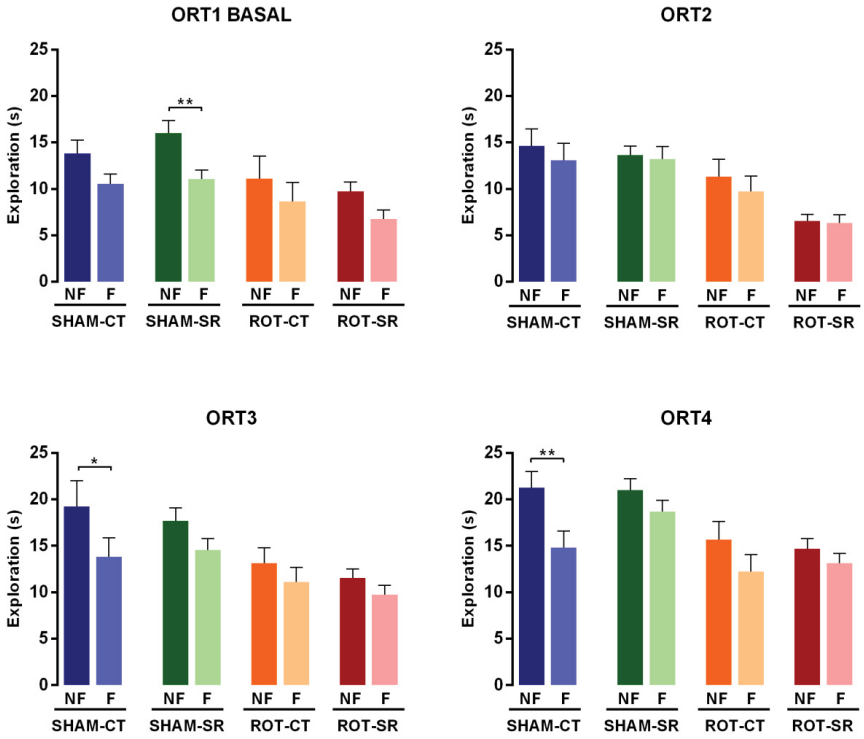

Figure S2. Duration of object exploration in Object Recognition Task.
The bars represent the mean ± SEM exploration time (s) before and during 3 weeks of sleep restriction (SR). *P < 0.05; **P ≤ 0.01 (two-way ANOVA followed by Fisher's LSD test). n = 24 SHAM-CT; n = 24 SHAM-SR; n = 20 ROT-CT; n = 20 ROT-SR. NF: Non-familiar object; F: familiar object.

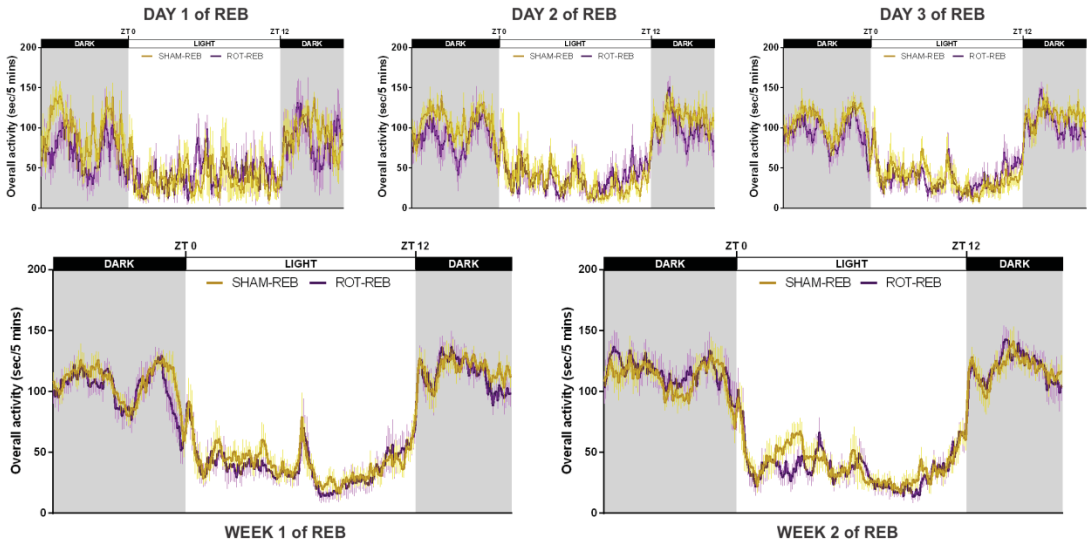

Figure S3. Rest-activity parameters.
(A) Daily activity pattern of each group (SHAM-REB and ROT-REB) during sleep rebound period (REB). Each line represents the mean activity (seconds/5 minutes) of the 21 days ± SEM. ZT0 = 07.00 h - lights on, n = 6 per group.

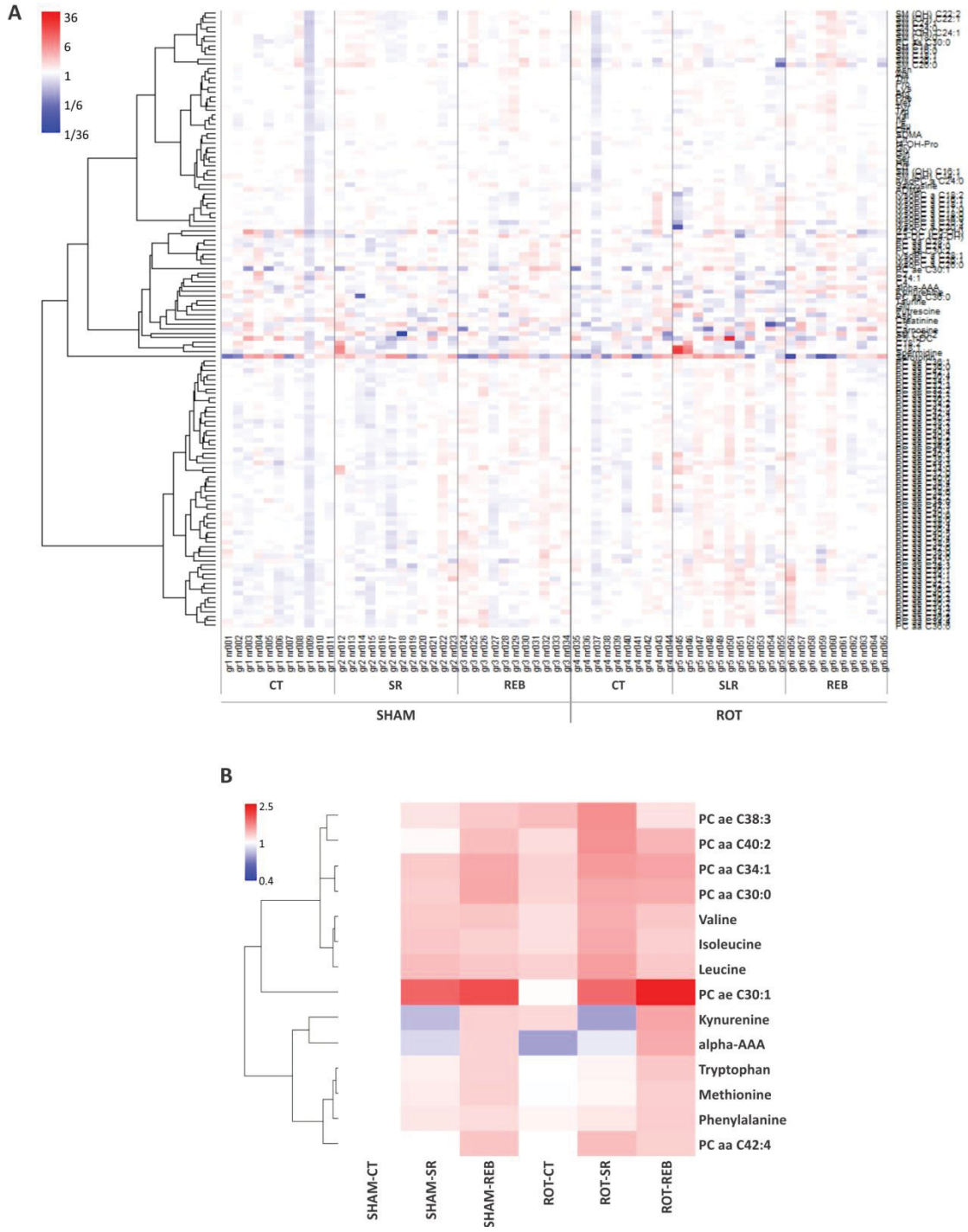

Figure S4. Multivariate analysis of LC/MS metabolomics data.

(A) Heat map combined with hierarchical clustering (Euclidean distance and Ward linkage) of metabolites and experimental groups (n = 6). Colour values are based on the relative value compared to the average value of each metabolite in the complete data set. Higher levels of metabolites are shown in red, lower levels are shown in blue.

(B) Hits from one-way and multivariate ANOVA of metabolites showing significant changes between the experimental groups. Higher levels of metabolites are shown in red, lower levels are shown in blue.

Table S1: OPLS-DA loadings (p(corr) values) of the measured metabolites in the different models

A. Phenotype SHAM vs ROT		B. Sleep restriction CT vs SR		C. Phenotype + sleep restriction	
SHAM-CT vs ROT-CT		SHAM-CT vs SHAM-SR		SHAM-CT vs ROT-SR	
Metabolite	p(corr)	Metabolite	p(corr)	Metabolite	p(corr)
alpha-Aminoadipic acid	-0.415	Creatinine	-0.554	Creatinine	-0.422
Propionylcarnitine	-0.336	Putrescine	-0.530	trans-4-hydroxyproline	-0.409
Glutamate	-0.282	Tetradecenoylcarnitine	-0.395	Acetylcarnitine	-0.386
Tyrosine	-0.279	Symmetric dimethylarginine	-0.354	Tetradecenoylcarnitine	-0.362
Asymmetric dimethylarginine	-0.277	Kynurenine	-0.320	Tyrosine	-0.277
Octadecadienylcarnitine	-0.257	alpha-Aminoadipic acid	-0.308	Asymmetric dimethylarginine	-0.266
Octadecanoylcarnitine	-0.233	trans-4-hydroxyproline	-0.301	Symmetric dimethylarginine	-0.237
Spermidine	-0.224	Glutaconylcarnitine	-0.293	Kynurenine	-0.235
Taurine	-0.221	Acetylcarnitine	-0.283	SM C26:0	-0.233
Acetylcarnitine	-0.209	Malonylhydroxybutyrylcarnitine	-0.247	Propionylcarnitine	-0.217
Creatinine	-0.195	lysoPC a C28:1	-0.237	Carnitine	-0.206
PC ae C36:5	-0.192	PC ae C42:1	-0.180	Butyrylcarnitine	-0.200
trans-4-hydroxyproline	-0.180	PC ae C36:5	-0.175	PC aa C36:0	-0.196
PC ae C44:6	-0.179	PC ae C30:2	-0.154	SM (OH) C14:1	-0.139
Symmetric dimethylarginine	-0.177	SM (OH) C22:1	-0.109	alpha-Aminoadipic acid	-0.137
PC aa C36:0	-0.173	PC aa C40:4	-0.095	SM (OH) C24:1	-0.124
PC aa C42:1	-0.159	Asymmetric dimethylarginine	-0.094	Sarcosine	-0.112
Tetradecanoylcarnitine	-0.157	PC aa C38:5	-0.084	SM (OH) C22:1	-0.090
Threonine	-0.154	Glutarylcarnitine	-0.084	Glutamine	-0.086
Malonylhydroxybutyrylcarnitine	-0.148	Tyrosine	-0.061	Putrescine	-0.064
lysoPC a C26:1	-0.141	PC aa C38:0	-0.043	SM C20:2	-0.060
Glutaconylcarnitine	-0.140	SM (OH) C14:1	-0.042	SM C26:1	-0.054
Serotonin	-0.134	lysoPC a C24:0	-0.035	lysoPC a C20:4	-0.047
SM C26:1	-0.131	PC aa C36:0	-0.028	SM (OH) C16:1	-0.045
SM C26:0	-0.126	Octadecadienylcarnitine	-0.026	Taurine	-0.026
Glutarylcarnitine	-0.109	PC aa C40:6	-0.021	Glutarylcarnitine	-0.025
PC ae C32:1	-0.086	PC ae C40:4	-0.011	Malonylhydroxybutyrylcarnitine	-0.010
Butyrylcarnitine	-0.081	PC aa C42:1	-0.008	Aspartate	0.003
PC aa C42:5	-0.080	PC ae C44:6	0.001	Citrulline	0.042
SM (OH) C14:1	-0.066	lysoPC a C26:1	0.002	Octadecadienylcarnitine	0.046
Carnosine	-0.060	PC ae C38:0	0.003	lysoPC a C28:1	0.060
Methionine	-0.059	PC aa C38:4	0.008	PC ae C44:6	0.070
Alanine	-0.053	SM C16:0	0.016	lysoPC a C18:2	0.087
PC aa C38:0	-0.052	PC ae C44:3	0.021	lysoPC a C26:1	0.091
Glycine	-0.052	SM C20:2	0.025	Glycine	0.097
Tryptophan	-0.050	SM C24:0	0.040	Serotonin	0.097
PC ae C30:2	-0.048	SM C18:1	0.050	SM (OH) C22:2	0.098
Putrescine	-0.029	PC ae C42:4	0.050	Carnosine	0.108
PC ae C44:3	-0.026	PC aa C42:5	0.065	SM C24:1	0.109
Aspartate	-0.010	lysoPC a C26:0	0.070	SM C16:0	0.121
SM C18:1	-0.001	PC aa C34:2	0.073	PC ae C42:1	0.128
PC aa C42:4	0.002	PC aa C32:3	0.073	lysoPC a C18:1	0.142
Serine	0.006	SM (OH) C24:1	0.079	Methionine	0.144
SM (OH) C16:1	0.012	SM (OH) C22:2	0.084	SM C24:0	0.151
PC ae C34:0	0.015	PC aa C36:4	0.096	Tryptophan	0.153
SM C16:0	0.018	PC aa C40:3	0.110	Threonine	0.197
SM (OH) C22:2	0.020	PC aa C40:5	0.115	PC ae C36:5	0.199
Glutamine	0.020	PC ae C38:5	0.120	Glutaconylcarnitine	0.213
Sarcosine	0.024	lysoPC a C20:4	0.120	SM C18:1	0.217
PC aa C32:0	0.027	Serotonin	0.130	PC aa C34:2	0.218
lysoPC a C26:0	0.029	Sarcosine	0.133	lysoPC a C24:0	0.226
PC aa C42:6	0.038	PC aa C34:4	0.134	PC ae C38:0	0.230
SM (OH) C24:1	0.039	PC ae C40:3	0.153	lysoPC a C17:0	0.232
PC aa C40:4	0.043	SM (OH) C16:1	0.160	Alanine	0.237
lysoPC a C28:1	0.055	PC aa C42:4	0.160	Histidine	0.245
Proline	0.056	Glutamine	0.162	PC ae C40:4	0.247
PC ae C32:2	0.060	PC aa C40:2	0.169	PC aa C42:1	0.248
Citrulline	0.066	PC aa C42:6	0.173	PC ae C42:3	0.257
Asparagine	0.070	Citrulline	0.182	PC aa C38:0	0.263
PC aa C24:0	0.074	PC ae C40:2	0.186	Glutamate	0.267
PC aa C36:6	0.076	PC aa C24:0	0.194	PC aa C38:5	0.274
PC aa C38:5	0.091	PC ae C32:2	0.194	lysoPC a C26:0	0.274
SM (OH) C22:1	0.092	PC ae C40:5	0.216	SM C18:0	0.291
PC ae C42:1	0.097	Octadecanoylcarnitine	0.218	lysoPC a C18:0	0.292

PC ae C42:4	0.112	SM C26:1	0.220	PC ae C32:1	0.292
Histidine	0.115	PC ae C32:1	0.221	Asparagine	0.292
SM C24:0	0.116	PC ae C38:4	0.240	Octadecanoylcarnitine	0.296
SM C20:2	0.121	SM C24:1	0.241	PC aa C32:3	0.298
PC aa C42:2	0.125	Propionylcarnitine	0.249	PC aa C42:6	0.305
lysoPC a C24:0	0.125	PC ae C40:1	0.252	PC aa C38:4	0.309
PC ae C38:5	0.129	PC aa C28:1	0.256	PC ae C38:6	0.311
PC aa C40:6	0.130	Glycine	0.258	PC ae C30:2	0.316
lysoPC a C20:4	0.131	PC aa C36:6	0.264	PC ae C42:4	0.318
PC ae C30:1	0.132	Butyrylcarnitine	0.266	PC ae C32:2	0.322
PC aa C36:5	0.133	Glutamate	0.270	PC ae C40:1	0.324
Kynurenine	0.144	PC aa C36:5	0.271	PC ae C38:5	0.324
PC ae C36:4	0.147	lysoPC a C18:0	0.273	PC aa C36:6	0.326
PC aa C32:3	0.149	PC ae C42:3	0.280	Spermidine	0.328
Phenylalanine	0.151	PC ae C36:4	0.281	Serine	0.330
Arginine	0.177	PC aa C38:3	0.282	PC ae C44:3	0.334
Lysine	0.180	SM C16:1	0.286	lysoPC a C16:0	0.336
PC aa C34:2	0.191	Serine	0.290	Phenylalanine	0.337
PC aa C38:4	0.191	Histidine	0.299	PC aa C42:5	0.344
PC aa C34:4	0.192	lysoPC a C18:1	0.311	Proline	0.347
SM C18:0	0.196	SM C18:0	0.329	lysoPC a C16:1	0.353
PC aa C36:4	0.197	PC ae C40:6	0.333	PC aa C38:6	0.361
PC aa C40:5	0.201	PC aa C34:3	0.338	PC aa C40:4	0.396
PC ae C38:0	0.211	PC aa C36:2	0.344	PC ae C30:1	0.401
SM C16:1	0.221	PC ae C38:2	0.344	PC ae C34:3	0.405
PC ae C40:3	0.236	PC ae C34:3	0.353	PC ae C40:6	0.409
PC aa C28:1	0.246	Tryptophan	0.363	lysoPC a C20:3	0.412
Carnitine	0.257	SM C26:0	0.369	PC ae C36:4	0.417
PC ae C40:4	0.277	PC ae C34:1	0.369	SM C16:1	0.419
PC ae C42:3	0.287	Asparagine	0.378	PC aa C34:4	0.421
PC aa C40:3	0.291	Spermidine	0.378	PC aa C40:3	0.424
SM C24:1	0.303	Taurine	0.384	PC aa C28:1	0.425
lysoPC a C18:2	0.308	PC ae C38:6	0.386	PC aa C40:6	0.436
PC ae C40:1	0.310	Threonine	0.392	Lysine	0.463
PC aa C40:2	0.311	Methionine	0.398	PC ae C36:0	0.468
lysoPC a C18:0	0.317	Carnosine	0.400	PC aa C36:5	0.485
PC ae C34:1	0.327	PC aa C32:1	0.406	PC aa C36:2	0.491
PC ae C34:3	0.331	PC ae C42:2	0.409	PC aa C32:0	0.492
PC aa C38:6	0.338	PC ae C36:0	0.414	PC ae C34:0	0.498
PC ae C36:0	0.345	lysoPC a C16:1	0.419	PC ae C38:2	0.501
PC aa C38:3	0.346	PC aa C32:0	0.425	PC ae C40:2	0.503
Isoleucine	0.347	PC ae C38:3	0.430	PC ae C38:4	0.509
PC ae C38:4	0.348	Aspartate	0.432	PC ae C34:1	0.510
lysoPC a C18:1	0.349	PC aa C42:2	0.436	PC aa C36:4	0.514
Ornithine	0.351	Lysine	0.444	Arginine	0.514
PC ae C40:2	0.355	Alanine	0.452	PC aa C42:4	0.521
lysoPC a C16:1	0.365	PC ae C36:3	0.453	PC ae C34:2	0.541
PC aa C36:1	0.367	lysoPC a C18:2	0.463	PC aa C24:0	0.546
PC ae C42:2	0.383	PC ae C36:1	0.467	PC aa C40:5	0.547
Valine	0.396	lysoPC a C16:0	0.471	PC ae C40:3	0.548
PC aa C30:0	0.398	Phenylalanine	0.471	PC ae C40:5	0.565
lysoPC a C20:3	0.402	PC ae C34:0	0.475	PC aa C42:2	0.577
lysoPC a C16:0	0.404	Carnitine	0.480	PC ae C36:3	0.588
PC ae C40:5	0.405	lysoPC a C17:0	0.496	PC aa C36:3	0.598
PC ae C38:6	0.405	Arginine	0.500	PC aa C34:3	0.599
PC aa C34:1	0.406	PC aa C38:6	0.504	PC ae C42:2	0.604
PC aa C36:2	0.413	PC ae C30:1	0.508	PC ae C36:1	0.629
PC aa C36:3	0.415	PC aa C36:1	0.530	PC aa C36:1	0.650
lysoPC a C17:0	0.436	PC aa C30:0	0.541	PC aa C40:2	0.674
PC aa C34:3	0.436	lysoPC a C20:3	0.549	PC aa C38:3	0.674
PC ae C36:3	0.439	Proline	0.549	PC aa C30:0	0.677
PC ae C40:6	0.452	PC aa C36:3	0.557	Ornithine	0.687
PC aa C32:1	0.458	PC aa C34:1	0.563	PC ae C36:2	0.701
PC ae C38:3	0.465	PC ae C34:2	0.565	PC ae C38:3	0.761
Leucine	0.469	Isoleucine	0.576	PC aa C34:1	0.780
PC ae C38:2	0.472	Valine	0.578	PC aa C32:1	0.789
PC ae C36:1	0.502	Leucine	0.580	Leucine	0.810
PC ae C36:2	0.509	PC ae C36:2	0.594	Isoleucine	0.814
PC ae C34:2	0.545	Ornithine	0.668	Valine	0.849

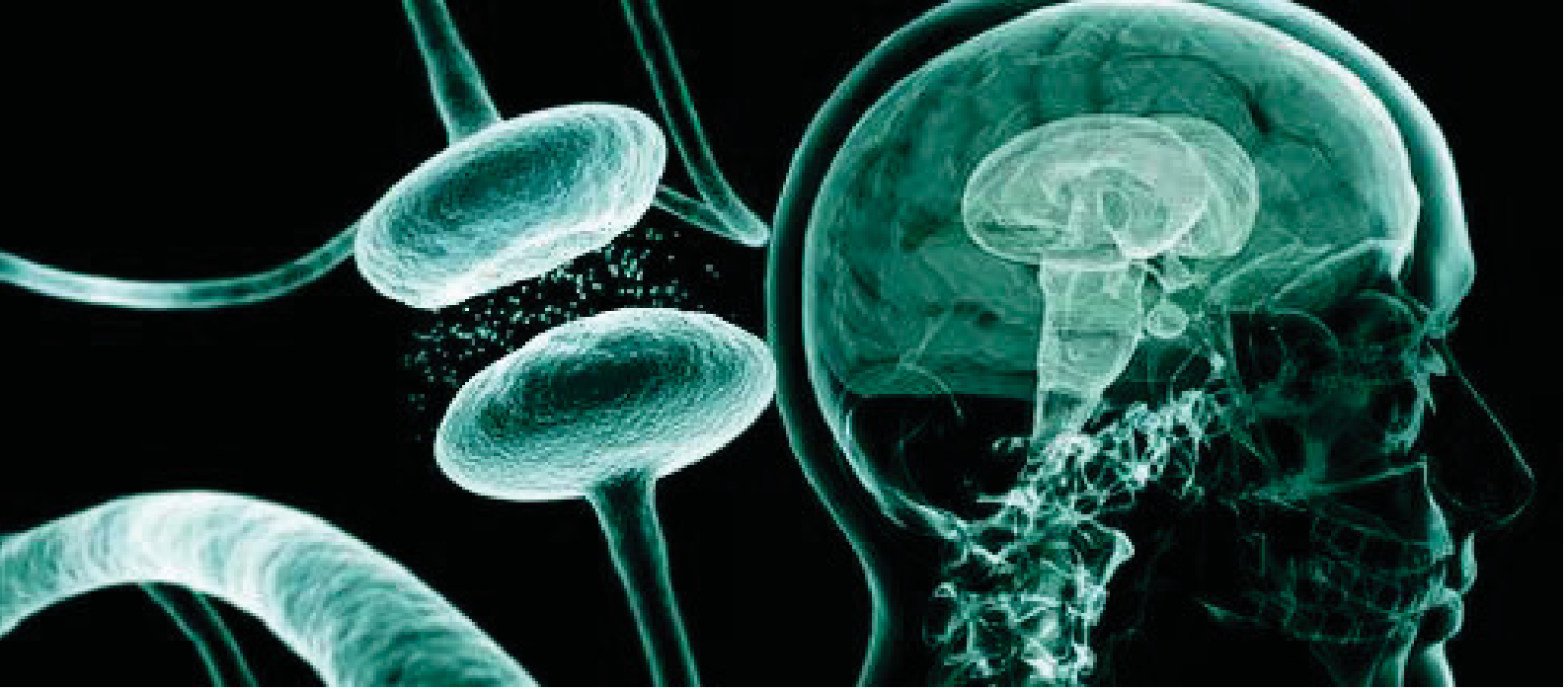

- CHAPTER 2 -

Neurochemical profile and Urine and Gut Content Metabolomic

Stability in metabolic phenotypes in face of chronic sleep restriction and rotenone-induced Parkinson's disease

Juliane Fagotti[1,2], Natasa Giallourou[3], Adriano D S Targa[1,3], Lais S Rodrigues[1,3], Ana Carolina D Noseda[1,3], Fernando M Louzada[1], Debra J Skene[4] Jonathan R Swann[2] and Marcelo M S Lima[1,3]*

Abstract

Parkinson's disease (PD) is the fastest-growing neurodegenerative disorder in the world, with prevalence rates doubling with each generation, making the search for a reliable, early-disease biomarker that reflects underlying pathology a high priority research. Although there is increasing research in the pathogenesis of PD, we still face challenges in the ability to make a definitive diagnosis. Still today, it relies in the clinical presentation of the disease, even if converging evidence suggests the initiation of PD-specific pathology prior to the initial presentation of these classical motor features by years or decades, characterised by non-motor symptoms, such as sleep disturbances. Therefore, the identification of PD biomarkers along with prodromal symptoms is inestimable to develop a sensible diagnostic and gain mechanistic insights into PDs pathogenesis. We previously showed differences in behaviour and plasma metabolic profiles of the rotenone PD-model in rats which became more prominent if challenged by chronic sleep restriction. In the present study, we aimed to further investigate whether alterations could also be seen in different tissues, revealing a global phenotypic metabolic fingerprint of the model. ^{1}H NMR spectroscopy has been applied to phenotype the metabolomes of urine and stool samples and the neurochemical profiles of brain extracts from substantia nigra pars compacta (SNpc), hippocampus and striatum. Supervised statistical analysis yielded no models that possessed statistically significant predictive value on the basis of the metabolic profile, confirming that metabolite profiles were remarkably unaffected either by chronic sleep restriction or rotenone infusion, indicating resilience of the metabolic network regardless observed plasma variations or suggesting that any metabolic disturbance associated with this model is untraceable with ^{1}H NMR.

Keywords: Parkinson's disease biomarkers, rotenone, metabolic profiling, metabolomics, metabolome, Nuclear Magnetic Resonance spectroscopy.

*Correspondent author: marcelomslima.neuro@gmail.com; mmslima@ufpr.br (M.M.S. Lima).
Federal University of Paraná (UFPR), Biological Sciences Division, Department of Physiology, Laboratory of Neurophysiology, Av. Francisco H. dos Santos s/n, ZIP: 81.531– 990, Caixa Postal: 19031, Curitiba, Paraná, Brazil.

[1] Department of Physiology, Federal University of Paraná, Curitiba, PR, Brazil.
[2] Department of Metabolism, Digestion and Reproduction, Faculty of Medicine, Imperial College London, South Kensington, London, UK
[3] Department of Pharmacology, Federal University of Paraná, Curitiba, PR, Brazil.
[4] Chronobiology, Faculty of Health and Medical Sciences, University of Surrey, Guildford, UK.

1. Introduction

Parkinson's disease (PD) is a complex, heterogeneous and progressive neurodegenerative disorder, and the fastest growing neurological disease in the world, affecting more than 6.1 million in the world, a number expected to double in the next generation (DORSEY; ELBAZ; NICHOLS; ABD-ALLAH *et al.*, 2018). Although there is increasing research regarding the pathogenesis of PD, we still face challenges in the ability to make a definitive diagnosis, which still today relies on the same symptoms seen in the first description of the disease, more than two hundred years ago (MARSILI; RIZZO; COLOSIMO, 2018). These symptoms, however, generally emerge when neurodegeneration has reached more than 50% of the substantia nigra pars compacta (SNpc), (FEARNLEY; LEES, 1991), the canonical feature of PD. Even though, diagnosis in this early stage of the clinical presentation of the disease has relatively poor accuracy (ADLER; BEACH; HENTZ; SHILL *et al.*, 2014), making the pursuit for biomarkers a surpassing need to improve diagnostic accuracy in living patients.

Notwithstanding, converging evidence from clinical, genetic, neuropathological and imaging studies suggests the initiation of PD-specific pathology prior to the initial presentation of these classical clinical motor features by years or even decades (TOLOSA; PONT-SUNYER, 2011). This prodromal phase is tied with non-motor symptoms (NMS), such as cognitive deficits, gastrointestinal dysfunction and sleep disturbances (LIMA, 2013; LIMA; MARTINS; DELATTRE; PROENCA *et al.*, 2012; TOLOSA; PONT-SUNYER, 2011; VIDENOVIC; GOLOMBEK, 2013) but they still fall poor in being taking into account in the diagnosis, even if sleep and some other NMS are currently more informative in following the progression of the disease than other markers (MOLLENHAUER; ZIMMERMANN; SIXEL-DORING; FOCKE *et al.*, 2016). In fact, sleep alterations, from rapid eye movement (REM) sleep behaviour disorder to reduced sleep efficiency and increased fragmentation, all leading to sleep loss, are an integral part of PD (GARCIA-BORREGUERO; LARROSA; BRAVO, 2003; TANDBERG; LARSEN; KARLSEN, 1998), and could be contributing for the progression of the disease itself and other NMS, modulating or even exacerbating parameters associated with disease progression (DOS SANTOS; CASTRO; JOSE; DELATTRE *et al.*, 2013; FAGOTTI; TARGA; RODRIGUES; NOSEDA *et al.*, 2019; JUNHO; KUMMER; CARDOSO; TEIXEIRA *et al.*, 2018; SOBREIRA; SOBREIRA-NETO; PENA-PEREIRA; CHAGAS *et al.*, 2019), possibly producing

detectable changes in peripheral tissues such as urine and the intestinal microbiota. Indeed, sleep quality can influence gut microbiome (ANDERSON; CARROLL; AZCARATE-PERIL; ROCHETTE *et al.*, 2017) and epidemiological studies have reported metabolic changes in microbiota due to aging, showing the importance of better understanding these processes in aging-related diseases (SWANN; SPAGOU; LEWIS; NICHOLSON *et al.*, 2013). Intestinal microbiota and its metabolites are strongly implicated in the pathogenesis and progression of PD as a promoting agent and even as a non-motor sign of the disease (KLINGELHOEFER; REICHMANN, 2017; SAMPSON; DEBELIUS; THRON; JANSSEN *et al.*, 2016).

Using the rotenone (ROT) model of PD in rats, we have previously showed that sleep restriction (SR), and in the PD context particularly, can engender several behavioural and biochemical alterations, revealing a metabolic signature of the disease in plasma (FAGOTTI; TARGA; RODRIGUES; NOSEDA *et al.*, 2019). Based on our previous findings, we hypothesized that other tissues would also exhibit modified biochemical profiles in face of rotenone (ROT) lesion and SR, which in turn could unravel metabolic pathways implicated in the disease. For that, we examined the functional potential of intestinal content and urine to provide biomarkers of early-stage PD associated with chronic sleep loss, in view of the fact that a combination of biomarkers can improve the diagnostic accuracy of individual biomarkers, especially if considered the heterogeneity of the disease. Even more, if associated with the information obtained from neurochemical analysis, these findings would contribute for neuroprotective therapies with upcoming disease-modifying drugs that might slow or even prevent the progression of PD.

2. Methods

2.1 Study Design

Subjects

The experiments were performed on healthy male Wistar rats, 90 days old, weighing 280-330 g, with normal immune status. Experimental animals were not involved in any previous test or drug treatment. The animals were group housed (4 per cage) in polypropylene cages with disposable bedding on a standard light-dark (L/D) cycle (12 h:12 h cycle) in a

temperature-controlled room (22 ± 2 ºC). Food and water were provided ad libitum throughout the experiment.

All animal procedures were approved by the Ethics Committee of the Federal University of Paraná (approval ID #858) and conducted according to the guidelines of ethics and experimental care and use of laboratory animals (SBCAL). The research protocols were reviewed by The University of Surrey Animal Welfare Ethical Review Body (AWERB) and by the Named Veterinary Surgeon (NVS) prior to any work, in accordance with the principles of UK legislation (Animals [Scientific Procedures] Act 1986).

Experimental design

Figure 1 shows the group distribution flowchart and a timeline diagram of the study design. Animals were randomly distributed in one of the four groups: SHAM-CT (vehicle infusion and control for sleep restriction) / SHAM-SR (vehicle infusion and sleep restriction condition) /ROT-CT (rotenone infusion and control for sleep restriction) / ROT-SR (rotenone infusion and sleep restriction condition). Sample size is specified in the figure. One week before the experiments begin, the animals were maintained in the room described above for habituation. On day 0, the animals underwent stereotaxic surgery. After a 10-day interval for recovery, the animals underwent to 21 days of sleep restriction. At day 32, the animals were sacrificed.

Stereotaxic surgery

The animals were initially sedated with intraperitoneal xylazine (10 mg/kg) and anaesthetized with ketamine (90 mg/kg). For rotenone (ROT) or vehicle (SHAM) (dimethyl sulfoxide - DMSO) infusion within the SNpc, the following coordinates was used, bregma as a reference: (AP) - 5.0 mm, (ML) ± 2.1 mm and (DV) - 8.0 mm (PAXINOS; WATSON, 2005). ROT (12 µg/µL) or DMSO infusions of 1 µL into each hemisphere were made at a rate of 0.33 µL/min for 3 min (RODRIGUES; TARGA; NOSEDA; AURICH *et al.*, 2014). These infusions were made using an electronic infusion pump (Insight Instruments, Ribeirão Preto, SP, Brazil).

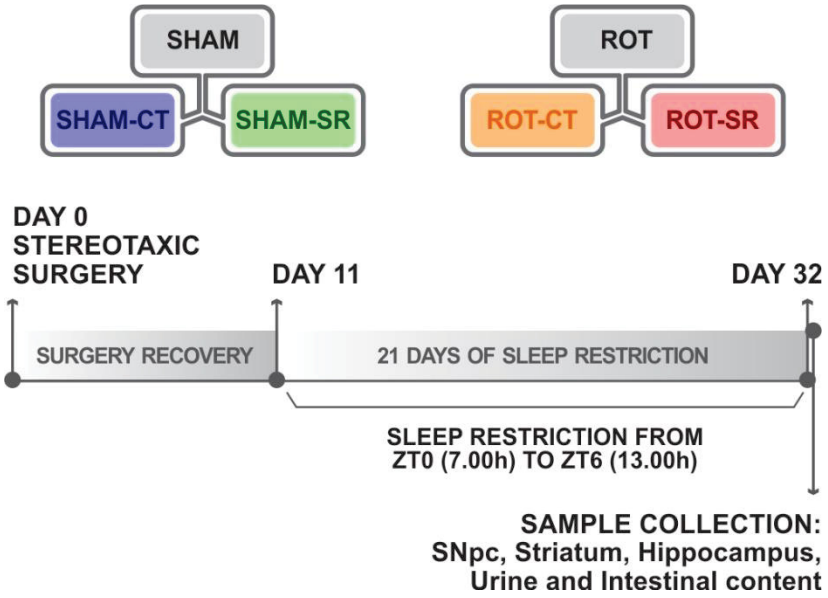

Figure 1. Group distribution and timeline diagram. Colours are representative of groups throughout the results. SR = Sleep Restriction; SHAM = vehicle; ROT = rotenone; SHAM-CT = sham control for SR (blue); ROT-CT = rotenone control for SR (orange); SHAM-SR = vehicle SR (green); ROT-SR = rotenone SR (red). SNpc, Striatum and Hippocampus, n=8/group (total n = 32); urine and intestinal content = 10/group (total n = 40).

Sleep restriction procedure

SR (4 groups) was performed using a gentle handling/stimulation protocol, which consisted of soft tapping on, gently shaking the cage or, when this was not enough to keep animals awake, gently disturbing the sleeping nest (FAGOTTI; TARGA; RODRIGUES; NOSEDA *et al.*, 2019; VAN DER BORGHT; FERRARI; KLAUKE; ROMAN *et al.*, 2006). CT animals (2 groups) were left undisturbed.

2.2 ^{1}H NMR -based metabolic profiling

Sample collection and preparation

Urine samples were collected from bladder puncture right after anaesthesia and stored at −80 °C (n=40, 10 per group). Before preparation, samples were thawed at room temperature. Then, 540 µL of sample was mixed with 60 µL ^{1}H NMR phosphate buffer (pH 7.4 in D_2O) containing 1 mM of internal standard, 3-(trimethyl-silyl)-[2,2,3,3,-2H4]-propionic acid (TSP) as a chemical shift reference. Samples were vortexed and particles were removed by centrifugation (16,000g for 10 min) before transferring 550 µL into a 5mm ^{1}H NMR tube.

Low intestine sections were collected right after anaesthesia and stored at −80 °C (n=40, 10 per group). Samples were thawed thoroughly at room temperature and the intestinal content was separated from the gut wall. 50mg of faeces were weighted and 1mL of HPLC-grade water was added. Samples were homogenised with a bead beater for 40s at 6,500 rpm, then centrifuged for 20 mins at 13,000 g. 400 µL of supernatant (faecal water) was combined with 200 µL ^{1}H NMR phosphate buffer (pH 7.4 in D_2O) containing 1 mM of internal standard (TSP) and faecal water was vortexed and centrifuged at 16,000 g for 10 min, before 550 µL of the supernatant was transferred to a 5 mm outer diameter ^{1}H NMR Tube.

SNpc (n=32, 8 per group), hippocampus (n=32, 8 per group), and striatum (n=32, 8 per group), were removed after decapitation. Aqueous metabolites were extracted using a tissue lyser, brain tissue was homogenized in 300 µL of chloroform:methanol (2:1 v/v). The homogenate was combined with 300 µL of water, mixed by vortexing and centrifuged at 13,000 g for 10 min. The upper aqueous phase was separated from the lower organic phase and the water: methanol was removed using a vacuum concentrator (SpeedVac). The aqueous phase was reconstituted in 550 µL of phosphate buffer (pH 7.4 in D_2O) containing 1 mM of TSP. Aqueous extracts were vortexed and centrifuged at 16,000 g for 10 min, before 550µL of the supernatant was transferred to a 5 mm outer diameter ^{1}H NMR tube.

Data acquisition - ^{1}H NMR spectroscopy

^{1}H NMR spectra of urine and brain tissue extracts was acquired at 300 K on a Bruker 600 MHz spectrometer (Bruker Biospin, Karlsruhe, Germany) and faecal water spectra was obtained in a 600 MHz Bruker 600 MHz AVANCE III HD BBI probe spectrometer (Rheinstetten, Germany), using the following standard one-dimensional pulse sequence with water peak suppression using a standard pulse sequence: relaxation delay (RD)−90◦-t−90◦-tm−90◦-acquire free induction decay (FID), where 90◦ represents the applied 90◦ radio frequency (rf) pulse, t is an interpulse delay set to a fixed interval, RD was 2 sand tm (mixing time) was 100 ms. For each sample, eight dummy scans were followed by 128 scans and collected in 64 K data points using a spectral width of 12 parts per million (ppm) for urine and brain tissue and 16 ppm for faecal water. Before data analysis, ^{1}H NMR spectra were

manually corrected for phase and baseline distortions if necessary, using the reference standard TSP.

Data Pre-processing

The ^{1}H NMR spectra (δ 0·2–10·0) were digitised into consecutive integrated spectral regions of equal width using MATLAB (version R2018b, The Mathworks, Inc.; Natwick, MA) using an in-house script (https://csmsoftware.github.io/docs/impacts/index.html). The raw spectra were referenced to the TSP singlet at δ 0.0 using TOPSPIN (version 3.1, Bruker BioSpin). The regions containing signals from urea (δ 5.5–6.0), residual water (δ 4·7–5·2) and TSP (δ -0.2–0.2) were removed to minimise baseline effects. Spectra were then manually aligned to adjust for variation in chemical shift and probabilistic quotient normalisation was applied to the spectra in order to control for the variability between samples and instrument response drifts (DIETERLE; ROSS; SCHLOTTERBECK; SENN, 2006).

Chemometric modelling/Data Analysis

Data were imported into SIMCA-P 16.0.1 (Umetrics, Umea, Sweden), mean-centred and Pareto-scaled. Unsupervised multivariate statistics and more specifically Principal Component Analysis (PCA) was performed to identify sources of variation in the metabolic data, in order to ensure that the observed variability had biological and not analytical/technical origin (batch, sample weight) and to create an overview and showing trends, groupings and outliers in the data. Any outstanding outlier was removed if necessary (dilution effects, contaminants, etc).

Following removal of extreme outliers, supervised multivariate statistics and Orthogonal Partial Least-Squares Discriminant Analysis (OPLS-DA) in particular, with 7-fold cross-validation (default) analysis, was applied in order to identify class-separating variables and to find pair-wise differences between groups. The Q^2 (predicted variation; “goodness of predictability”) and R^2 (explained variation; “goodness of fit”) parameters were used to evaluate the models, followed by permutation test by 100 for validation and pCV-ANOVA for significance. Results were visualized using the OPLS-DA scores produced on SIMCA and

loadings plots by an in-house developed script on MATLAB (https://csmsoftware.github.io/docs/impacts/index.html).

The corresponding chemical shift regions assignments in were based in the Human Metabolome Database (HMDB, http://www.hmdb.ca), an in-house chemical shift assignments list and the software Chenomx Profiler – Chenomx NMR Suite 8.4 (Chenomx Inc., Edmonton, Canada) and further confirmed by Statistical Total Correlation Spectroscopy (STOCSY) on MATLAB (HOLMES; CLOAREC; NICHOLSON, 2006).

2.3 Chemicals and reagents

Xylazine and ketamine were obtained from Syntec do Brasil Ltda. (Brazil). Rotenone and DMSO were purchased from Sigma-Aldrich® (St. Louis, MO, United States). Chloroform, methanol, 3-(trimethylsilyl)-[2,2,3,3,-2H4]-propionic acid (TSP) 3-[2,2,3,3-2H4] trimethylsilyl propionate sodium salt (TSP), ammonium acetate, sodium dihydrogen phosphate and disodium hydrogen phosphate were purchased from Sigma-Aldrich Company, Ltd (Gillingham, UK). NMR -grade deuterium oxide (D_2O), was obtained from Goss Scientific Instruments (Nantwich, UK).

3. Results

Using untargeted ^{1}H NMR spectroscopy, we investigated the putative effects of SR in the ROT/PD model on the metabolic profiles of brain structures commonly affected in PD, urine and gut content, in order to integrate with previously reported alterations in plasma metabolic phenotype. ^{1}H NMR-based metabolic profiling was chosen for its relatively quantitative ability and highly reproducible nature (EMWAS; ROY; MCKAY; TENORI *et al.*, 2019; PAN; RAFTERY, 2007).

PCA analysis was first carried out on ^{1}H NMR-derived data to provide an overview of the variations. PCA is an unsupervised method for assessing variation among samples that ignores the correlation between sample characteristics. For this reason, we also performed OPLS-DA (a supervised classification method) that considers the correlation of variables, including class membership of samples. Whereas PCA looks at overall variation (unsupervised), OPLS-DA distinguishes between class-predictive (discriminating) variation

(supervised) and non-predictive (orthogonal) variation. The use of these methods allows insight into the extent of underlying patterns and class-predictive variation within the data set as a whole.

Brain structures metabolomic profile

Analysis of SNpc, hippocampus and striatum did not display a clear discriminatory metabolic profile. In the SNpc (Figure 2), the first glimpse at data showed 3 spectra that had to be removed (one had a very intense peak on sucrose which was interfering with subsequent analysis and 2 samples were too diluted). After removing these, PCA in non-normalised data revealed a clustering unrelated to a condition (group/weight/batch) (Figure 2A). Loading plots showed that this separation was not being led by any specific signals (Figure 2B), giving no reason to remove these samples. Therefore, to account for any sort of analytical variation across samples, a normalisation with the probabilistic quotient method was applied to achieve a higher quality dataset. PCA from normalised data showed no clustering (Figure 2C) and two outliers were identified. Since inclusion or exclusion of these points made little difference to subsequent supervised analysis, only the analysis with them retained is shown. A pairwise (OPLS-DA) model was obtained comparing the metabolic profiles of SHAM-CT with ROT-CT (Figure 2D) ($R^2X = 0.586$; $R^2Y = 0.843$; $Q^2Y = 0.216$; A = 1 + 3 components). This model was not significant (CV ANOVA $P > 0.05$). The corresponding loading plot is shown in Figure 2E. Even if some features were identified, the loading plot shows a model distinguished by the contribution of very many metabolites, each of which contributing with a small amount of discriminatory power. In same manner, For SHAM-CT vs SHAM-SR, the OPLS-DA model was not significant either (CV ANOVA $P > 0.05$ $R^2X = 0.55$; $R^2Y = 0.918$; $Q^2(cum) = 0.194$; A = 1 + 3 components) and no model was obtained by comparing the groups SHAM-CT and ROT-SR.

For Striatum (Figure 3), 4 samples had to be removed from dataset (2 samples were found to be contaminated with polyethylene glycol – 3.66 ppm and 2 samples had a very intense peak on sucrose). PCA on aligned data showed no trends, either for groups (3A) or weight (3B), and, in this dataset, normalisation by probabilistic quotient generated bad spectra (3C), therefore supervised analyses were performed using the aligned dataset. While an extreme outlier was observed in PCA (sample 3J), the exclusion of this sample made no

difference in subsequent OPLS-DA analysis, which no model was possible to be built for the biochemical profile of striatum between groups.

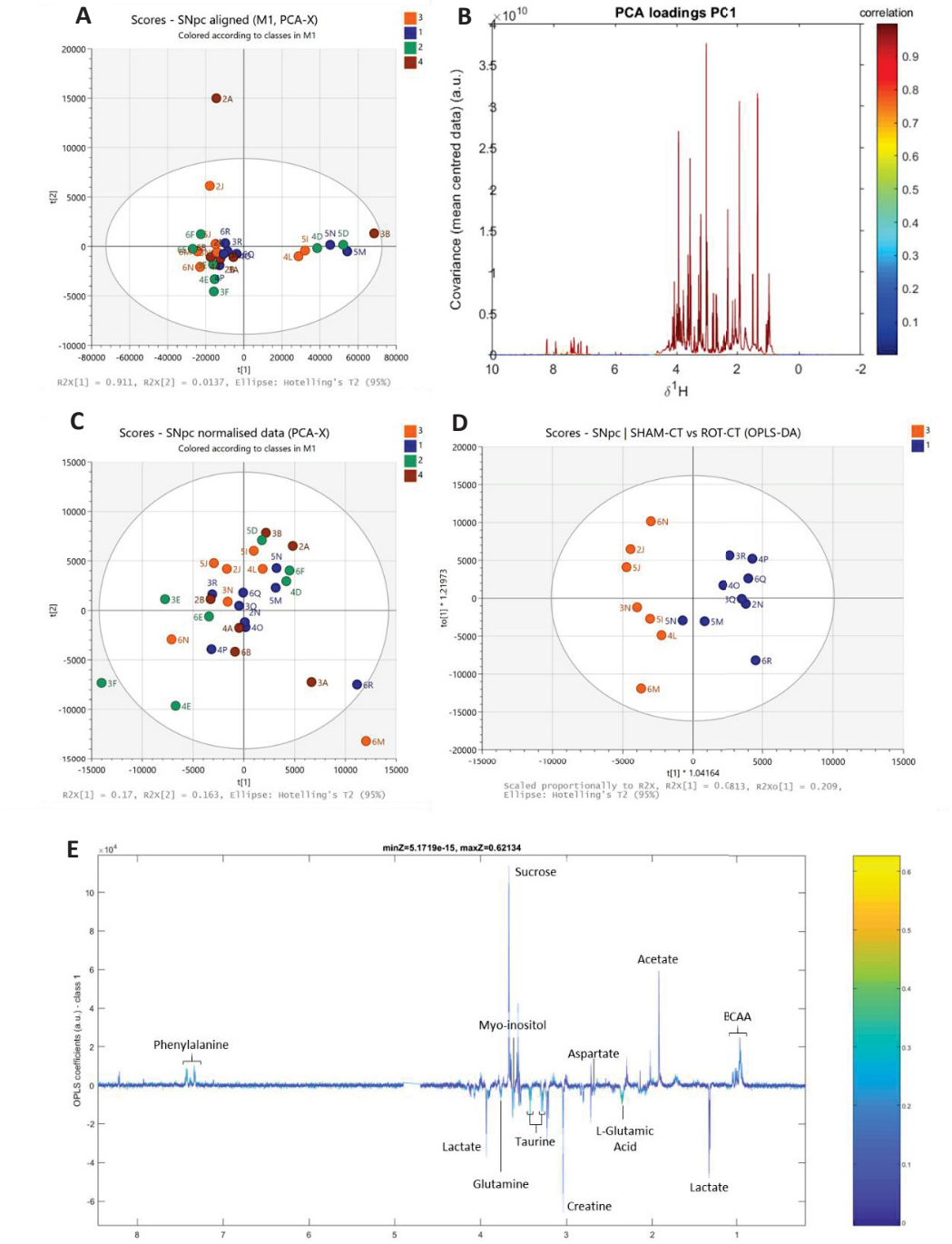

Figure 2. Analysis of SNpc. A) PCA of aligned spectra (n=29, R^2X = 0.94, Q^2(cum) = 0.878, A=4), showing a cluster on t[1], led by B) the many different signals. C) PCA of normalised spectra showing no trends (n=29, R^2X = 0.617, Q^2(cum) = 0.199, A=5), first two principal components shown. D) 600 MHz ^{1}H NMR spectra obtained after normalisation by weight. E) 600 MHz ^{1}H NMR spectra with median fold normalisation.

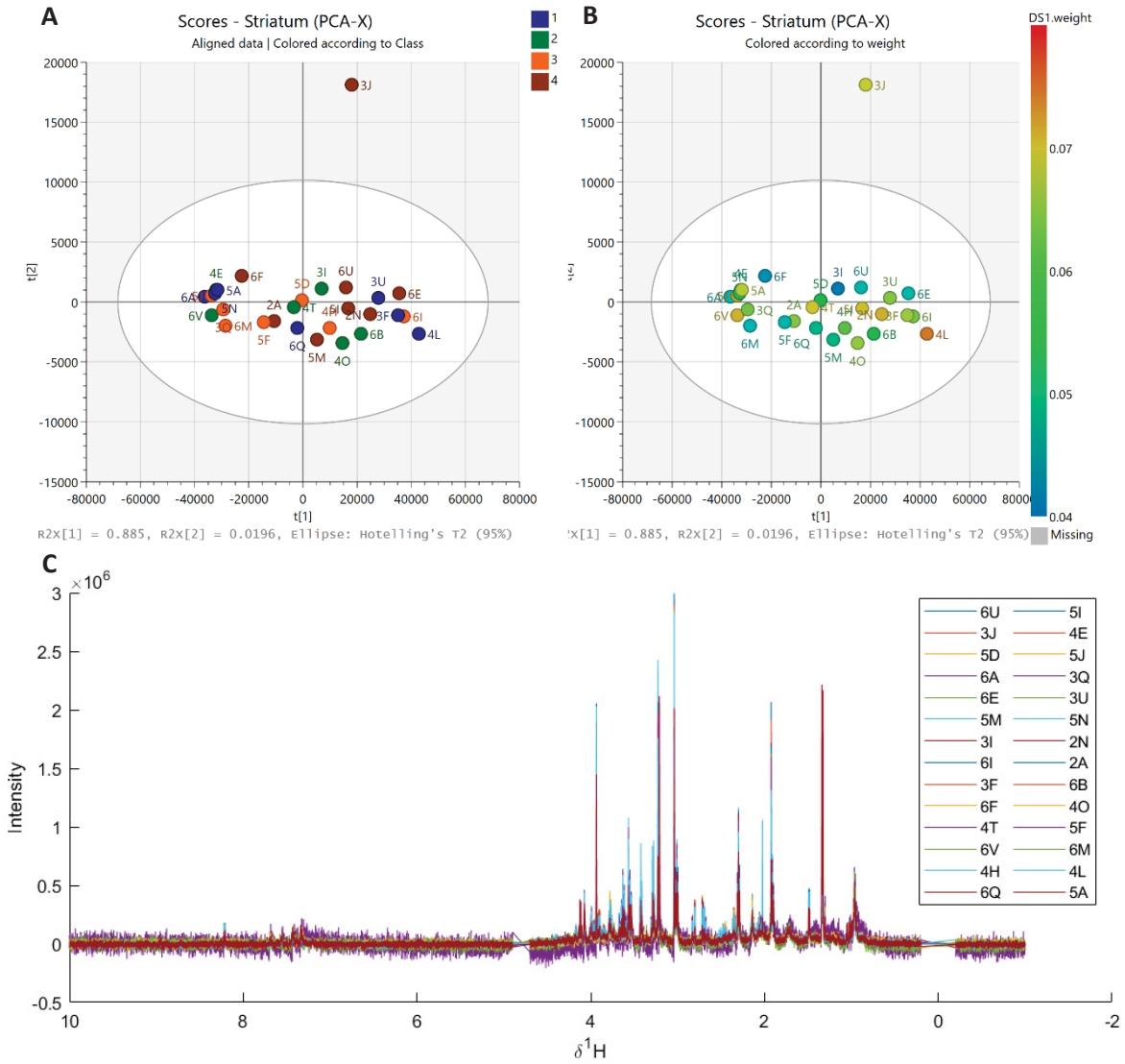

Figure 3. Analysis of Striatum. A) PCA of only aligned spectra, showing no clear separation for groups (n=28, R^2X = 0.937, Q^2(cum) = 0.878, A=4). B) PCA with samples coloured by weight, showing no trend due to sample weight variation. C) 600 MHz ^{1}H NMR spectra obtained by median-fold normalisation.

Hippocampus (Figure 4) samples had a clustering on PCA, which could not be accounted by any group (Figure 4A), although it shows a small tendency for sample weight (Figure 4B), which was not eliminated by sample weight normalisation (Figure 4C and 4D). Normalisation with the probabilistic quotient method could not be used due to bad spectra quality (4E), therefore the subsequent supervised analysis was performed in aligned data only, then again it was not possible to build any model with discriminating groups.

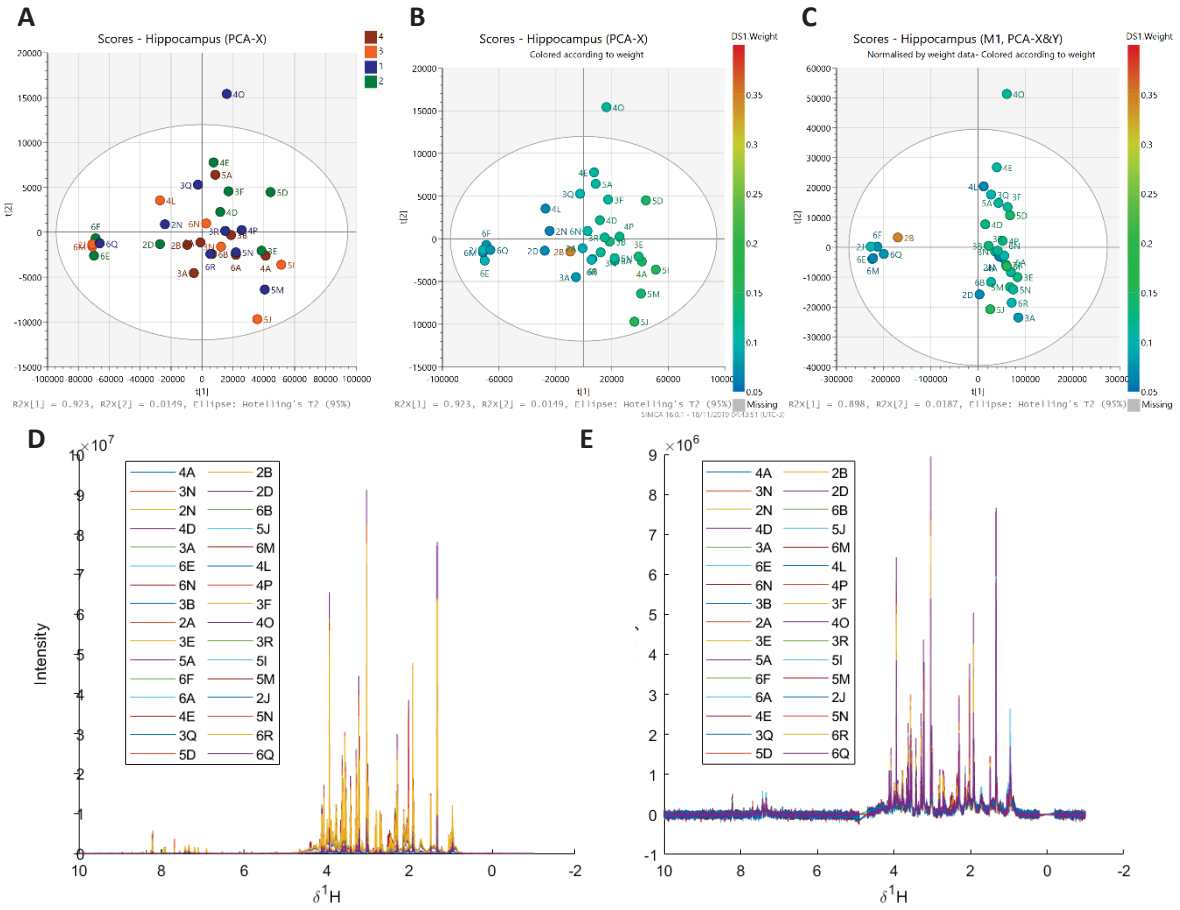

Figure 4. Analysis of Hippocampus. A) PCA of aligned spectra (n=32, R^2X = 0.957, Q^2(cum) = 0.939, A=4), showing a cluster on t[1]. B) PCA with samples coloured by weight, showing a small trend due to sample weight variation. C) PCA of dataset normalised by weight (n=32, R^2X = 0.933, Q^2(cum) = 0.912, A=3), showing a cluster on t[1]. D) 600 MHz ^{1}H NMR spectra obtained by median-fold normalisation. D) 600 MHz ^{1}H NMR spectra after normalisation by weight.

Urine profile

Urine spectra were manually aligned, where 2 samples were removed due to extreme dilution, followed by probabilistic quotient normalisation. Analysis of urine metabolites is shown in Figure 5. PCA (Figure 5A) revealed no clustering and the identification of two outliers, which were included to subsequent supervised analysis with OPLS-DA, since inclusion or exclusion of these points made little difference in the models. Pairwise OPLS-DA revealed a model discriminating the groups SHAM-CT and ROT-CT (Figure 5B), but further validation showed no significance for this model (CV ANOVA P > 0.05).

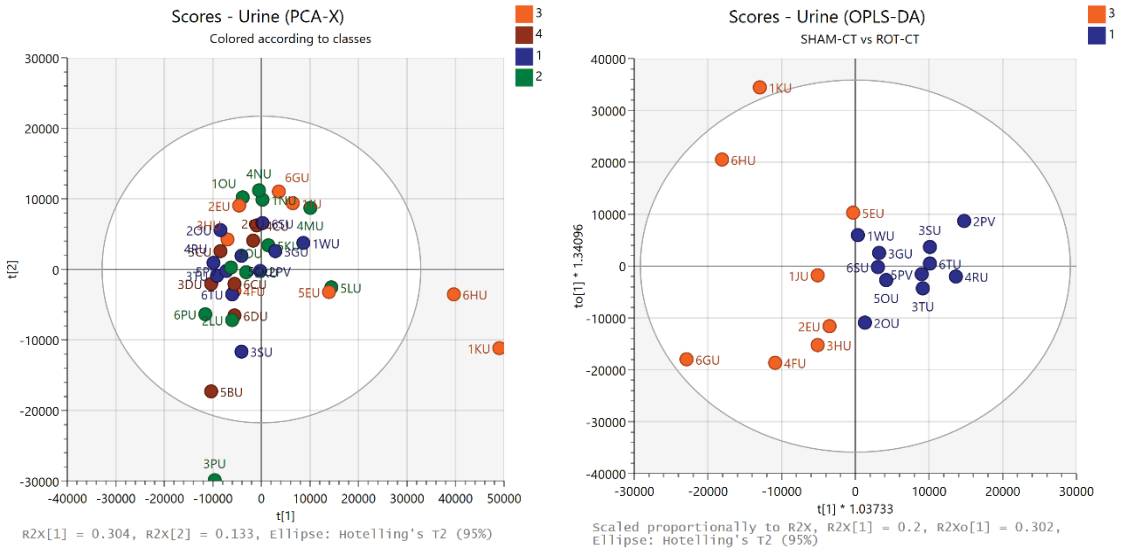

Figure 5. Urine metabolic profile. A) PCA of aligned and normalised spectra (n=37, R^2X = 0.621, Q^2(cum) = 0 .205, A=6). B) OPLS DA model of SHAM CT (dark blue) vs ROT-CT (orange), showing the first two principal components (R^2X = 0.502; R^2Y = 0.668; Q^2Y = 0.277; A = 1 + 1 components; CV ANOVA P=0.3).

Intestinal Content profile

Intestinal content analysis showed a clustering in t[1] after PCA in aligned plus normalised data (Figure 6A), which was not present in the only aligned dataset (Figure 6B). However, by performing supervised analysis with comparison between different groups, no discriminatory metabolic profile was built. Analysing the loadings of the normalised data (Figure 6C) identified that the cluster was a result of increased content of cholic acid, independent of group/batch. Since concentrations of cholic acid can vary along the intestine (DAWSON; KARPEN, 2015), this cluster could be a result of technical/sampling issues, and subsequent analyses were performed after removing these samples. Subsequent pairwise (OPLS-DA) model was obtained comparing the metabolic profiles of SHAM-CT with ROT-CT (Figure 6D) (R^2X = 0.291; R^2Y = 0.801; Q^2Y = 0.136; A = 1 + 1 components), but it was not successfully validated (CV ANOVA P > 0.05). Further non-significant models (CV ANOVA P > 0.05) were also obtained comparing SHAM-CT vs SHAM-SR (6E) (R^2X = 0.443; R^2Y = 0.906; Q^2Y = 0.283; A = 1 + 2 components) and SHAM-CT vs ROT-SR (6F) (R^2X = 0.79; R^2Y = 0.997; Q^2Y = 0.452; A = 1 + 5 components). For the 3 models, there was no clear metabolite-driven discriminatory power, with a diverse set of signals contributing for the dissimilarity.

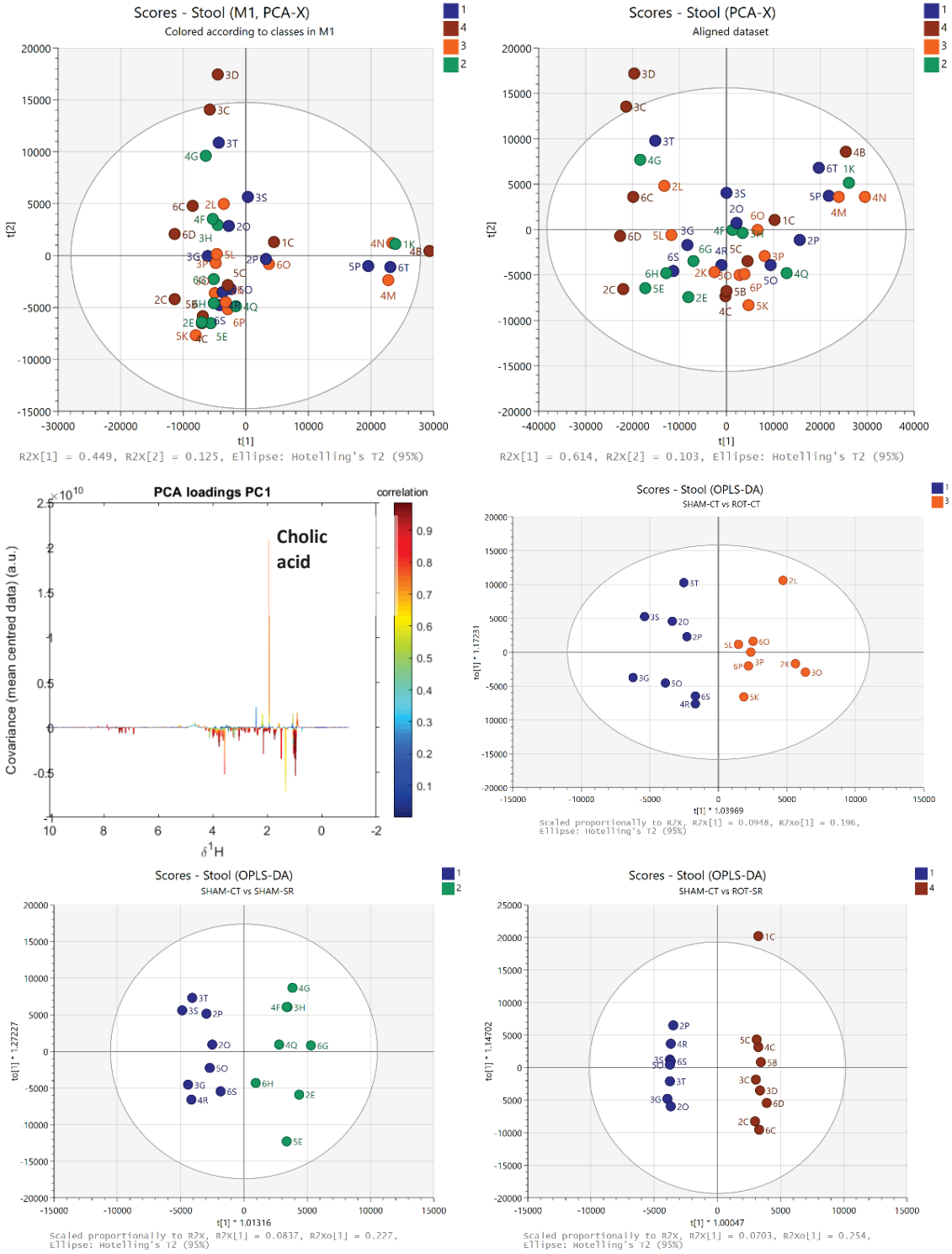

Figure 6. Stool metabolic profile. PCA of aligned and normalised spectra (n=39, R^2X = 0.449, Q^2(cum) = 0.1254, A=4), showing a cluster on t[1]. B) PCA of aligned dataset only (n=39, R^2X = 0.817, Q^2(cum) = 0.714, A=4). C) PCA loadings of normalised dataset showing chemical shift assignment for Cholic acid, (R^2X = 0.933, Q^2(cum) = 0.912, A=3), showing a cluster on t[1].). D) OPLS-DA model of SHAM-CT (dark blue) vs ROT-CT (orange), showing the first two principal components (R^2X =0.291; R^2Y = 0.801; Q^2Y = 0.136; A = 1 + 1 components; (CV ANOVA P > 0.05). E) OPLS-DA model of SHAM-CT (dark blue) vs SHAM-SR (green), showing the first two principal components (R^2X = 0.443; R^2Y = 0.906; Q^2Y = 0.283; A = 1 + 2 components; (CV ANOVA P > 0.05). F) OPLS-DA model of SHAM-CT (dark blue) vs ROT-SR (dark red), showing the first two principal components (R^2X = 0.79; R^2Y = 0.997; Q^2Y = 0.452; A = 1 + 5 components; CV ANOVA P > 0.05).

4. Discussion

We showed previously that SR combined with PD altered several behavioural and plasma metabolic parameters (mainly branched-chain amino acids, tryptophan pathway, phenylalanine, and lipoproteins, all pointing to mitochondrial impairment) in the rat rotenone model (FAGOTTI; TARGA; RODRIGUES; NOSEDA *et al.*, 2019). To shed light on further putative metabolic changes, we performed a metabolite analysis of urine, gut content and brain samples. Our data indicate a stable pattern of phenotyping due to SR and ROT exposition, suggesting that metabolic pathways remain stable in these matrices, showing that changes in plasma metabolome are not necessarily accompanied by different biofluids and brain tissue.

The use of ^{1}H NMR spectroscopy for the analysis of biofluids and tissue extracts provides a convenient means of performing untargeted metabolic profiling for a wide range of abundant metabolites (SWANN; GARCIA-PEREZ; BRANISTE; WILSON *et al.*, 2017). Using this untargeted approach, spectroscopy feature annotation identified a variety of unique metabolite structures, however, it is important to stress that none of these metabolites or a combination of them was discriminatory in any of the investigated biological matrices, once again highlighting the stability of the metabolic phenotype. Interestingly, all obtained spectra had a considerable variability in peak intensity among samples showing that this technique is sensible enough to reveal differences in metabolic pools, but the nature of the observed variability hampers any inference related to the models.

Regarding brain tissue, remarkably we didn't find any reliable variation of biological origin, although nigral rotenone infusion was already shown to produce neurochemical alterations in brains structures (MOREIRA; BARBIERO; ARIZA; DOMBROWSKI *et al.*, 2012; RODRIGUES; TARGA; NOSEDA; AURICH *et al.*, 2014). However, is important to highlight that ^{1}H NMR is 10 to 100 times less sensitive than targeted approaches, like mass spectrometry, with limits of detection on the order of 10 μM (EMWAS; ROY; MCKAY; TENORI *et al.*, 2019; PAN; RAFTERY, 2007) and DA levels and its metabolites, for instance, are in the order of nanograms (RODRIGUES; TARGA; NOSEDA; AURICH *et al.*, 2014). In fact, in another study, using spectroscopy approaches, differences between PD-models and control in brain structures were not identified either (CHASSAIN; BIELICKI; KELLER; RENOU *et al.*, 2010).

However, more recent studies, using multivariate analysis for interpretation of ^{1}H NMR data, have obtained success in differentiate lesioned animals from control (GRAHAM; REY; YILMAZ; KUMAR *et al.*, 2018; LU; ZHANG; ZHAO; YANG *et al.*, 2018; PODELL; HADJICONSTANTINOU; SMITH; NEFF, 2003; VIREL; DUDKA; LATERVEER; AF BJERKEN, 2019; ZHENG; ZHAO; XIA; XU *et al.*, 2016), however different models and protocols were used. Regarding the fact that some samples showed high levels of sucrose in brain sample, unrelated to a specific group, could be accredited to an increase in blood-brain barrier permeability (ALQAHTANI; CHOWDHURY; BHATTACHARYA; NOORANI *et al.*, 2018) lead by DMSO (BRINK; STEIN, 1967; KLEINDIENST; DUNBAR; GLISSON; OUKUNO *et al.*, 2006).

Urine, which contains abundant metabolites, is fairly investigated by untargeted metabolomics in PD research, nonetheless these promising findings reported in the literature were not replicated thus far, mainly due to huge variability in methodologies (COVA; PRIORI, 2018; LUAN; LIU; TANG; ZHANG *et al.*, 2015; MICHELL; MOSEDALE; GRAINGER; BARKER, 2008) and because of the heterogeneity of the disease *per se*, where the etiological variability and its progressive nature is accompanied by the evolution and alterations in physiological markers. As matter of fact, MOLLENHAUER; ZIMMERMANN; SIXEL-DORING; FOCKE *et al.* (2016) have reported that 33% of identified PD biomarkers changed in the course of 24 months. Considering SR, some studies have shown differences in urine metabolites using NMR due to sleep disturbances, like sleep apnoea, and acute sleep deprivation, with some overlapping metabolites, but then again with some variability (GISKEODEGARD; DAVIES; REVELL; KEUN *et al.*, 2015; ZABEK; STANIMIROVA; DEJA; BARG *et al.*, 2015). Our results come together with this lack of reproducible data of urinary fingerprinting. Nonetheless, given the easy availability and non-invasive sampling of urine, it is a very promising matrix for biomarkers for clinical practice, therefore extensive efforts should be applied in finding metabolic signatures in this biofluid.

Faecal metabolome can provide information to look upon the metabolic interactions between host, diet, and gut microbes, presenting a promising avenue to “fingerprint” the functional status of the intestinal microbiota and explore links between microbiome and host phenotypes (SHAO; LE, 2019). Recent investigations have highlighted the crucial role of the gut microbiota in the development of neurodegenerative diseases, including PD (BEDARF; HILDEBRAND; GOESER; BORK *et al.*, 2019; BOERTIEN; PEREIRA; AHO;

SCHEPERJANS, 2019; BOULOS; YAGHI; EL HAYECK; HERAOUI *et al.*, 2019; CHIANG; LIN, 2019; KLINGELHOEFER; REICHMANN, 2015; LUBOMSKI; TAN; LIM; HOLMES *et al.*, 2019; SANTOS; DE OLIVEIRA; YAMADA; NEVES *et al.*, 2019; SMITH; PARR-BROWNLIE, 2019; VAN; DERKINDEREN, 2019). Faecal metabolomic approaches have been widely explored in biomarker discovery, however, only recently it started to be applied in the investigation of neurodegenerative diseases. In PD, some studies have highlighted a reduction of faecal short chain fatty acids (SCFAs) in PD (SHAO; LE, 2019) and even if NMR analysis is able to identify these metabolites, we didn't see a specific fingerprint in ROT and/or SR faecal samples. These results might be due to the fact that our model was based in direct lesion of SNpc; in this case, these results would come against the bi-directional hypothesis of gut-brain axis, once the disruption in the central nervous system doesn't seem to be able to inflict any alteration in the enteric nervous system (SANTOS; DE OLIVEIRA; YAMADA; NEVES *et al.*, 2019). On the other hand, as previously discussed, gut microbiota is the main source of intestinal metabolites, and in this sense, SR was already shown to have no effect in altering gut microbiome composition (ZHANG; BAI; GOEL; BAILEY *et al.*, 2017). Nonetheless, our models from stool samples showed some separation, whilst a poor predictive ability, due to the over-fitting of data, which is relatively common in exploratory studies, because of the large number of metabolites and the relatively small sample size, and the OPLS-DA analysis forces scores in which classes are separated (WORLEY; POWERS, 2013).

Considering SR, independent of PD, despite the effects on overall health, there is no established clinical biomarkers for insufficient sleep. Acute sleep deprivation was shown to induce metabolomic shifts (DAVIES; ANG; REVELL; HOLMES *et al.*, 2014; GISKEODEGARD; DAVIES; REVELL; KEUN *et al.*, 2015; MEJRI; YOUSFI; HAMMOUDA; TAYECH *et al.*, 2017), underscoring the effects on metabolic networks, which may be related to modulation of many physiological functions. But, considering chronic sleep loss, results are not unanimous (MA; SONG; WANG; SHI *et al.*, 2019; MINAMI; TAKAHASHI; SASAKI; MATSUMOTO *et al.*, 2012), and even if we have previously demonstrated plasma metabolic alterations due to SR, our current results face the fact that changes might not affect global metabolic networks or the variability between subjects interfere in the construction of a valid statistical model. Indeed, sleep deficiency shows robust individual responses across subjects due to phenotypic characteristics, and currently the pursuit for sleep loss biomarkers have focused

in identify and predict these phenotypic differences that reflects in an increased vulnerability to neurobehavioural deficits (GOEL, 2015).

In conclusion, our results confirm that metabolic profiles are remarkably unaffected either by SR or rotenone infusion, indicating resilience of the metabolic network regardless previous observed plasma variations or suggesting that any metabolic disturbance associated with PD or SR is untraceable in ^{1}H NMR. Interestingly, previous studies have showed diverse metabolomic variations due to PD status, yet most of them unreproducible. Albeit some of these candidate biomarkers have relatively high diagnostic performance or predictive value for PD and may have the potential to be applied in clinical practice, biomarkers with the function of identifying a population by confirming the clinical diagnosis are still far from being unexceptionally used and we still lack standard evaluations, specificity and sensitivity (LI; LE, 2019). As a matter of fact, even with 20 years of research pursuing these indicators for PD, none of them is specific enough for diagnosis, prediction or determination of disease progression (YILMAZ; HOPFNER; VAN EIMEREN; BERG, 2019). Metabolomic appliance, even with the immense progress in the field, is still at its standardisation phase, with many aspects to tackle, particularly for brain studies (VASILOPOULOU; MARGARITY; KLAPA, 2016).

On the other hand, the lack of variation could be due to the nature of the model, which mimics an early stage of the disease, while previous studies mainly emphasise the biochemical measurements of biofluids in the symptomatic evaluation of PD. An important feature of ROT infusion is that, independent of the route, it leads to a nigrostriatal dopaminergic neurodegeneration with different degrees of severity (BETARBET; SHERER; MACKENZIE; GARCIA-OSUNA *et al.*, 2000; HOGLINGER; FEGER; PRIGENT; MICHEL *et al.*, 2003; SHERER; BETARBET; GREENAMYRE, 2002). This variation of susceptibility among individuals could explain the variability within the group that hinds a standard metabolic phenotype. Moreover, the rotenone model with direct infusion shows absence of overall toxicity, targeting only DA neurons (VOITENKO; NIKONENKO, 2015), and triggers an increase in serotonin levels 30 days after rotenone injection, suggesting a compensatory mechanism due to dopaminergic depletion (MOREIRA; BARBIERO; ARIZA; DOMBROWSKI *et al.*, 2012). This compensatory mechanism could be globalized, with other systems involved, and the absence of variation here observed could be facing a neurorestorative process. Considering

that samples were collected 32 days after the lesion, it would be very plausible to have missed the ideal window of metabolic changes, especially those in the brain. Furthermore, NMR permits a glance in a small fraction of the metabolome, far from a full coverage. Therefore, it may not be the ideal tool to detect more restricted molecular traits.

Alternatively, analytical and technical issues should be addressed: (i) with ^{1}H NMR, metabolites present in very low amounts cannot be detected and, since variations are given in abundances and not in absolute concentrations, small variations might not be evidenced with untargeted, not fully quantitative approaches; (ii) transport – samples may have thawed and degraded, masking possible differences; (iii) sample collection – whereas collection is standardized and no batch effect was noticed, there may be variations, which were evidenced by differences in sample weight. In this sense, even factors that are not taken into account could be underlying the study, like cage environment, which was shown to be capable of inflict metabolic changes in the urine of rats (LEES; SWANN; POUCHER; HOLMES *et al.*, 2019). Besides all the above mentioned, our study had a narrow time window, and perhaps the plasma changes we previously reported are a correspondence of a metabolic reservoir that would allow a higher concentration of the molecules involved. Nevertheless, these shortcomings open a research agenda to further explore the metabolic fingerprint of rotenone induced PD pathophysiology and the extension of its progression in face sleep disturbance.

Declarations

Availability of data and materials

The datasets used and/or analysed during the current study are included in this published article [and its supplementary information files]. If any additional information is required, it is available from the corresponding author on reasonable request.

Competing interests

The authors declare that they have no competing interests.

Funding

This work was supported by the Newton Fund, the Research Councils UK (RCUK), the Conselho Nacional das Fundações de Amparo à Pesquisa (CONFAP) and Fundação Araucária, Research Grant MR/N006321/1 (D.J.S.), Fundação Araucária (Programa de Apoio a Núcleos de Excelência – PRONEX) and in part by the Conselho Nacional de Desenvolvimento Científico e Tecnológico – CNPq. M.M.S.L. is the recipient of a CNPq fellowship, Research Grants 431279/2016-0, 305986/2016-3 and CAPES - Coordenação de Aperfeiçoamento de Pessoal de Nível Superior.

Author contributions

Conceptualization, M.M.L., D.J.S. and F.M.L.; Methodology, M.M.L., J.R.S., N.G., J.F.; Formal Analysis, J.F., N.G. and J.R.S. Investigation, J.F., A.D.S.T., A.C.D.N., L.S.R., N.G. and J.R.S.; Resources, M.M.L. and J.R.S.; Data Curation, J.F. and N.G.; Writing – Original Draft, J.F.; Writing – Review & Editing, M.M.L.; Visualization, J.F and N.G..; Supervision, M.M.L. and J.R.S.; Project Administration, J.F., J.R.S., D.J.S. and M.M.L.; Funding Acquisition, D.J.S., M.M.L., F.M.L., B.M. and J.R.S.

All authors read and approved the final manuscript.

Acknowledgments

We thank the support of Flavia Dorieux Wastner Cunha e Franciele Franco Scarante for the endless days of chronic sleep restriction. We wish to express our sincere gratitude to the Cross-Faculty NMR Centre at Imperial College London and its staff.

References

ADLER, C. H.; BEACH, T. G.; HENTZ, J. G.; SHILL, H. A. *et al.* Low clinical diagnostic accuracy of early vs advanced Parkinson disease: clinicopathologic study. **Neurology**, 83, n. 5, p. 406-412, Jul 29 2014.

ALQAHTANI, F.; CHOWDHURY, E. A.; BHATTACHARYA, R.; NOORANI, B. *et al.* Brain Uptake of [(13)C] and [(14)C]Sucrose Quantified by Microdialysis and Whole Tissue Analysis in Mice. **Drug Metab Dispos**, 46, n. 11, p. 1514-1518, Nov 2018.

ANDERSON, J. R.; CARROLL, I.; AZCARATE-PERIL, M. A.; ROCHETTE, A. D. *et al.* A preliminary examination of gut microbiota, sleep, and cognitive flexibility in healthy older adults. **Sleep Med**, 38, p. 104-107, Oct 2017.

BEDARF, J. R.; HILDEBRAND, F.; GOESER, F.; BORK, P. *et al.* [The gut microbiome in Parkinson's disease]. **Nervenarzt**, 90, n. 2, p. 160-166, Feb 2019.

BETARBET, R.; SHERER, T. B.; MACKENZIE, G.; GARCIA-OSUNA, M. *et al.* Chronic systemic pesticide exposure reproduces features of Parkinson's disease. **Nat Neurosci**, 3, n. 12, p. 1301-1306, Dec 2000.

BOERTIEN, J. M.; PEREIRA, P. A. B.; AHO, V. T. E.; SCHEPERJANS, F. Increasing Comparability and Utility of Gut Microbiome Studies in Parkinson's Disease: A Systematic Review. **J Parkinsons Dis**, Sep 4 2019.

BOULOS, C.; YAGHI, N.; EL HAYECK, R.; HERAOUI, G. N. *et al.* Nutritional Risk Factors, Microbiota and Parkinson's Disease: What Is the Current Evidence? **Nutrients**, 11, n. 8, Aug 14 2019.

BRINK, J. J.; STEIN, D. G. Pemoline levels in brain: enhancement by dimethyl sulfoxide. **Science**, 158, n. 3807, p. 1479-1480, Dec 15 1967.

CHASSAIN, C.; BIELICKI, G.; KELLER, C.; RENOU, J. P. *et al.* Metabolic changes detected in vivo by 1H MRS in the MPTP-intoxicated mouse. **NMR Biomed**, 23, n. 6, p. 547-553, Jul 2010.

CHIANG, H. L.; LIN, C. H. Altered Gut Microbiome and Intestinal Pathology in Parkinson's Disease. **J Mov Disord**, 12, n. 2, p. 67-83, May 2019.

COVA, I.; PRIORI, A. Diagnostic biomarkers for Parkinson's disease at a glance: where are we? **J Neural Transm (Vienna)**, 125, n. 10, p. 1417-1432, Oct 2018.

DAVIES, S. K.; ANG, J. E.; REVELL, V. L.; HOLMES, B. *et al.* Effect of sleep deprivation on the human metabolome. **Proc Natl Acad Sci U S A**, 111, n. 29, p. 10761-10766, Jul 22 2014.

DAWSON, P. A.; KARPEN, S. J. Intestinal transport and metabolism of bile acids. **J Lipid Res**, 56, n. 6, p. 1085-1099, Jun 2015.

DIETERLE, F.; ROSS, A.; SCHLOTTERBECK, G.; SENN, H. Probabilistic quotient normalization as robust method to account for dilution of complex biological mixtures. Application in 1H NMR metabonomics. **Anal Chem**, 78, n. 13, p. 4281-4290, Jul 1 2006.

DORSEY, E. R.; ELBAZ, A.; NICHOLS, E.; ABD-ALLAH, F. *et al.* Global, regional, and national burden of Parkinson's disease, 1990–2016: a systematic analysis for the Global Burden of Disease Study 2016. **The Lancet Neurology**, 17, n. 11, p. 939-953, 2018.

DOS SANTOS, A. C.; CASTRO, M. A.; JOSE, E. A.; DELATTRE, A. M. *et al.* REM sleep deprivation generates cognitive and neurochemical disruptions in the intranigral rotenone model of Parkinson's disease. **J Neurosci Res**, 91, n. 11, p. 1508-1516, Nov 2013.

EMWAS, A. H.; ROY, R.; MCKAY, R. T.; TENORI, L. *et al.* NMR Spectroscopy for Metabolomics Research. **Metabolites**, 9, n. 7, Jun 27 2019.

FAGOTTI, J.; TARGA, A. D. S.; RODRIGUES, L. S.; NOSEDA, A. C. D. *et al.* Chronic sleep restriction in the rotenone Parkinson's disease model in rats reveals peripheral early-phase biomarkers. **Sci Rep**, 9, n. 1, p. 1898, Feb 13 2019.

FEARNLEY, J. M.; LEES, A. J. Ageing and Parkinson's disease: substantia nigra regional selectivity. **Brain**, 114 (Pt 5), p. 2283-2301, Oct 1991.

GARCIA-BORREGUERO, D.; LARROSA, O.; BRAVO, M. Parkinson's disease and sleep. **Sleep Med Rev**, 7, n. 2, p. 115-129, Apr 2003.

GISKEODEGARD, G. F.; DAVIES, S. K.; REVELL, V. L.; KEUN, H. *et al.* Diurnal rhythms in the human urine metabolome during sleep and total sleep deprivation. **Sci Rep**, 5, p. 14843, Oct 9 2015.

GOEL, N. "Omics" Approaches for Sleep and Circadian Rhythm Research: Biomarkers for Identifying Differential Vulnerability to Sleep Loss. **Current Sleep Medicine Reports**, 1, n. 1, p. 38-46, 2015.

GRAHAM, S. F.; REY, N. L.; YILMAZ, A.; KUMAR, P. *et al.* Biochemical Profiling of the Brain and Blood Metabolome in a Mouse Model of Prodromal Parkinson's Disease Reveals Distinct Metabolic Profiles. **J Proteome Res**, 17, n. 7, p. 2460-2469, Jul 6 2018.

HOGLINGER, G. U.; FEGER, J.; PRIGENT, A.; MICHEL, P. P. *et al.* Chronic systemic complex I inhibition induces a hypokinetic multisystem degeneration in rats. **J Neurochem**, 84, n. 3, p. 491-502, Feb 2003.

HOLMES, E.; CLOAREC, O.; NICHOLSON, J. K. Probing latent biomarker signatures and in vivo pathway activity in experimental disease states via statistical total correlation spectroscopy (STOCSY) of biofluids: application to HgCl2 toxicity. **J Proteome Res**, 5, n. 6, p. 1313-1320, Jun 2006.

JUNHO, B. T.; KUMMER, A.; CARDOSO, F. E.; TEIXEIRA, A. L. *et al.* Sleep quality is associated with the severity of clinical symptoms in Parkinson's disease. **Acta Neurol Belg**, 118, n. 1, p. 85-91, Mar 2018.

KLEINDIENST, A.; DUNBAR, J. G.; GLISSON, K.; OUKUNO, K. *et al.* Effect of dimethyl sulfoxide on blood-brain barrier integrity following middle cerebral artery occlusion in the rat. **Acta Neurochir**, 96, p. 258-262, 2006.

KLINGELHOEFER, L.; REICHMANN, H. Parkinson's Disease and Gastrointestinal Non Motor Symptoms: Diagnostic and Therapeutic Options - A Practise Guide. **J Parkinsons Dis**, 5, n. 3, p. 647-658, 2015.

KLINGELHOEFER, L.; REICHMANN, H. The Gut and Nonmotor Symptoms in Parkinson's Disease. **Int Rev Neurobiol**, 134, p. 787-809, 2017.

LEES, H. J.; SWANN, J. R.; POUCHER, S.; HOLMES, E. *et al.* Obesity and Cage Environment Modulate Metabolism in the Zucker Rat: A Multiple Biological Matrix Approach to Characterizing Metabolic Phenomena. **J Proteome Res**, 18, n. 5, p. 2160-2174, May 3 2019.

LI, T.; LE, W. Biomarkers for Parkinson's Disease: How Good Are They? **Neurosci Bull**, Oct 23 2019.

LIMA, M. M. Sleep disturbances in Parkinson's disease: the contribution of dopamine in REM sleep regulation. **Sleep Med Rev**, 17, n. 5, p. 367-375, Oct 2013.

LIMA, M. M.; MARTINS, E. F.; DELATTRE, A. M.; PROENCA, M. B. *et al.* Motor and non-motor features of Parkinson's disease - a review of clinical and experimental studies. **CNS Neurol Disord Drug Targets**, 11, n. 4, p. 439-449, Jun 1 2012.

LU, Y.; ZHANG, X.; ZHAO, L.; YANG, C. *et al.* Metabolic Disturbances in the Striatum and Substantia Nigra in the Onset and Progression of MPTP-Induced Parkinsonism Model. **Front Neurosci**, 12, p. 90, 2018.

LUAN, H.; LIU, L. F.; TANG, Z.; ZHANG, M. *et al.* Comprehensive urinary metabolomic profiling and identification of potential noninvasive marker for idiopathic Parkinson's disease. **Sci Rep**, 5, p. 13888, Sep 14 2015.

LUBOMSKI, M.; TAN, A. H.; LIM, S. Y.; HOLMES, A. J. *et al.* Parkinson's disease and the gastrointestinal microbiome. **J Neurol**, Apr 30 2019.

MA, W.; SONG, J.; WANG, H.; SHI, F. *et al.* Chronic paradoxical sleep deprivation-induced depression-like behavior, energy metabolism and microbial changes in rats. **Life Sci**, 225, p. 88-97, May 15 2019.

MARSILI, L.; RIZZO, G.; COLOSIMO, C. Diagnostic Criteria for Parkinson's Disease: From James Parkinson to the Concept of Prodromal Disease. **Front Neurol**, 9, p. 156, 2018.

MEJRI, M. A.; YOUSFI, N.; HAMMOUDA, O.; TAYECH, A. *et al.* One night of partial sleep deprivation increased biomarkers of muscle and cardiac injuries during acute intermittent exercise. **J Sports Med Phys Fitness**, 57, n. 5, p. 643-651, May 2017.

MICHELL, A. W.; MOSEDALE, D.; GRAINGER, D. J.; BARKER, R. A. Metabolomic analysis of urine and serum in Parkinson's disease. **Metabolomics**, 4, n. 3, p. 191-201, 2008.

MINAMI, M.; TAKAHASHI, H.; SASAKI, T.; MATSUMOTO, S. *et al.* The effect of sleep restriction and psychological load on the diurnal metabolic changes in tryptamine-related compounds in human urine. **Environ Health Prev Med**, 17, n. 2, p. 87-97, Mar 2012.

MOLLENHAUER, B.; ZIMMERMANN, J.; SIXEL-DORING, F.; FOCKE, N. K. *et al.* Monitoring of 30 marker candidates in early Parkinson disease as progression markers. **Neurology**, 87, n. 2, p. 168-177, Jul 12 2016.

MOREIRA, C. G.; BARBIERO, J. K.; ARIZA, D.; DOMBROWSKI, P. A. *et al.* Behavioral, neurochemical and histological alterations promoted by bilateral intranigral rotenone administration: a new approach for an old neurotoxin. **Neurotox Res**, 21, n. 3, p. 291-301, Apr 2012.

PAN, Z.; RAFTERY, D. Comparing and combining NMR spectroscopy and mass spectrometry in metabolomics. **Anal Bioanal Chem**, 387, n. 2, p. 525-527, Jan 2007.

PAXINOS, G.; WATSON, C. **The rat brain in stereotaxic coordinates**. Elsevier Academic Press, 2005.

PODELL, M.; HADJICONSTANTINOU, M.; SMITH, M. A.; NEFF, N. H. Proton magnetic resonance imaging and spectroscopy identify metabolic changes in the striatum in the MPTP feline model of parkinsonism. **Exp Neurol**, 179, n. 2, p. 159-166, Feb 2003.

RODRIGUES, L. S.; TARGA, A. D.; NOSEDA, A. C.; AURICH, M. F. *et al.* Olfactory impairment in the rotenone model of Parkinson's disease is associated with bulbar dopaminergic D2 activity after REM sleep deprivation. **Front Cell Neurosci**, 8, p. 383, 2014.

SAMPSON, T. R.; DEBELIUS, J. W.; THRON, T.; JANSSEN, S. *et al.* Gut Microbiota Regulate Motor Deficits and Neuroinflammation in a Model of Parkinson's Disease. **Cell**, 167, n. 6, p. 1469-1480 e1412, Dec 1 2016.

SANTOS, S. F.; DE OLIVEIRA, H. L.; YAMADA, E. S.; NEVES, B. C. *et al.* The Gut and Parkinson's Disease-A Bidirectional Pathway. **Front Neurol**, 10, p. 574, 2019.

SHAO, Y.; LE, W. Recent advances and perspectives of metabolomics-based investigations in Parkinson's disease. **Mol Neurodegener**, 14, n. 1, p. 3, Jan 11 2019.

SHERER, T. B.; BETARBET, R.; GREENAMYRE, J. T. Environment, mitochondria, and Parkinson's disease. **Neuroscientist**, 8, n. 3, p. 192-197, Jun 2002.

SMITH, L. M.; PARR-BROWNLIE, L. C. A neuroscience perspective of the gut theory of Parkinson's disease. **Eur J Neurosci**, 49, n. 6, p. 817-823, Mar 2019.

SOBREIRA, E. S. T.; SOBREIRA-NETO, M. A.; PENA-PEREIRA, M. A.; CHAGAS, M. H. N. *et al.* Global cognitive performance is associated with sleep efficiency measured by polysomnography in patients with Parkinson's disease. **Psychiatry Clin Neurosci**, 73, n. 5, p. 248-253, May 2019.

SWANN, J. R.; GARCIA-PEREZ, I.; BRANISTE, V.; WILSON, I. D. *et al.* Application of (1)H NMR spectroscopy to the metabolic phenotyping of rodent brain extracts: A metabonomic study of gut microbial influence on host brain metabolism. **J Pharm Biomed Anal**, 143, p. 141-146, Sep 5 2017.

SWANN, J. R.; SPAGOU, K.; LEWIS, M.; NICHOLSON, J. K. *et al.* Microbial-mammalian cometabolites dominate the age-associated urinary metabolic phenotype in Taiwanese and American populations. **J Proteome Res**, 12, n. 7, p. 3166-3180, Jul 5 2013.

TANDBERG, E.; LARSEN, J. P.; KARLSEN, K. A community-based study of sleep disorders in patients with Parkinson's disease. **Mov Disord**, 13, n. 6, p. 895-899, Nov 1998.

TOLOSA, E.; PONT-SUNYER, C. Progress in defining the premotor phase of Parkinson's disease. **J Neurol Sci**, 310, n. 1-2, p. 4-8, Nov 15 2011.

VAN DER BORGHT, K.; FERRARI, F.; KLAUKE, K.; ROMAN, V. *et al.* Hippocampal cell proliferation across the day: increase by running wheel activity, but no effect of sleep and wakefulness. **Behav Brain Res**, 167, n. 1, p. 36-41, Feb 15 2006.

VAN, I. S. C. D.; DERKINDEREN, P. The Intestinal Barrier in Parkinson's Disease: Current State of Knowledge. **J Parkinsons Dis**, Sep 20 2019.

VIDENOVIC, A.; GOLOMBEK, D. Circadian and sleep disorders in Parkinson's disease. **Exp Neurol**, 243, p. 45-56, May 2013.

VIREL, A.; DUDKA, I.; LATERVEER, R.; AF BJERKEN, S. (1)H NMR profiling of the 6-OHDA parkinsonian rat brain reveals metabolic alterations and signs of recovery after N-acetylcysteine treatment. **Mol Cell Neurosci**, 98, p. 131-139, Jul 2019.

VOITENKO, L. P.; NIKONENKO, A. G. [Modification of experimental rotenone model of Parkinson's disease]. **Fiziol Zh**, 61, n. 1, p. 83-90, 2015.

WORLEY, B.; POWERS, R. Multivariate Analysis in Metabolomics. **Curr Metabolomics**, 1, n. 1, p. 92-107, 2013.

YILMAZ, R.; HOPFNER, F.; VAN EIMEREN, T.; BERG, D. Biomarkers of Parkinson's disease: 20 years later. **J Neural Transm (Vienna)**, 126, n. 7, p. 803-813, Jul 2019.

ZABEK, A.; STANIMIROVA, I.; DEJA, S.; BARG, W. *et al.* Fusion of the (1)H NMR data of serum, urine and exhaled breath condensate in order to discriminate chronic obstructive pulmonary disease and obstructive sleep apnea syndrome. **Metabolomics**, 11, n. 6, p. 1563-1574, 2015.

ZHANG, S. L.; BAI, L.; GOEL, N.; BAILEY, A. *et al.* Human and rat gut microbiome composition is maintained following sleep restriction. **Proc Natl Acad Sci U S A**, 114, n. 8, p. E1564-E1571, Feb 21 2017.

ZHENG, H.; ZHAO, L.; XIA, H.; XU, C. *et al.* NMR-Based Metabolomics Reveal a Recovery from Metabolic Changes in the Striatum of 6-OHDA-Induced Rats Treated with Basic Fibroblast Growth Factor. **Mol Neurobiol**, 53, n. 10, p. 6690-6697, Dec 2016.

4 CONCLUSIONS

In conclusion, SR in the ROT model has been shown to be an interesting model for investigating the interactions between them and the consequent behavioural and metabolic alterations. We have observed that chronic SR produces behavioural and plasma metabolic alterations that revealed a set of metabolic pathways, which are involved in PD pathophysiology. Nevertheless, these alterations were not replicated in brain tissue, urine and stool, facing an even more complex universe in the search of the metabolic fingerprint of PD. Disregarding putative technical issues, perhaps the plasma changes are a correspondence of a homeostatic reservoir of metabolic shifts, therefore with higher concentrations of the molecules involved.

Interestingly, SR appears to have a stronger effect in both metabolic and behavioural alterations, having a synergistic drift with ROT, highlighting the importance of better understanding the mechanisms underlying the observed results. These aspects contribute to the view that the sleep disorders are not merely subsidiary aspect of PD, but an interdependent outspread. Collectively, our findings reinforce the concept that SR in PD exacerbate and modulate metabolic shifts early in the disease, and might contributes to the development and progression, therefore having the potential to be established as reliable early-phase predictive biomarker.

On the other hand, the lack of variation in other matrices supports the characteristic heterogeneity of the ROT (which is correlated with PD variability as well) and sleep loss likelihood, revealing the need for differently designed studies to take this inconsistency into account and the time-dependency of the models.

4.1 FUTURE PERSPECTIVES

Perform a temporal metabolomic curve for the model, with correspondent neurodegeneration stage, establishing correlations and thus understanding the kinetics and relevance of each.

5 REFERENCES

ABBOTT, R. D.; ROSS, G. W.; WHITE, L. R.; TANNER, C. M. *et al.* Excessive daytime sleepiness and subsequent development of Parkinson disease. **Neurology**, 65, n. 9, p. 1442-1446, Nov 8 2005.

ADLER, C. H.; THORPY, M. J. Sleep issues in Parkinson's disease. **Neurology**, 64, n. 12 Suppl 3, p. S12-20, Jun 28 2005.

ALAM, M.; SCHMIDT, W. J. Rotenone destroys dopaminergic neurons and induces parkinsonian symptoms in rats. **Behav Brain Res**, 136, n. 1, p. 317-324, Oct 17 2002.

AMBERG, A.; RIEFKE, B.; SCHLOTTERBECK, G.; ROSS, A. *et al.* NMR and MS Methods for Metabolomics. **Methods Mol Biol**, 1641, p. 229-258, 2017.

ASCHERIO, A.; SCHWARZSCHILD, M. A. The epidemiology of Parkinson's disease: risk factors and prevention. **The Lancet Neurology**, 15, n. 12, p. 1257-1272, 2016.

ASKENASY, J. J.; YAHR, M. D. Reversal of sleep disturbance in Parkinson's disease by antiparkinsonian therapy: a preliminary study. **Neurology**, 35, n. 4, p. 527-532, Apr 1985.

BALL, N.; TEO, W. P.; CHANDRA, S.; CHAPMAN, J. Parkinson's Disease and the Environment. **Front Neurol**, 10, p. 218, 2019.

BARBOSA, M. T.; CARAMELLI, P.; MAIA, D. P.; CUNNINGHAM, M. C. *et al.* Parkinsonism and Parkinson's disease in the elderly: a community-based survey in Brazil (the Bambui study). **Mov Disord**, 21, n. 6, p. 800-808, Jun 2006.

BARNUM, C. J.; TANSEY, M. G. Neuroinflammation and non-motor symptoms: the dark passenger of Parkinson's disease? **Curr Neurol Neurosci Rep**, 12, n. 4, p. 350-358, Aug 2012.

BEAL, M. F. Mitochondria, oxidative damage, and inflammation in Parkinson's disease. **Ann N Y Acad Sci**, 991, p. 120-131, Jun 2003.

BETARBET, R.; SHERER, T. B.; MACKENZIE, G.; GARCIA-OSUNA, M. *et al.* Chronic systemic pesticide exposure reproduces features of Parkinson's disease. **Nat Neurosci**, 3, n. 12, p. 1301-1306, Dec 2000.

BILLINGSLEY, K. J.; BANDRES-CIGA, S.; SAEZ-ATIENZAR, S.; SINGLETON, A. B. Genetic risk factors in Parkinson's disease. **Cell Tissue Res**, 373, n. 1, p. 9-20, Jul 2018.

BOSE, A.; BEAL, M. F. Mitochondrial dysfunction in Parkinson's disease. **J Neurochem**, 139 Suppl 1, p. 216-231, Oct 2016.

BOVE, C.; TRAVAGLI, R. A. Neurophysiology of the brain stem in Parkinson's disease. **J Neurophysiol**, 121, n. 5, p. 1856-1864, May 1 2019.

BOVE, J.; PROU, D.; PERIER, C.; PRZEDBORSKI, S. Toxin-induced models of Parkinson's disease. **NeuroRx**, 2, n. 3, p. 484-494, Jul 2005.

BRAAK, H.; DEL TREDICI, K. Neuropathological staging of brain pathology in sporadic Parkinson's disease: separating the wheat from the chaff. **J Parkinsons Dis**, 7, n. s1, p. S73-S87, 2017.

BRAAK, H.; DEL TREDICI, K.; RUB, U.; DE VOS, R. A. *et al.* Staging of brain pathology related to sporadic Parkinson's disease. **Neurobiol Aging**, 24, n. 2, p. 197-211, Mar-Apr 2003.

BRAAK, H.; GHEBREMEDHIN, E.; RUB, U.; BRATZKE, H. *et al.* Stages in the development of Parkinson's disease-related pathology. **Cell Tissue Res**, 318, n. 1, p. 121-134, Oct 2004.

CANNON, J. R.; TAPIAS, V.; NA, H. M.; HONICK, A. S. *et al.* A highly reproducible rotenone model of Parkinson's disease. **Neurobiol Dis**, 34, n. 2, p. 279-290, May 2009.

CARRIERE, C. H.; KANG, N. H.; NILES, L. P. Bilateral upregulation of alpha-synuclein expression in the mouse substantia nigra by intracranial rotenone treatment. **Exp Toxicol Pathol**, 69, n. 2, p. 109-114, Feb 2017.

CHEN-PLOTKIN, A. S. Unbiased approaches to biomarker discovery in neurodegenerative diseases. **Neuron**, 84, n. 3, p. 594-607, Nov 05 2014.

CHEN, H.; BURTON, E. A.; ROSS, G. W.; HUANG, X. *et al.* Research on the premotor symptoms of Parkinson's disease: clinical and etiological implications. **Environ Health Perspect**, 121, n. 11-12, p. 1245-1252, Nov-Dec 2013.

COMELLA, C. L. Sleep disturbances and excessive daytime sleepiness in Parkinson disease: an overview. **J Neural Transm Suppl**, n. 70, p. 349-355, 2006.

DAUER, W.; PRZEDBORSKI, S. Parkinson's disease: mechanisms and models. **Neuron**, 39, n. 6, p. 889-909, Sep 11 2003.

DAVIES, S. K.; ANG, J. E.; REVELL, V. L.; HOLMES, B. *et al.* Effect of sleep deprivation on the human metabolome. **Proc Natl Acad Sci U S A**, 111, n. 29, p. 10761-10766, Jul 22 2014.

DEL TREDICI, K.; BRAAK, H. Lewy pathology and neurodegeneration in premotor Parkinson's disease. **Mov Disord**, 27, n. 5, p. 597-607, Apr 15 2012.

DEL TREDICI, K.; BRAAK, H. Sporadic Parkinson's disease: development and distribution of alpha-synuclein pathology. **Neuropathol Appl Neurobiol**, Dec 13 2015.

Doença de Parkinson. Blog da Saúde. http://www.blog.saude.gov.br/index.php/34589-doenca-de-parkinson: Ministério da Saúde 2014.

DORSEY, E. R.; ELBAZ, A.; NICHOLS, E.; ABD-ALLAH, F. *et al.* Global, regional, and national burden of Parkinson's disease, 1990–2016: a systematic analysis for the Global Burden of Disease Study 2016. **The Lancet Neurology**, 17, n. 11, p. 939-953, 2018.

DOS SANTOS, A. C.; CASTRO, M. A.; JOSE, E. A.; DELATTRE, A. M. *et al.* REM sleep deprivation generates cognitive and neurochemical disruptions in the intranigral rotenone model of Parkinson's disease. **J Neurosci Res**, 91, n. 11, p. 1508-1516, Nov 2013.

DUMAS, M. E.; KINROSS, J.; NICHOLSON, J. K. Metabolic phenotyping and systems biology approaches to understanding metabolic syndrome and fatty liver disease. **Gastroenterology**, 146, n. 1, p. 46-62, Jan 2014.

FAHN, S. Description of Parkinson's disease as a clinical syndrome. **Ann N Y Acad Sci**, 991, p. 1-14, Jun 2003.

FEARNLEY, J. M.; LEES, A. J. Ageing and Parkinson's disease: substantia nigra regional selectivity. **Brain**, 114 (Pt 5), p. 2283-2301, Oct 1991.

FERRARI, E.; PUCA, F.; MARGHERITA, G. [Anomalies of the Spindles during Sleep in Patients with Parkinson's Disease]. **Riv Neurol**, 34, p. 48-55, Jan-Feb 1964.

FIEHN, O. Metabolomics--the link between genotypes and phenotypes. **Plant Mol Biol**, 48, n. 1-2, p. 155-171, Jan 2002.

GALATI, S.; SALVADE, A.; PACE, M.; SARASSO, S. *et al.* Evidence of an association between sleep and levodopa-induced dyskinesia in an animal model of Parkinson's disease. **Neurobiol Aging**, 36, n. 3, p. 1577-1589, Mar 2015.

GAO, H. M.; KOTZBAUER, P. T.; URYU, K.; LEIGHT, S. *et al.* Neuroinflammation and oxidation/nitration of alpha-synuclein linked to dopaminergic neurodegeneration. **J Neurosci**, 28, n. 30, p. 7687-7698, Jul 23 2008.

GARCIA-BORREGUERO, D.; LARROSA, O.; BRAVO, M. Parkinson's disease and sleep. **Sleep Med Rev**, 7, n. 2, p. 115-129, Apr 2003.

GARCIA-DOMINGUEZ, I.; VESELA, K.; GARCIA-REVILLA, J.; CARRILLO-JIMENEZ, A. *et al.* Peripheral Inflammation Enhances Microglia Response and Nigral Dopaminergic Cell Death in an in vivo MPTP Model of Parkinson's Disease. **Front Cell Neurosci**, 12, p. 398, 2018.

GARCIA-GARCIA, F.; PONCE, S.; BROWN, R.; CUSSEN, V. *et al.* Sleep disturbances in the rotenone animal model of Parkinson disease. **Brain Res**, 1042, n. 2, p. 160-168, May 3 2005.

GARCIA, A.; BARBAS, C. Gas chromatography-mass spectrometry (GC-MS)-based metabolomics. **Methods Mol Biol**, 708, p. 191-204, 2011.

GASSER, T.; HARDY, J.; MIZUNO, Y. Milestones in PD genetics. **Mov Disord**, 26, n. 6, p. 1042-1048, May 2011.

GORELL, J. M.; PETERSON, E. L.; RYBICKI, B. A.; JOHNSON, C. C. Multiple risk factors for Parkinson's disease. **J Neurol Sci**, 217, n. 2, p. 169-174, Feb 15 2004.

GREENLAND, J. C.; WILLIAMS-GRAY, C. H.; BARKER, R. A. The clinical heterogeneity of Parkinson's disease and its therapeutic implications. **Eur J Neurosci**, 49, n. 3, p. 328-338, Feb 2019.

GRUNEWALD, A.; KUMAR, K. R.; SUE, C. M. New insights into the complex role of mitochondria in Parkinson's disease. **Prog Neurobiol**, 177, p. 73-93, Jun 2019.

HANCOCK, D. B.; MARTIN, E. R.; MAYHEW, G. M.; STAJICH, J. M. *et al.* Pesticide exposure and risk of Parkinson's disease: a family-based case-control study. **BMC Neurol**, 8, p. 6, 2008.

HANG, L.; THUNDYIL, J.; LIM, K. L. Mitochondrial dysfunction and Parkinson disease: a Parkin-AMPK alliance in neuroprotection. **Ann N Y Acad Sci**, 1350, p. 37-47, Sep 2015.

HAWKES, C. H.; DEL TREDICI, K.; BRAAK, H. A timeline for Parkinson's disease. **Parkinsonism Relat Disord**, 16, n. 2, p. 79-84, Feb 2010.

HOGLINGER, G. U.; FEGER, J.; PRIGENT, A.; MICHEL, P. P. *et al.* Chronic systemic complex I inhibition induces a hypokinetic multisystem degeneration in rats. **J Neurochem**, 84, n. 3, p. 491-502, Feb 2003.

HOLMES, E.; LI, J. V.; MARCHESI, J. R.; NICHOLSON, J. K. Gut microbiota composition and activity in relation to host metabolic phenotype and disease risk. **Cell Metab**, 16, n. 5, p. 559-564, Nov 7 2012.

HOLMES, E.; WILSON, I. D.; NICHOLSON, J. K. Metabolic phenotyping in health and disease. **Cell**, 134, n. 5, p. 714-717, Sep 05 2008.

HUGHES, A. J.; DANIEL, S. E.; LEES, A. J. Improved accuracy of clinical diagnosis of Lewy body Parkinson's disease. **Neurology**, 57, n. 8, p. 1497-1499, Oct 23 2001.

IBGE. Projeções da População do Brasil e Unidades da Federação por sexo e idade: 2010-2060. 2018.

ICKENSTEIN, G. W.; KLOTZ, J. M.; LANGOHR, H. D. [Virus encephalitis with symptomatic Parkinson syndrome, diabetes insipidus and panhypopituitarism]. **Fortschr Neurol Psychiatr**, 67, n. 10, p. 476-481, Oct 1999.

JELLINGER, K. A. Neuropathology of sporadic Parkinson's disease: evaluation and changes of concepts. **Mov Disord**, 27, n. 1, p. 8-30, Jan 2012.

JOHNSON, C. H.; IVANISEVIC, J.; SIUZDAK, G. Metabolomics: beyond biomarkers and towards mechanisms. **Nat Rev Mol Cell Biol**, 17, n. 7, p. 451-459, Jul 2016.

JOHNSON, M. E.; BOBROVSKAYA, L. An update on the rotenone models of Parkinson's disease: their ability to reproduce the features of clinical disease and model gene-environment interactions. **Neurotoxicology**, 46, p. 101-116, Jan 2015.

JOHNSON, M. E.; STECHER, B.; LABRIE, V.; BRUNDIN, L. *et al.* Triggers, Facilitators, and Aggravators: Redefining Parkinson's Disease Pathogenesis. **Trends Neurosci**, 42, n. 1, p. 4-13, Jan 2019.

KALES, A.; ANSEL, R. D.; MARKHAM, C. H.; SCHARF, M. B. *et al.* Sleep in patients with Parkinson's disease and normal subjects prior to and following levodopa administration. **Clin Pharmacol Ther**, 12, n. 2, p. 397-406, Mar-Apr 1971.

KAUR, R.; MEHAN, S.; SINGH, S. Understanding multifactorial architecture of Parkinson's disease: pathophysiology to management. **Neurol Sci**, 40, n. 1, p. 13-23, Jan 2019.

KIM, S.; KWON, S. H.; KAM, T. I.; PANICKER, N. *et al.* Transneuronal Propagation of Pathologic alpha-Synuclein from the Gut to the Brain Models Parkinson's Disease. **Neuron**, 103, n. 4, p. 627-641 e627, Aug 21 2019.

KRUGER, R.; HARDT, C.; TSCHENTSCHER, F.; JACKEL, S. *et al.* Genetic analysis of immunomodulating factors in sporadic Parkinson's disease. **J Neural Transm (Vienna)**, 107, n. 5, p. 553-562, 2000.

LANE, E.; DUNNETT, S. Animal models of Parkinson's disease and L-dopa induced dyskinesia: how close are we to the clinic? **Psychopharmacology (Berl)**, 199, n. 3, p. 303-312, Aug 2008.

LANG, A. E.; LOZANO, A. M. Parkinson's disease. First of two parts. **N Engl J Med**, 339, n. 15, p. 1044-1053, Oct 8 1998.

LANGSTON, J. W.; BALLARD, P. A., Jr. Parkinson's disease in a chemist working with 1-methyl-4-phenyl-1,2,5,6-tetrahydropyridine. **N Engl J Med**, 309, n. 5, p. 310, Aug 4 1983.

LARIVE, C. K.; BARDING, G. A., Jr.; DINGES, M. M. NMR spectroscopy for metabolomics and metabolic profiling. **Anal Chem**, 87, n. 1, p. 133-146, Jan 6 2015.

LE, W.; SAYANA, P.; JANKOVIC, J. Animal models of Parkinson's disease: a gateway to therapeutics? **Neurotherapeutics**, 11, n. 1, p. 92-110, Jan 2014.

LEI, S.; POWERS, R. NMR metabolomics analysis of Parkinson's disease. **Curr Metabolomics**, 1, n. 3, p. 191-209, 2013.

LI, J. V.; SWANN, J.; MARCHESI, J. R. Biology of the Microbiome 2: Metabolic Role. **Gastroenterol Clin North Am**, 46, n. 1, p. 37-47, Mar 2017.

LIMA, M. M. Sleep disturbances in Parkinson's disease: the contribution of dopamine in REM sleep regulation. **Sleep Med Rev**, 17, n. 5, p. 367-375, Oct 2013.

LIMA, M. M.; ANDERSEN, M. L.; REKSIDLER, A. B.; FERRAZ, A. C. *et al.* Paradoxical sleep deprivation modulates tyrosine hydroxylase expression in the nigrostriatal pathway and attenuates motor deficits induced by dopaminergic depletion. **CNS Neurol Disord Drug Targets**, 11, n. 4, p. 359-368, Jun 1 2012.

LIMA, M. M.; ANDERSEN, M. L.; REKSIDLER, A. B.; SILVA, A. *et al.* Blockage of dopaminergic D(2) receptors produces decrease of REM but not of slow wave sleep in rats after REM sleep deprivation. **Behav Brain Res**, 188, n. 2, p. 406-411, Apr 9 2008.

LIMA, M. M.; ANDERSEN, M. L.; REKSIDLER, A. B.; VITAL, M. A. *et al.* The role of the substantia nigra pars compacta in regulating sleep patterns in rats. **PLoS One**, 2, n. 6, p. e513, 2007.

LIMA, M. M.; MARTINS, E. F.; DELATTRE, A. M.; PROENCA, M. B. *et al.* Motor and non-motor features of Parkinson's disease - a review of clinical and experimental studies. **CNS Neurol Disord Drug Targets**, 11, n. 4, p. 439-449, Jun 1 2012.

LINDON, J. C.; NICHOLSON, J. K.; HOLMES, E.; EVERETT, J. R. Metabonomics: Metabolic processes studied by NMR spectroscopy of biofluids. **Concepts in Magnetic Resonance**, 12, n. 5, p. 289-320, 2000.

LUTH, E. S.; STAVROVSKAYA, I. G.; BARTELS, T.; KRISTAL, B. S. *et al.* Soluble, prefibrillar alpha-synuclein oligomers promote complex I-dependent, Ca2+-induced mitochondrial dysfunction. **J Biol Chem**, 289, n. 31, p. 21490-21507, Aug 1 2014.

MANDER, B. A.; WINER, J. R.; WALKER, M. P. Sleep and human aging. **Neuron**, 94, n. 1, p. 19-36, Apr 05 2017.

MARSILI, L.; RIZZO, G.; COLOSIMO, C. Diagnostic Criteria for Parkinson's Disease: From James Parkinson to the Concept of Prodromal Disease. **Front Neurol**, 9, p. 156, 2018.

MEERLO, P.; MISTLBERGER, R. E.; JACOBS, B. L.; HELLER, H. C. *et al.* New neurons in the adult brain: the role of sleep and consequences of sleep loss. **Sleep Med Rev**, 13, n. 3, p. 187-194, Jun 2009.

MILLER, D. B.; O'CALLAGHAN, J. P. Biomarkers of Parkinson's disease: present and future. **Metabolism**, 64, n. 3 Suppl 1, p. S40-46, Mar 2015.

MOLLENHAUER, B.; ZIMMERMANN, J.; SIXEL-DORING, F.; FOCKE, N. K. *et al.* Monitoring of 30 marker candidates in early Parkinson disease as progression markers. **Neurology**, 87, n. 2, p. 168-177, Jul 12 2016.

MORAIS, L. H.; LIMA, M. M.; MARTYNHAK, B. J.; SANTIAGO, R. *et al.* Characterization of motor, depressive-like and neurochemical alterations induced by a short-term rotenone administration. **Pharmacol Rep**, 64, n. 5, p. 1081-1090, 2012.

MOREIRA, C. G.; BARBIERO, J. K.; ARIZA, D.; DOMBROWSKI, P. A. *et al.* Behavioral, Neurochemical and Histological Alterations Promoted by Bilateral Intranigral Rotenone Administration: A New Approach for an Old Neurotoxin. **Neurotox Res**, 21, n. 3, p. 291-301, Sep 28 2012.

MOREIRA, C. G.; BARBIERO, J. K.; ARIZA, D.; DOMBROWSKI, P. A. *et al.* Behavioral, neurochemical and histological alterations promoted by bilateral intranigral rotenone administration: a new approach for an old neurotoxin. **Neurotox Res**, 21, n. 3, p. 291-301, Apr 2012.

MOURET, J. Differences in sleep in patients with Parkinson's disease. **Electroencephalogr Clin Neurophysiol**, 38, n. 6, p. 653-657, Jun 1975.

OSORIO, R. S.; PIRRAGLIA, E.; AGUERA-ORTIZ, L. F.; DURING, E. H. *et al.* Greater risk of Alzheimer's disease in older adults with insomnia. **J Am Geriatr Soc**, 59, n. 3, p. 559-562, Mar 2011.

PAN-MONTOJO, F.; SCHWARZ, M.; WINKLER, C.; ARNHOLD, M. *et al.* Environmental toxins trigger PD-like progression via increased alpha-synuclein release from enteric neurons in mice. **Sci Rep**, 2, p. 898, 2012.

PARK, M.; COMELLA, C. L.; LEURGANS, S. E.; FAN, W. *et al.* Association of daytime napping and Parkinsonian signs in Alzheimer's disease. **Sleep Med**, 7, n. 8, p. 614-618, Dec 2006.

PARKINSON, J. An essay on the shaking palsy. 1817. **J Neuropsychiatry Clin Neurosci**, 14, n. 2, p. 223-236; discussion 222, Spring 2002.

PEDERSEN, H. K.; GUDMUNDSDOTTIR, V.; NIELSEN, H. B.; HYOTYLAINEN, T. *et al.* Human gut microbes impact host serum metabolome and insulin sensitivity. **Nature**, 535, n. 7612, p. 376-381, Jul 21 2016.

PERIER, C.; BOVE, J.; VILA, M.; PRZEDBORSKI, S. The rotenone model of Parkinson's disease. **Trends Neurosci**, 26, n. 7, p. 345-346, Jul 2003.

POSTUMA, R. B.; BERG, D. Prodromal Parkinson's Disease: The Decade Past, the Decade to Come. **Mov Disord**, 34, n. 5, p. 665-675, May 2019.

POSTUMA, R. B.; GAGNON, J. F.; MONTPLAISIR, J. Clinical prediction of Parkinson's disease: planning for the age of neuroprotection. **J Neurol Neurosurg Psychiatry**, 81, n. 9, p. 1008-1013, Sep 2010.

PRIYADARSHI, A.; KHUDER, S. A.; SCHAUB, E. A.; PRIYADARSHI, S. S. Environmental risk factors and Parkinson's disease: a metaanalysis. **Environ Res**, 86, n. 2, p. 122-127, Jun 2001.

PROENCA, M. B.; DOMBROWSKI, P. A.; DA CUNHA, C.; FISCHER, L. *et al.* Dopaminergic D2 receptor is a key player in the substantia nigra pars compacta neuronal activation mediated by REM sleep deprivation. **Neuropharmacology**, 76 Pt A, p. 118-126, Jan 2014.

PUSHPANATHAN, M. E.; LOFTUS, A. M.; THOMAS, M. G.; GASSON, N. *et al.* The relationship between sleep and cognition in Parkinson's disease: A meta-analysis. **Sleep Med Rev**, 26, p. 21-32, Apr 2016.

RIEDER, C. R. M. Audiência Pública sobre o Projeto de Lei 605/2015: Diretrizes para a política de atenção integral aos portadores da doença de Parkinson no âmbito do Sistema Único de Saúde –SUS. Basília 2016.

RIEDERER, P.; BERG, D.; CASADEI, N.; CHENG, F. *et al.* alpha-Synuclein in Parkinson's disease: causal or bystander? **J Neural Transm (Vienna)**, 126, n. 7, p. 815-840, Jul 2019.

RITZ, B.; YU, F. Parkinson's disease mortality and pesticide exposure in California 1984-1994. **Int J Epidemiol**, 29, n. 2, p. 323-329, Apr 2000.

ROBERTS, L. D.; SOUZA, A. L.; GERSZTEN, R. E.; CLISH, C. B. Targeted metabolomics. **Curr Protoc Mol Biol**, Chapter 30, p. Unit 30 32 31-24, Apr 2012.

RODRIGUES, L. S.; FAGOTTI, J.; A, D. S. T.; AC, D. N. *et al.* Potential new therapies against a toxic relationship: neuroinflammation and Parkinson's disease. **Behav Pharmacol**, 30, n. 8, p. 676-688, Dec 2019.

RODRIGUES, L. S.; TARGA, A.; NOSEDA, A. C. D.; AURICH, M. F. *et al.* Olfactory impairment in the rotenone model of Parkinson's disease is associated with bulbar dopaminergic D2 activity after REM sleep deprivation. **Frontiers in Cellular Neuroscience**, 8, 2014-December-1 2014. Original Research.

ROTHMAN, S. M.; HERDENER, N.; FRANKOLA, K. A.; MUGHAL, M. R. *et al.* Chronic mild sleep restriction accentuates contextual memory impairments, and accumulations of cortical Abeta and pTau in a mouse model of Alzheimer's disease. **Brain Res**, 1529, p. 200-208, Sep 5 2013.

SCHAPIRA, A. H. V.; CHAUDHURI, K. R.; JENNER, P. Non-motor features of Parkinson disease. **Nat Rev Neurosci**, 18, n. 8, p. 509, Aug 2017.

SCHRIMPE-RUTLEDGE, A. C.; CODREANU, S. G.; SHERROD, S. D.; MCLEAN, J. A. Untargeted Metabolomics Strategies-Challenges and Emerging Directions. **J Am Soc Mass Spectrom**, 27, n. 12, p. 1897-1905, Dec 2016.

SCHULER, F.; CASIDA, J. E. The insecticide target in the PSST subunit of complex I. **Pest Manag Sci**, 57, n. 10, p. 932-940, Oct 2001.

SCHULZ-SCHAEFFER, W. J. The synaptic pathology of alpha-synuclein aggregation in dementia with Lewy bodies, Parkinson's disease and Parkinson's disease dementia. **Acta Neuropathol**, 120, n. 2, p. 131-143, Aug 2010.

SHAO, Y.; LE, W. Recent advances and perspectives of metabolomics-based investigations in Parkinson's disease. **Mol Neurodegener**, 14, n. 1, p. 3, Jan 11 2019.

SHARMA, S.; MOON, C. S.; KHOGALI, A.; HAIDOUS, A. *et al.* Biomarkers in Parkinson's disease (recent update). **Neurochem Int**, 63, n. 3, p. 201-229, Sep 2013.

SHERER, T. B.; BETARBET, R.; GREENAMYRE, J. T. Environment, mitochondria, and Parkinson's disease. **Neuroscientist**, 8, n. 3, p. 192-197, Jun 2002.

SHERER, T. B.; BETARBET, R.; TESTA, C. M.; SEO, B. B. *et al.* Mechanism of toxicity in rotenone models of Parkinson's disease. **J Neurosci**, 23, n. 34, p. 10756-10764, Nov 26 2003.

SILVEIRA-MORIYAMA, L.; LEES, A. J. Parkinson disease: how reliable are prodromal indicators of Parkinson disease? **Nat Rev Neurol**, 11, n. 1, p. 5-6, Jan 2015.

SKENE, D. J.; MIDDLETON, B.; FRASER, C. K.; PENNINGS, J. L. *et al.* Metabolic profiling of presymptomatic Huntington's disease sheep reveals novel biomarkers. **Sci Rep**, 7, p. 43030, Feb 22 2017.

SU, X.; FEDEROFF, H. J. Immune responses in Parkinson's disease: interplay between central and peripheral immune systems. **Biomed Res Int**, 2014, p. 275178, 2014.

SUBRAMANIAM, S. R.; CHESSELET, M. F. Mitochondrial dysfunction and oxidative stress in Parkinson's disease. **Prog Neurobiol**, 106-107, p. 17-32, Jul-Aug 2013.

TANDBERG, E.; LARSEN, J. P.; KARLSEN, K. A community-based study of sleep disorders in patients with Parkinson's disease. **Mov Disord**, 13, n. 6, p. 895-899, Nov 1998.

TARGA, A. D.; RODRIGUES, L. S.; NOSEDA, A. C.; AURICH, M. F. *et al.* Unraveling a new circuitry for sleep regulation in Parkinson's disease. **Neuropharmacology**, 108, p. 161-171, Sep 2016.

THOLFSEN, L. K.; LARSEN, J. P.; SCHULZ, J.; TYSNES, O. B. *et al.* Development of excessive daytime sleepiness in early Parkinson disease. **Neurology**, 85, n. 2, p. 162-168, Jul 14 2015.

TOLOSA, E.; PONT-SUNYER, C. Progress in defining the premotor phase of Parkinson's disease. **J Neurol Sci**, 310, n. 1-2, p. 4-8, Nov 15 2011.

VIDENOVIC, A.; GOLOMBEK, D. Circadian and sleep disorders in Parkinson's disease. **Exp Neurol**, 243, p. 45-56, May 2013.

VOITENKO, L. P.; NIKONENKO, A. G. [Modification of experimental rotenone model of Parkinson's disease]. **Fiziol Zh**, 61, n. 1, p. 83-90, 2015.

WAHNER, A. D.; SINSHEIMER, J. S.; BRONSTEIN, J. M.; RITZ, B. Inflammatory cytokine gene polymorphisms and increased risk of Parkinson disease. **Arch Neurol**, 64, n. 6, p. 836-840, Jun 2007.

WISHART, D. S. Emerging applications of metabolomics in drug discovery and precision medicine. **Nat Rev Drug Discov**, 15, n. 7, p. 473-484, Jul 2016.

WORLEY, B.; POWERS, R. Multivariate Analysis in Metabolomics. **Curr Metabolomics**, 1, n. 1, p. 92-107, 2013.

YILMAZ, R.; HOPFNER, F.; VAN EIMEREN, T.; BERG, D. Biomarkers of Parkinson's disease: 20 years later. **J Neural Transm (Vienna)**, 126, n. 7, p. 803-813, Jul 2019.

ZANELLATI, M. C.; MONTI, V.; BARZAGHI, C.; REALE, C. *et al.* Mitochondrial dysfunction in Parkinson disease: evidence in mutant PARK2 fibroblasts. **Front Genet**, 6, p. 78, 2015.

ZHANG, J.; XU, C. Y.; LIU, J. Meta-analysis on the prevalence of REM sleep behavior disorder symptoms in Parkinson's disease. **BMC Neurol**, 17, n. 1, p. 23, Feb 4 2017.

ZHANG, X.; SUN, X.; WANG, J.; TANG, L. *et al.* Prevalence of rapid eye movement sleep behavior disorder (RBD) in Parkinson's disease: a meta and meta-regression analysis. **Neurol Sci**, 38, n. 1, p. 163-170, Jan 2017.

ZHOU, B.; XIAO, J. F.; TULI, L.; RESSOM, H. W. LC-MS-based metabolomics. **Mol Biosyst**, 8, n. 2, p. 470-481, Feb 2012.

APPENDIX – CO-AUTHOR REFEREED FULL ARTICLES

SANTOS, P. D.; TARGA, A. D. S.; NOSEDA, A. C. D.; RODRIGUES, L. S. et al. Cholinergic Oculomotor Nucleus Activity Is Induced by REM Sleep Deprivation Negatively Impacting on Cognition. **Mol Neurobiol,** 54, n. 7, p. 5721-5729, Sep 2017.

Mol Neurobiol (2017) 54:5721–5729
DOI 10.1007/s12035-016-0112-z

Cholinergic Oculomotor Nucleus Activity Is Induced by REM Sleep Deprivation Negatively Impacting on Cognition

Patrícia Dos Santos [1] · Adriano D. S. Targa [1] · Ana Carolina D. Noseda [1] · Lais S. Rodrigues [1] · Juliane Fagotti [1] · Marcelo M. S. Lima [1]

Received: 5 February 2016 / Accepted: 7 September 2016 / Published online: 22 September 2016

Abstract Several efforts have been made to understand the involvement of rapid eye movement (REM) sleep for cognitive processes. Consolidation or retention of recognition memories is severely disrupted by REM sleep deprivation (REMSD). In this regard, pedunculopontine tegmental nucleus (PPT) and other brainstem nuclei, such as pontine nucleus (Pn) and oculomotor nucleus (OCM), appear to be candidates to take part in this REM sleep circuitry with potential involvement in cognition. Therefore, the objective of this study was to investigate a possible association between the performance of Wistar rats in a declarative memory and PPT, Pn, and OCM activities after different periods of REMSD. We examined c-Fos and choline acetyltransferase (ChaT) expressions as indicators of neuronal activity as well as a familiarity-based memory test. The animals were distributed in groups: control, REMSD, and sleep rebound (REB). At the end of the different REMSD (24, 48, 72, and 96 h) and REB (24 h) time points, the rats were immediately tested in the object recognition test and then the brains were collected. Results indicated that OCM neurons presented an increased activity, due to ChaT-labeling associated with REMSD that negatively correlated ($r = -0.32$) with the cognitive performance. This suggests the existence of a cholinergic compensatory mechanism within the OCM during REMSD. We also showed that 24 h of REMSD impacted similarly in memory, compared to longer periods of REMSD. These data extend the notion that REM sleep is influenced by areas other than PPT, i.e., Pn and OCM, which could be key players in both sleep processes and cognition.

Keywords Oculomotor nucleus · Pontine nucleus · Pedunculopontine tegmental nucleus · REM sleep deprivation · Object recognition test · Cognition

Abbreviations

ChaT	Choline acetyltransferase
DI	Discrimination index
OCM	Oculomotor nucleus
PD	Parkinson's disease
PPT	Pedunculopontine tegmental nucleus
Pn	Pontine nucleus
REM	Rapid eye movement
REMSD	REM sleep deprivation
REB	Rebound

Introduction

Several efforts have been made to comprehend the involvement of rapid eye movement (REM) sleep for cognitive processes, including attention, meaning, and memory consolidation [1, 2]. After repetitive exposure to a cognitive task, the patterns of hippocampal discharges, reflecting up to several minutes of behavioral experience, are reproduced during REM sleep, suggesting that episodic memory traces are reactivated during REM sleep [3]. The time course of REM sleep deprivation (REMSD) over these reactivations has not yet been thoroughly investigated.

Electronic supplementary material The online version of this article (doi:10.1007/s12035-016-0112-z) contains supplementary material, which is available to authorized users.

✉ Marcelo M. S. Lima
mmslima@ufpr.br; marcelomslima.neuro@gmail.com

[1] Laboratório de Neurofisiologia, Departamento de Fisiologia, Setor de Ciências Biológicas, Universidade Federal do Paraná, Av. Francisco H. dos Santos s/n, Caixa Postal: 19031, Curitiba, Paraná 81.531-990, Brazil

ILKIW, J. L.; KMITA, L. C.; TARGA, A. D. S.; NOSEDA, A. C. D. et al. Dopaminergic Lesion in the Olfactory Bulb Restores Olfaction and Induces Depressive-Like Behaviors in a 6-OHDA Model of Parkinson's Disease. **Mol Neurobiol**, 56, n. 2, p. 1082-1095, Feb 2019.

Molecular Neurobiology (2019) 56:1082–1095
https://doi.org/10.1007/s12035-018-1134-5

Dopaminergic Lesion in the Olfactory Bulb Restores Olfaction and Induces Depressive-Like Behaviors in a 6-OHDA Model of Parkinson's Disease

Jessica L. Ilkiw[1] · Luana C. Kmita[1] · Adriano D. S. Targa[1] · Ana Carolina D. Noseda[1] · Lais S. Rodrigues[1] · Flávia W. C. Dorieux[1] · Juliane Fagotti[1] · Patrícia dos Santos[1] · Marcelo M. S. Lima[1]

Received: 4 April 2018 / Accepted: 15 May 2018 / Published online: 5 June 2018

Abstract
Olfactory impairments and depressive behavior are commonly reported by individuals with Parkinson's disease (PD) being observed before motor symptoms. The mechanisms underlying these clinical manifestations are not fully elucidated. However, the imbalance in dopaminergic neurotransmission seems to play an important role in this context. In patients and animal models of PD, an increase in the dopaminergic interneurons of the glomerular layer in olfactory bulb (OB-gl) is observed, which may contribute to the olfactory impairment. In addition, neuronal imbalance in OB is related to depressive symptoms, as demonstrated by chemical olfactory bulbectomy. In view of that, we hypothesized that a reduction in the number or density of dopaminergic neurons present in OB could promote an olfactory improvement and, in contrast, would accentuate the depressive-like behaviors in the 6-hydroxydopamine (6-OHDA) model of PD. Therefore, we performed single or double injections of 6-OHDA within the substantia nigra pars compacta (SNpc) and/or in the OB-gl. We observed that, after 7 days, the group with nigral lesion exhibited olfactory impairment, as well as the group with the lesion in the OB-gl. However, the combination of the lesions prevented the occurrence of hyposmia. In relation to depressive-like behaviors, we observed that the SNpc injury promoted depressive-like behavior, being accentuated after a double injury. Our results demonstrated the importance of the dopaminergic neurons of the OB-gl in different non-motor features of PD, since the selective reduction of these periglomerular neurons was able to induce olfactory impairment and depressive-like behaviors.

Keywords Depression · Dopaminergic neurons · Olfaction · Parkinson's disease

Introduction

Parkinson's disease (PD) is the second most prevalent neurodegenerative disease [1, 2], accounting for 4.5–19 cases per 100,000 inhabitants per year [3, 4]. Olfactory impairment is the first pre-motor alteration of PD [5, 6], affecting more than 90% of the patients [7–9]. Currently, non-motor disturbances, such as depression, anxiety, hyposmia, constipation, and rapid eye movement (REM) sleep disorders, are gaining more attention in the literature since they appear before the motor signs [5, 10, 11].

✉ Marcelo M. S. Lima
mmslima@ufpr.br; marcelomslima.neuro@gmail.com

[1] Laboratório de Neurofisiologia. Departamento de Fisiologia, Universidade Federal do Paraná, Av. Francisco H. dos Santos s/n, , Curitiba, PR 81531-990, Brazil

Studies with relatives of PD patients had established that hyposmia may precede motor symptoms in 5 years [7], but other studies affirm that this disturbance is found decades before the motor onset [12]. In fact, it has been reported a significant increase in the number of the dopaminergic periglomerular interneurons located within the glomerular layer of the olfactory bulb (OB-gl), which are responsible for modulating olfactory transmission by inhibiting olfactory receptor cells and mitral/tufted neurons [8] in both humans [13, 14] and rats [15]. Hence, this mechanism raises the hypothesis that this increased dopaminergic activity could be a compensatory response to the loss of dopaminergic neurons in the substantia nigra pars compacta (SNpc), possibly being related to olfactory impairment observed in such condition [5, 16].

Depression is a psychiatric comorbidity that affects 30–50% of PD patients [17–22] and is characterized by depressed mood, loss of interest, and fatigue [23]. Depressive symptoms are normally observed before motor alterations [11], and it is a

RODRIGUES, L. S.; FAGOTTI, J.; A, D. S. T.; AC, D. N. et al. Potential new therapies against a toxic relationship: neuroinflammation and Parkinson's disease**. Behav Pharmacol**, 30, n. 8, p. 676-688, Dec 2019.

Potential new therapies against a toxic relationship: neuroinflammation and Parkinson's disease

Lais S. Rodrigues[a], Juliane Fagotti[a], Adriano D.S. Targa[b], Ana Carolina D. Noseda[a], Jéssica L. Ilkiw[a], Ana Paula Chuproski[a], Flavia W.C. Dorieux[a], Patricia D. dos Santos[a] and Marcelo M.S. Lima[a,c]

Parkinson's disease (PD) is a neurodegenerative disorder classically associated with motor symptoms, but several nonmotor disturbances appear decades before the clinical diagnosis of the disease. A variety of hypotheses exist to explain the onset of PD, and neuroinflammation is one of the most investigated processes. In fact, strong evidence suggests that PD begins with an inflammatory process; currently, however, no anti-inflammatory therapy is clinically employed to alleviate the typical motor and the prodromal disturbances such as olfactory loss, cognitive impairments, depression and anxiety, sleep disturbances, and autonomic disorders. In fact, the classical dopaminergic therapies are not effective in alleviating these symptoms and there is no other specific therapy for these outcomes. Therefore, in this review, we will discuss novel potential pharmacological therapeutic strategies focusing on cannabinoids, caffeine, melatonin, and dietary compounds, which could act as adjuvants to regular PD therapy. These described chemicals have been extensively investigated as anti-inflammatory agents possibly promoting beneficial effects on nonmotor symptoms of PD. The investigation of the inflammatory process at different stages of PD progression should give us a better view of the therapeutic scenario and could improve our understanding of the mechanisms of this disease. *Behavioural Pharmacology* **30: 675–687**

Behavioural Pharmacology 2019, 30:675–687

Keywords: caffeine, cannabinoids, melatonin, microglia, neuroinflammation, nonmotor symptoms, Parkinson's disease, polyunsaturated fatty acids

[a]Neurophysiology Laboratory, Department of Physiology, Federal University of Parana, Curitiba, Parana, Brazil; [b]Biomedical Research Institute of Lleida (IRBLleida), University of Lleida, Lleida, Catalonia, Spain; and [c]Department of Pharmacology, Federal University of Parana, Curitiba, Parana, Brazil

Correspondence to Marcelo M.S. Lima, PhD, Universidade Federal do Parana, Setor de Ciências Biologicas, Departamento de Fisiologia, Av. Francisco H. dos Santos s/n, 81.531 – 980, Caixa Postal: 19031, Curitiba, Parana, Brazil
E-mail: mmslima@utpr.br/marcelomslima.neuro@gmail.com

Received 15 July 2019 **Accepted as revised** 18 September 2019

Introduction

The inflammatory process is a protective mechanism that regenerates and repairs cells and damaged tissues, and removes parasites, infectious agents, and toxins from the body. The inflammatory responses are carried out by several immune and inflammatory cells, including T cells, neutrophils, macrophages, microglia, and mast cells (Kulkarni *et al.*, 2016). Within the central nervous system, inflammation is a protective mechanism that restores damaged glial and neuronal cells. However, a long-term or an excessive inflammatory response may inhibit neuronal regeneration (Kempuraj *et al.*, 2016). Neuroinflammation can be triggered by different circumstances such as dementia, trauma, stroke, hypertension, depression, diabetes, tumors, infections, toxins, and drugs, which can lead to a persistent production of proinflammatory molecules (Barrientos *et al.*, 2015). The normal aging process itself is known to drive a process of neuroinflammation, along with decreased adult neurogenesis, increased synaptic abnormalities, metabolic stress, cognitive decline, neurobehavioral deficits, and increased reactivity to any immunological challenge (Barrientos *et al.*, 2015). Several studies have identified neuroinflammation as a constant factor in neurodegenerative diseases that could be related to their etiology and/or their progression.

Parkinson's disease (PD) is a progressive and chronic neurodegenerative disorder that affects mostly elderly population – the peak incidence of symptoms is in people between 70 and 79 years old – typical for a neuroinflammatory disease (Muangpaisan *et al.*, 2011). In addition, it is the most common neurodegenerative disorder after Alzheimer's disease, with an increasing prevalence according to the age (41 per 100 000 at 40–49 years; 107 per 100 000 at 50–59 years; 173 per 100 000 at 55–64 years; 428 per 100 000 at 60–69 years; 425 per 100 000 at 65–74 years; 1087 per 100 000 at 70–79 years; and 1903 per 100 000 at over age 80) (Pringsheim *et al.*, 2014). PD is characterized by the death of dopaminergic neurons in the substantia nigra pars compacta (SNpc), the main responsible for the motor symptoms, and also by the presence of α-synuclein (Lewy bodies) protein accumulation in the neurons (Braak *et al.*, 2004). Despite the profound knowledge about PD motor symptoms – well established since the first description of PD by James Parkinson (1817) as bradykinesia, muscular rigidity, and resting tremor – its etiology is not fully understood but

DOI: 10.1097/FBP.0000000000000512